Westinghouse Non-Proprietary Class 3

WCAP-15916
Revision 0

September 2002

Analysis of Capsule X from the Florida Power and Light Company Turkey Point Unit 3 Reactor Vessel Radiation Surveillance Program

Westinghouse

WCAP-15916, Revision 0

Analysis of Capsule X from the Florida Power and Light Company Turkey Point Unit 3 Reactor Vessel Radiation Surveillance Program

J. H. Ledger
G. K. Roberts
J. Conermann

September 2002

Approved: _____
J. A. Gresham, Manager
Engineering & Materials Technology

Westinghouse Electric Company LLC
Energy Systems
P.O. Box 355
Pittsburgh, PA 15230-0355

TABLE OF CONTENTS

LIST OF TABLES

LIST OF TABLES (Cont.)

LIST OF FIGURES

LIST OF FIGURES (Cont.)

PREFACE

This report has been technically reviewed and verified by:

Reviewer:

Sections 1 through 5, 7, 8, Appendices B, C and D	T. J. Laubham	T. J. Laubham
Section 6 and Appendix A	S. L. Anderson	S. L. Anderson

EXECUTIVE SUMMARY

The purpose of this report is to document the results of the testing of surveillance Capsule X specimens and dosimeters from the Turkey Point Unit 3 reactor vessel. Capsule X was removed at 19.85 EFPY and post irradiation mechanical testing of the Capsule X Charpy V-notch and tensile specimens was performed along with a fluence evaluation. The surveillance Capsule X fluence was 2.90×10^{19} n/cm^2 after 19.85 EFPY of plant operation. A brief summary of the Charpy V-notch testing results can be found in Section 1 and the updated capsule removal schedule can be found in Section 7. The results of the capsule analysis are within the expected range for both materials tested and dosimetry calculations.

1 SUMMARY OF RESULTS

The analysis of the reactor vessel materials contained in surveillance Capsule X, the fourth capsule to be removed from the Turkey Point Unit 3 reactor pressure vessel, resulted in the following conclusions:

- Capsule X received an average fast neutron calculated fluence (E > 1.0 MeV) of 2.90 x 10^{19} n/cm^2 after 19.85 effective full power years of operation. This capsule was relocated from the "X" position to the "T" position in 1990 in order to accelerate neutron accumulation and better suit the program intent.

- Irradiation of the reactor vessel lower shell forging 123S266VA1 Charpy specimens, oriented with the longitudinal axis of the specimen parallel to the major working direction of the plate (tangential orientation), to 2.90 x 10^{19} n/cm^2 (E> 1.0MeV) resulted in a 30 ft-lb transition temperature increase of 72.44°F and a 50 ft-lb transition temperature increase of 63.4°F. This results in an irradiated 30 ft-lb transition temperature of 9.14°F and an irradiated 50 ft-lb transition temperature of 27.95°F for the longitudinally oriented specimens.

- Irradiation of the weld metal Charpy specimens to 2.90 x 10^{19} n/cm^2 (E> 1.0MeV) resulted in a 30 ft-lb transition temperature increase of 191.06°F. This results in an irradiated 30 ft-lb transition temperature of 190.97°F.

- Irradiation of the weld Heat-Affected-Zone (HAZ) metal Charpy specimens to 2.90 x 10^{19} n/cm^2 (E> 1.0 MeV) resulted in a 30 ft-lb transition temperature increase of 26°F and a 50 ft-lb transition temperature increase of 18.72°F. This results in an irradiated 30 ft-lb transition temperature of –45.77°F and an irradiated 50 ft-lb transition temperature of –30.55°F.

- Irradiation of the Correlation Monitor Material Charpy specimens to 2.90 x 10^{19} n/cm^2 (E> 1.0 MeV) resulted in a 30 ft-lb transition temperature increase of 126.86°F and a 50 ft-lb transition temperature increase of 127.45°F. This results in an irradiated 30 ft-lb transition temperature of 156.96°F and an irradiated 50 ft-lb transition temperature of 202.03°F.

- The average upper shelf energy of the lower shell forging 123S266VA1 (tangential orientation) resulted in no energy decrease after irradiation to 2.90 x 10^{19} n/cm^2 (E> 1.0 MeV). This results in an irradiated average upper shelf energy of 148 ft-lb for the tangentially oriented specimens.

- The average upper shelf energy of the weld metal Charpy specimens resulted an average energy decrease of 19.7 ft-lb after irradiation to 2.90 x 10^{19} n/cm^2 (E> 1.0 MeV). Hence, this results in an irradiated average upper shelf energy of 45 ft-lb for the weld metal specimens. As expected, this result is below the 10CFR50 Appendix G requirement. The required analysis is documented in reference 19.

- The average upper shelf energy of the weld HAZ metal Charpy specimens resulted in an average energy decrease of 19 ft-lb after irradiation to 2.90 x 10^{19} n/cm^2 (E> 1.0MeV). This results in an irradiated average upper shelf energy of 158 ft-lb for the weld HAZ metal.

- The average upper shelf energy of the Correlation Monitor Material Charpy specimens resulted in an average energy decrease of 0.5 ft-lb after irradiation to 2.90×10^{19} n/cm^2 (E> 1.0MeV). This results in an irradiated average upper shelf energy of 67 ft-lb for the Correlation Monitor Material.

- A comparison of the Turkey Point Unit 3 Reactor Vessel beltline materials test results with the Regulatory Guide 1.99 Revision 2 predictions led to the following conclusions:

  - The measured 30 ft-lb shift in transition temperature values of the lower shell forging contained in Capsule X (Tangential) is greater than Regulatory Guide 1.99 Revision 2 predictions. However, the shift value is less than two sigma allowance by Regulatory Guide 1.99 Revision 2.

  - The measured 30 ft-lb shift in transition temperature values of the weld metal contained in Capsule X is less than the Regulatory Guide 1.99 Revision 2 predictions.

  - The measured percent decrease in upper shelf energy of the Capsule X surveillance materials is less than the Regulatory Guide 1.99 Revision 2 predictions.

- The peak calculated end-of-license (32 EFPY) and end-of-license renewal (48 EFPY) neutron fluence (E> 1.0 MeV) at the core midplane for the Turkey Point Unit 3 reactor vessel using the Regulatory Guide 1.99, Revision 2 attenuation formula (ie. Equation # 3 in the guide; $f_{(depth\ x)} = f_{surface} * e^{(-0.24x)}$) is as follows:

<u>Calculated (32 EFPY):</u>	Vessel inner radius* = 4.03×10^{19} n/cm^2
	Vessel 1/4 thickness = 2.53×10^{19} n/cm^2
	Vessel 3/4 thickness = 9.98×10^{18} n/cm^2
<u>Calculated (48 EFPY):</u>	Vessel inner radius* = 5.91×10^{19} n/cm^2
	Vessel 1/4 thickness = 3.71×10^{19} n/cm^2
	Vessel 3/4 thickness = 1.46×10^{19} n/cm^2

*Clad/base metal interface

Note: These fluence levels are calculated without the use of part length burnable absorber (Hf) assemblies in the core.

2 INTRODUCTION

This report presents the results of the examination of Capsule X, the fourth capsule removed from the reactor in the continuing surveillance program which monitors the effects of neutron irradiation on the Florida Power and Light Company Turkey Point Unit 3 reactor pressure vessel materials under actual operating conditions.

The surveillance program for the Turkey Point Unit 3 reactor pressure vessel materials was designed and recommended by the Westinghouse Electric Corporation. A description of the surveillance program and the preirradiation mechanical properties of the reactor vessel materials is presented in WCAP-7656, entitled "Florida Power and Light Co. Turkey Point Unit No. 3 Reactor Vessel Radiation Surveillance Program" by S. E. Yanichko, [1]. The surveillance program was planned to cover the 40-year design life of the reactor pressure vessel and was based on ASTM E185-66, "Recommended Practice for Surveillance Tests on Structural Materials in Nuclear Reactors"[13].

Subsequently, the Unit 3 program was integrated with the Unit 4 program. This is documented in reference 20 and approved by the NRC in reference 21. Program integration was facilitated by the fact that both units have the identical limiting material, weld SA-1101 in the lower to intermediate girth welds. Both surveillance programs contain weldments made of the same weld wire, Page wire heat 71249. Therefore the results of this capsule represent results for both units 3 and 4.

Capsule X was removed from the reactor after 19.85 EFPY of exposure and shipped to the Westinghouse Science and Technology Center Hot Cell Facility, where the postirradiation mechanical testing of the Charpy V-notch impact and tensile surveillance specimens was performed.

This report summarizes the analysis of the post-irradiation data obtained from surveillance Capsule X removed from the Florida Power and Light Company Turkey Point Unit 3 reactor vessel and discusses the analysis of the data.

3 BACKGROUND

The ability of the large steel pressure vessel containing the reactor core and its primary coolant to resist fracture constitutes an important factor in ensuring safety in the nuclear industry. The beltline region of the reactor pressure vessel is the most critical region of the vessel because it is subjected to significant fast neutron bombardment. The overall effects of fast neutron irradiation on the mechanical properties of low alloy, ferritic pressure vessel steels such as SA508 Class 2 (base material of the Turkey Point Unit 3 reactor pressure vessel forging) are well documented in the literature. Generally, low alloy ferritic materials show an increase in hardness and tensile properties and a decrease in ductility and toughness during high energy irradiation.

A method for ensuring the integrity of reactor pressure vessels has been presented in "Fracture Toughness Criteria for Protection Against Failure," Appendix G to Section XI of the ASME Boiler and Pressure Vessel Code[4]. The method uses fracture mechanics concepts and is based on the reference nil-ductility transition temperature (RT_{NDT}).

RT_{NDT} is defined as the greater of either the drop weight nil-ductility transition temperature (NDTT per ASTM E-208[5]) or the temperature 60°F less than the 50 ft-lb (and 35-mil lateral expansion) temperature as determined from Charpy specimens oriented normal to the major working direction of the material. The RT_{NDT} of a given material is used to index that material to a reference stress intensity factor curve (K_{Ic} curve) which appears in Appendix G to the ASME Code. The K_{Ic} curve is a lower bound of static fracture toughness results obtained from several heats of pressure vessel steel. When a given material is indexed to the K_{Ic} curve, allowable stress intensity factors can be obtained for this material as a function of temperature. Allowable operating limits can then be determined using these allowable stress intensity factors.

RT_{NDT} and, in turn, the operating limits of nuclear power plants can be adjusted to account for the effects of radiation on the reactor vessel material properties. The radiation embrittlement changes in mechanical properties of a given reactor pressure vessel steel can be monitored by a reactor surveillance program, such as the Turkey Point Unit 3 reactor vessel radiation surveillance program[1], in which a surveillance capsule is periodically removed from the operating nuclear reactor and the encapsulated specimens tested. The increase in the average Charpy V-notch 30 ft-lb temperature (ΔRT_{NDT}) due to irradiation is added to the initial RT_{NDT} along with a margin term(M) to cover uncertainties, to adjust the RT_{NDT} for radiation embrittlement. This RT_{NDT} (RT_{NDT} initial + M + ΔRT_{NDT}) is used to index the material to the K_{Ic} curve and, in turn, to set operating limits for the nuclear power plant that take into account the effects of irradiation on the reactor vessel materials.

4 DESCRIPTION OF PROGRAM

Eight surveillance capsules for monitoring the effects of neutron exposure on the Turkey Point Unit 3 reactor pressure vessel core region material were inserted in the reactor vessel prior to initial plant startup. The capsules were positioned in the reactor vessel between the thermal shield and the vessel wall at locations shown in Figure 4-1. The vertical center of the capsules is opposite the vertical center of the core.

Capsule X (Figure 4-2) was removed after 19.85 Effective Full Power Years (EFPY) of plant operation. This capsule was relocated from the "X" position to the "T" position in 1990 in order to accelerate neutron accumulation and better suit the program intent. This capsule contained Charpy V-notch, tensile specimens and WOL fracture mechanics specimens from the reactor vessel lower shell forging 123S266VA1, weld metal representative of the beltline region weld seams, Charpy V-notch specimens from weld heat-affected zone (HAZ) material and Charpy V-notch specimens from ASTM correlation monitor material (A302 Grade B).

The chemistry and heat treatment of the surveillance material are presented in Table 4-1 and Table 4-2, respectively. The chemical analyses reported in table 4-1 were obtained from unirradiated material used in the surveillance program.

All test specimens were machined from the ¼ thickness location. Test specimens represent material taken at least one forging thickness from the quenched end of the forging. All base material Charpy V-notch impact and tensile specimens were oriented with the longitudinal axis of the specimen parallel to (tangential orientation) the principal working direction of the forging. Charpy V-notch specimens from the weld metal were oriented with the longitudinal axis of the specimens transverse to the weld direction. Tensile specimens were oriented with the longitudinal axis of the specimens parallel to the weld. The WOL test specimens were machined with the simulated crack of the specimen to the surfaces and hoop direction of the forging.

Capsule X contained dosimeters of Copper, Nickel and Aluminum-Cobalt wire (cadmium-shielded and unshielded), and Neptunium (Np^{237}) and Uranium (U^{238}) which measure the integrated flux at specific neutron energy levels.

Thermal monitors were made from two low-melting eutectic alloys and sealed in Pyrex tubes that were included in the capsule and were located as shown in Figure 4-2. The two eutectic alloys and their melting points are:

2.5% Ag, 97.5% Pb	Melting Point 579°F (304°C)
1.75% Ag, 0.75% Sn, 97.5% Pb	Melting Point 590°F (310°F)

The arrangement of the various mechanical test specimens, dosimeters and thermal monitors contained in Capsule X are shown in Figure 4-2.

Table 4-1***Chemical Composition of the Turkey Point Unit 3 Reactor Vessel Surveillance Materials			
Element	Intermediate Shell Forging 123P461VA1	Lower Shell Forging 123S266VA1	Weld Metal
C	0.20	0.19 / 0 21	0 076
Mn	0.64 / 0.64	0 61 / 0.62	1.26
P	0.010	0 010	0.011
S	0.010	0.008	0.018
Si	0.26	0 20 / 0.19	0.66
Ni	0.70	0.68 / 0.66	0.57
Cr	0.40 / 0.39	0 38	0.14
V	0 02	0.02	0.002
Mo	0 62	0.58 / 0.59	0.42
Co	0.011 / 0 010	0 015 / 0.016	0.001
Cu	0 058 (0.07)**	0.079 (0.07)**	0.31
Sn	0 010	0 008	0.004
Zn	0.001	0 001	0 003
Al	0 005	0 005	0.015
N_2	0 003	0.003	0.012
Ti	0.001*	0 001*	0.001
Sb	0.001*	0 001*	0 001
A_s	0.005*	0 005*	0.005
B	0 003*	0.003*	0.003*
Zr	0 001*	0.001*	0 001

* Not Detected The number indicates the minimum limit of detection

** Copper Content Reported by Bethlehem Steel Co.

*** Table taken directly from WCAP-7656[11]

Table 4-2* Heat Treatment of the Turkey Point Unit 3 Reactor Vessel Surveillance Materials

Material	Temperature (°F)	Time (hr)	Coolant
Intermediate and Lower Shell Forgings	1550	13	Water quenched
	1210	18	Air Cooled
	1125	10.5	Furnace Cooled
Weldment	1125	10.25	Furnace Cooled

* Taken directly from WCAP-7656[11]

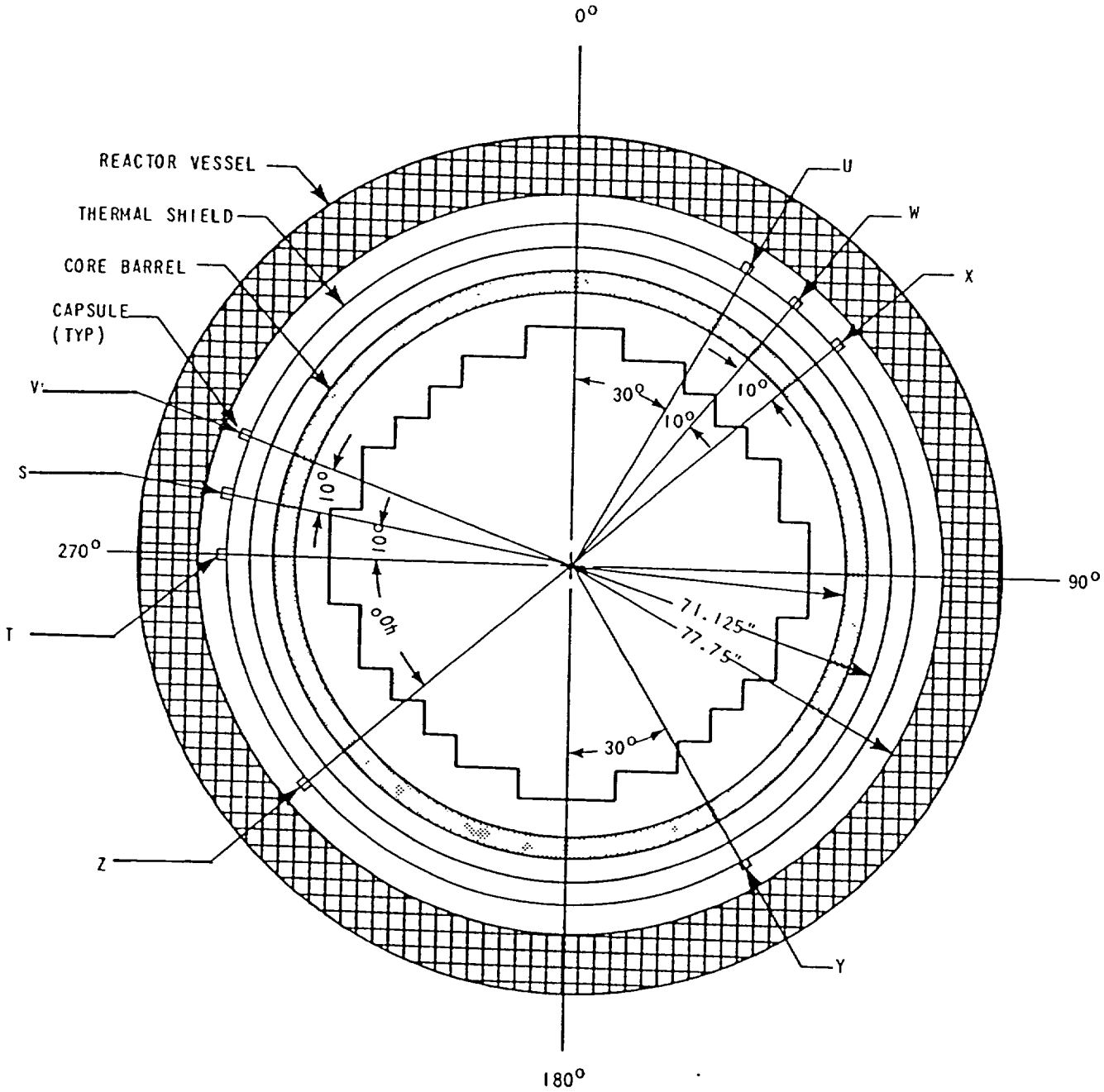

Figure 4-1 Original Arrangement of Surveillance Capsules in the Turkey Point Unit 3 Reactor Vessel

SPECIMEN NUMBERING CODE

S- Forging 123S266-VA1
W- Weld Metal
H- Heat-Affected-Zone
R- ASTM Correlation Monitor Material

SURVEILLANCE CAPSULE X

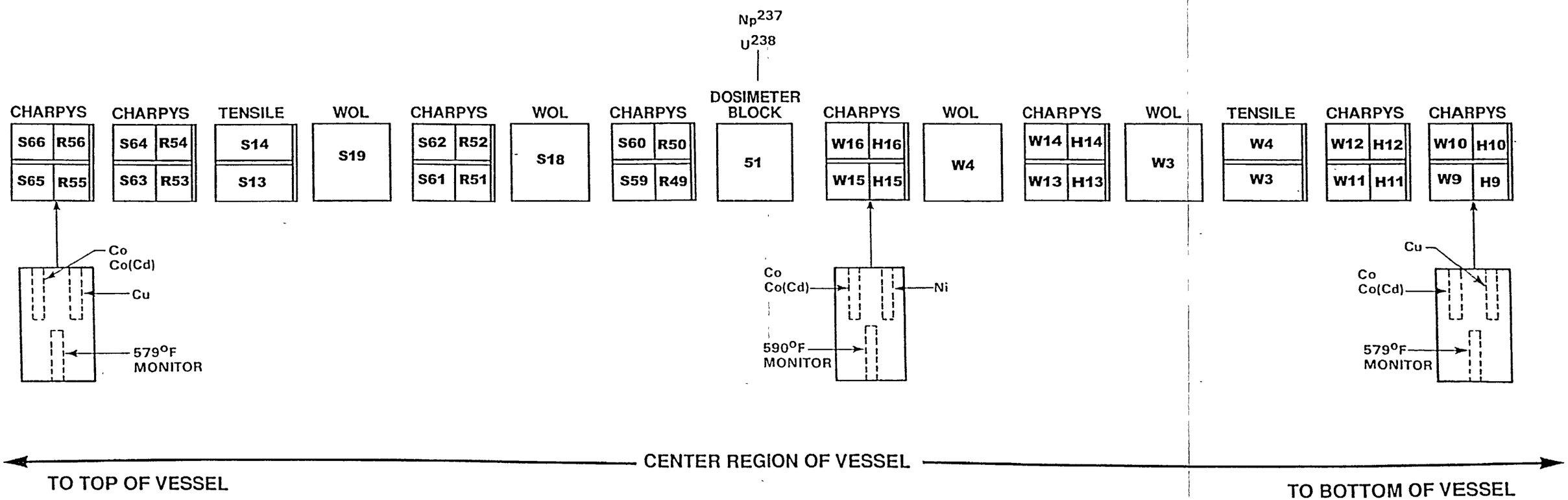

Figure 4-2 **Capsule X Diagram Showing the Location of Specimens, Thermal Monitors, and Dosimeters**

5 TESTING OF SPECIMENS FROM CAPSULE X

5.1 OVERVIEW

The post-irradiation mechanical testing of the Charpy V-notch and tensile specimens was performed at the Westinghouse Science and Technology Center Laboratory with consultation by Westinghouse Energy Systems personnel. Testing was performed in accordance with 10CFR50, Appendices G and H[2], ASTM Specification E185-82[6], and Westinghouse Remote Metallographic Facility (RMF) Procedure RMF 8402, Revision 1 and 8103, Revision 1.

Upon receipt of the capsule at the hot cell laboratory, the capsule was visually examinated and photographed for identification purposes. The specimens and spacer blocks were carefully removed, inspected for identification number, and checked against the master list in WCAP-7656[1]. No discrepancies were found.

Examination of the two low-melting point 304°C (579°F) and 310°C (590°F) eutectic alloys indicated no melting of either type of thermal monitor. Based on this examination, the maximum temperature to which the test specimens were exposed was less than 304°C (579°F).

The Charpy impact tests were performed per ASTM Specification E23-98[8] and RMF Procedure 8103, Revision 1, on a Tinius-Olsen Model 74, 358J machine. The tup (striker) of the Charpy impact test machine is instrumented with a GRC 930-I instrumentation system feeding information into an IBM compatible computer. With this system, load-time and energy-time signals can be recorded in addition to the standard measurement of Charpy energy (E_D). From the load-time curve (Appendix A), the load of general yielding (P_{GY}), the time to general yielding (t_{GY}), the maximum load (P_M), and the time to maximum load (t_M) can be determined. Under some test conditions, a sharp drop in load indicative of fast fracture was observed. The load at which fast fracture was initiated is identified as the fast fracture load (P_F), and the load at which fast fracture terminated is identified as the arrest load (P_A).

The energy at maximum load (E_M) was determined by comparing the energy-time record and the load-time record. The energy at maximum load is approximately equivalent to the energy required to initiate a crack in the specimen. Therefore, the propagation energy for the crack (E_p) is the difference between the total energy to fracture (E_D) and the energy at maximum load (E_M).

The yield stress (σ_Y) was calculated from the three-point bend formula having the following expression:

$$\sigma_Y = (P_{GY} * L) / [B * (W - a)^2 * C] \qquad (1)$$

where:
- L = distance between the specimen supports in the impact machine
- B = the width of the specimen measured parallel to the notch
- W = height of the specimen, measured perpendicularly to the notch
- a = notch depth

The constant C is dependent on the notch flank angle (ϕ), notch root radius (ρ) and the type of loading (i.e., pure bending or three-point bending). In three-point bending, for a Charpy specimen in which ϕ= 45° and ρ = 0.010 inch, Equation 1 is valid with C = 1.21. Therefore, (for L = 4W),

$$\sigma_y = (P_{GY} * L) / [B * (W - a)^2 * 1.21] = (3.33 * P_{GY} * W) / [B * (W - a)^2] \quad (2)$$

For the Charpy specimen, B = 0.394 inch, W = 0.394 inch and a = 0.079 inch. Equation 2 then reduces to:

$$\sigma_y = 33.3 * P_{GY} \quad (3)$$

where σ_y is in units of psi and P_{GY} is in units of lbs. The flow stress was calculated from the average of the yield and maximum loads, also using the three-point bend formula.

The symbol A in columns 4, 5, and 6 of Tables 5-5 through 5-8 is the cross-section area under the notch of the Charpy specimens:

$$A = B * (W - a) = 0.1241 \text{ sq.in.} \quad (4)$$

Percent shear was determined from post-fracture photographs using the ratio-of-areas methods in compliance with ASTM Specification E23-98[8] and A370-97a[9]. The lateral expansion was measured using a dial gage rig similar to that shown in the same specification.

Tensile tests were performed on a 20,000-pound Instron, split-console test machine (Model 1115) per ASTM Specification E8-99[10] and E21-92(1998)[11], and RMF Procedure 8102, Revision 1. All pull rods, grips, and pins were made of Inconel 718. The upper pull rod was connected through a universal joint to improve axiality of loading. The tests were conducted at a constant crosshead speed of 0.05 inches per minute throughout the test.

Extension measurements were made with a linear variable displacement transducer (LVDT) extensometer. The extensometer knife edges were spring-loaded to the specimen and operated through specimen failure. The extensometer gage length was 1.00 inch. The extensometer is rated as Class B-2 per ASTM E83-93[12].

Elevated test temperatures were obtained with a three-zone electric resistance split-tube furnace with a 9-inch hot zone. All tests were conducted in air.

The yield load, ultimate load, fracture load, total elongation, and uniform elongation were determined directly from the load-extension curve. The yield strength, ultimate strength, and fracture strength were calculated using the original cross-sectional area. The final diameter and final gage length were determined from post-fracture photographs. The fracture area used to calculate the fracture stress (true stress at fracture) and percent reduction in area was computed using the final diameter measurement.

5.2 CHARPY V-NOTCH IMPACT TEST RESULTS

The results of the Charpy V-notch impact tests performed on the various materials contained in Capsule X irradiated to approximately 2.90 x 10^{19} n/cm^2 in 19.85EFPY are presented in Tables 5-1 through 5-8, and are compared with unirradiated results as shown in Figures 5-1 through 5-12. The transition temperature increases and upper shelf energy decreases for the Capsule X material are shown in Table 5-10.

- Capsule X received an average fast neutron calculated fluence (E > 1.0 MeV) of 2.90 x 10^{19} n/cm^2 after 19.85 effective full power years of operation.

- Irradiation of the reactor vessel lower shell forging 123S266VA1 Charpy specimens, oriented with the longitudinal axis of the specimen parallel to the major working direction of the plate (tangential orientation), to 2.90 x 10^{19} n/cm^2 (E> 1.0MeV) resulted in a 30 ft-lb transition temperature increase of 72.44°F and a 50 ft-lb transition temperature increase of 63.4°F. This results in an irradiated 30 ft-lb transition temperature of 9.14°F and an irradiated 50 ft-lb transition temperature of 27.95°F for the longitudinally oriented specimens.

- Irradiation of the weld metal Charpy specimens to 2.90 x 10^{19} n/cm^2 (E> 1.0MeV) resulted in a 30 ft-lb transition temperature increase of 191.06°F. This results in an irradiated 30 ft-lb transition temperature of 190.97°F.

- Irradiation of the weld Heat-Affected-Zone (HAZ) metal Charpy specimens to 2.90 x 10^{19} n/cm^2 (E> 1.0 MeV) resulted in a 30 ft-lb transition temperature increase of 26°F and a 50 ft-lb transition temperature increase of 18.72°F. This results in an irradiated 30 ft-lb transition temperature of –45.77°F and an irradiated 50 ft-lb transition temperature of –30.55°F.

- Irradiation of the Correlation Monitor Material Charpy specimens to 2.90 x 10^{19} n/cm^2 (E> 1.0 MeV) resulted in a 30 ft-lb transition temperature increase of 126.86°F and a 50 ft-lb transition temperature increase of 127.45°F. This results in an irradiated 30 ft-lb transition temperature of 156.96°F and an irradiated 50 ft-lb transition temperature of 202.03°F.

- The average upper shelf energy of the lower shell forging 123S266VA1 (tangential orientation) resulted in no energy decrease after irradiation to 2.90 x 10^{19} n/cm^2 (E> 1.0 MeV). This results in an irradiated average upper shelf energy of 148 ft-lb for the tangentially oriented specimens.

- The average upper shelf energy of the weld metal Charpy specimens resulted an average energy decrease of 19.7 ft-lb after irradiation to 2.90 x 10^{19} n/cm^2 (E> 1.0 MeV). Hence, this results in an irradiated average upper shelf energy of 45 ft-lb for the weld metal specimens.

- The average upper shelf energy of the weld HAZ metal Charpy specimens resulted in an average energy decrease of 19 ft-lb after irradiation to 2.90 x 10^{19} n/cm^2 (E> 1.0MeV). This results in an irradiated average upper shelf energy of 158 ft-lb for the weld HAZ metal.

- The average upper shelf energy of the Correlation Monitor Material Charpy specimens resulted in an average energy decrease of 0.5 ft-lb after irradiation to 2.90 x 10^{19} n/cm^2 (E> 1.0MeV). This results in an irradiated average upper shelf energy of 67 ft-lb for the Correlation Monitor Material.

- The Fracture appearance of each irradiated Charpy specimen from the various materials is shown in Figures 5-13 through 5-16 shows an increasingly ductile or tougher appearance with increasing test temperature.

- The load time records for individual instrumented Charpy specimens tests are shown in Appendix B.

- A comparison of the Turkey Point Unit 3 Reactor Vessel beltline materials test results with the Regulatory Guide 1.99 Revision 2 predictions led to the following conclusions:

  - The measured 30 ft-lb shift in transition temperature values of the lower shell forging contained in Capsule X (Tangential) is greater than Regulatory Guide 1.99 Revision 2 predictions. However, the shift value is less than two sigma allowance by Regulatory Guide 1.99 Revision 2.

  - The measured 30 ft-lb shift in transition temperature values of the weld metal contained in Capsule X is less than the Regulatory Guide 1.99 Revision 2 predictions.

  - The measured percent decrease in upper shelf energy of the Capsule X surveillance materials is less than the Regulatory Guide 1.99 Revision 2 predictions.

- The Charpy V-Notch data presented in this report is based on a re-plot of all capsule data using CVGRAPH, Version 4.1, which is a hyperbolic tangent curve fitting program. Appendix C presents the CVGRAPH, Version 4.1, Charpy V-Notch plots and the program input data.

5.3 TENSILE TEST RESULTS

The results of the tensile tests performed on forging 123S266VA1 (tangential orientation) and weld metal irradiated to 2.90 x 10^{19} n/cm^2 are shown in Table 5-11 and are compared to the unirradiated results as shown in Figures 5-17 and 5-18.

The results of the tensile tests performed on the Lower Shell Forging 123S266VA1 indicated that irradiation to 2.90 x 10^{19} n/cm^2 (E>1.0 MeV) caused an approximate increase of 10 to 15 ksi in the 0.2 percent offset yield strength and approximately 8 to 12 ksi increase in the ultimate tensile strength when compared to the unirradiated data[1] (Figure 5-17).

The results of the tensile tests performed on the Weld material indicated that irradiation to 2.90 x 10^{19} n/cm^2 (E>1.0 MeV) caused an approximate increase of 18 to 20 ksi in the 0.2 percent offset yield strength and approximately 16 to 18 ksi increase in the ultimate tensile strength when compared to the unirradiated data[1] (Figure 5-18).

Fractured tension specimens for each of the materials are shown in Figures 5-19 and 5-20. Typical stress-strain curves for the tension specimens are shown in Figures 5-21 and 5-22.

5.4 COMPACT TENSION TESTS

Per the surveillance capsule testing contract with Florida Power and Light Company, the WOL Fracture Mechanics specimens will not be tested and will be stored at the Hot Cell at the Westinghouse Science and Technology Center.

Table 5-1 Charpy V-notch Impact Data for the Turkey Point Unit 3 Reactor Vessel Lower Shell Forging 123S266 Irradiated to a Fluence of 2.90 x 10^{19} n/cm^2 (E> 1.0 MeV) (Tangential Orientation)

Sample	Temperature		Impact Energy		Lateral Expansion		Shear
Number	F	C	ft-lbs	Joules	mils	mm	%
S62	0	-18	6	8	0	0.00	2
S60	25	-4	46	62	30	0.76	10
S63	50	10	97	132	59	1.50	20
S65	90	32	122	165	67	1.70	35
S66	130	54	144	195	82	2.08	80
S64	150	66	150	203	86	2.18	100
S61	160	71	164	222	80	2.03	100
S59	180	82	173	235	82	2.08	100

Table 5-2 Charpy V-notch Impact Data for the Turkey Point Unit 3 Reactor Vessel Weld Data Irradiated to a Fluence of 2.90 x 10^{19} n/cm^2 (E> 1.0 MeV)

Sample	Temperature		Impact Energy		Lateral Expansion		Shear
Number	F	C	ft-lbs	Joules	mils	mm	%
W13	20	-7	5	7	0	0.00	5
W12	80	27	10	14	4	0.10	15
W10	125	52	10	14	4	0.10	25
W14	150	66	18	24	7	0.18	20
W11	175	79	27	37	18	0.46	35
W16	225	107	36	49	20	0.51	65
W15	250	121	42	57	29	0.74	95
W9	325	163	48	65	33	0.84	100

Table 5-3 Charpy V-notch Impact Data for the Turkey Point Unit 3 Reactor Vessel HAZ Metal Irradiated to a Fluence of 2.90 x 10^{19} n/cm^2 (E> 1.0 MeV)

Sample	Temperature		Impact Energy		Lateral Expansion		Shear
Number	F	C	ft-lbs	Joules	mils	mm	%
H9	-30	-34	22	30	8	0.20	5
H12	-30	-34	130	176	72	1.83	90
H11	-10	-23	12	16	7	0.18	20
H10	20	-7	187	254	86	2.18	100
H14	25	-4	134	182	72	1.83	60
H16	75	24	142	193	79	2.01	70
H15	100	38	148	201	87	2.21	100
H13	130	54	167	226	86	2.18	100

Table 5-4 Charpy V-notch Impact Data for the Turkey Point Unit 3 ASTM Correlation Monitor Material Irradiated to a Fluence of 2.90 x 10^{19} n/cm^2 (E> 1.0 MeV)

Sample	Temperature		Impact Energy		Lateral Expansion		Shear
Number	F	C	ft-lbs	Joules	mils	mm	%
R51	60	16	8	11	1	0.03	5
R50	100	38	14	19	9	0.23	25
R49	150	66	27	37	18	0.46	30
R55	200	93	38	52	28	0.71	60
R54	225	107	67	91	44	1.12	90
R56	250	121	65	88	47	1.19	100
R52	275	135	68	92	45	1.14	100
R53	325	163	69	94	55	1.40	100

Table 5-5 Instrumented Charpy Impact Test Results for the Turkey Point Unit 3 Lower Shell Forging 123S266VA1 Reactor Vessel Irradiated to a Fluence of 2.90 x 10^{19} n/cm^2 (E> 1.0 MeV) (Tangential Orientation)

Sample Number	Test Temp (°F)	Charpy Energy (ft-lb)	Normalized Energies (ft-lb/in^2)			Yield Load (kips)	Time to Yield (µsec)	Maximum Load (kips)	Time to Maximum (µsec)	Fracture Load (kips)	Arrest Load (kips)	Yield Stress (ksi)	Flow Stress (ksi)
			Charpy Ed/A	Maximum Em/A	Prop Ep/A								
S62	0	6	48	25	23	9.72	0.1681	2592.4	0.1598	2589.97	0	0	43
S60	25	46	371	327	44	3485.11	0.1549	4533.08	0.6856	4508.7	0	116	134
S63	50	97	782	320	462	3212.39	0.1427	4386.76	0.6942	3572.04	0	107	127
S65	90	122	983	307	676	3122.08	0.144	4272.83	0.6881	3102.66	405.43	104	123
S66	130	144	1160	298	862	2992.8	0.1464	4208.94	0.6844	1740.12	675.09	100	120
S64	150	150	1209	311	898	3080.7	0.144	4369.39	0.6881	n/a	n/a	103	124
S61	160	164	1321	292	1029	2838.65	0.1427	4122.97	0.6905	n/a	n/a	95	116
S59	180	173	1394	290	1104	2794.61	0.1415	4070.62	0.6942	n/a	n/a	93	114

Table 5-6 Instrumented Charpy Impact Test Results for the Turkey Point Unit 3 Reactor Vessel Weld Metal Irradiated to a Fluence of 2.90 x 10^{19} n/cm^2 (E> 1.0 MeV)

Sample Number	Test Temp (°F)	Charpy Energy (ft-lb)	Normalized Energies (ft-lb/in^2)			Yield Load (kips)	Time to Yield (μsec)	Maximum Load (kips)	Time to Maximum (μsec)	Fracture Load (kips)	Arrest Load (kips)	Yield Stress (ksi)	Flow Stress (ksi)
			Charpy Ed/A	Maximum Em/A	Prop Ep/A								
W13	20	5	40	17	24	2150.21	0.1171	2172.08	0.1232	2172.08	0	72	72
W12	80	10	81	44	37	3833.72	0.1537	4063.26	0.1732	4053.49	0	128	131
W10	125	10	81	44	37	3662.22	0.1476	4061.3	0.1757	4061.3	0	122	129
W14	150	18	145	75	70	3553.97	0.144	4596.24	0.2269	4523.01	0	118	136
W11	175	27	218	91	127	4031.42	0.1915	4636.86	0.2696	4605.25	325.82	134	144
W16	225	36	290	182	108	3545.57	0.1598	4567.26	0.4209	4484.75	1050.81	118	135
W15	250	42	338	163	176	3504.34	0.144	4542.94	0.3758	4051.75	1263.42	117	134
W9	325	48	387	173	214	3360.16	0.1464	4417.05	0.405	n/a	n/a	112	129

Table 5-7 Instrumented Charpy Impact Test Results for the Turkey Point Unit 3 Reactor Vessel HAZ Metal Irradiated to a Fluence of 2.90 x 10^{19} n/cm^2 (E> 1.0 MeV)

Sample Number	Test Temp (°F)	Charpy Energy (ft-lb)	Normalized Energies (ft-lb/in^2)			Yield Load (kips)	Time to Yield (µsec)	Maximum Load (kips)	Time to Maximum (µsec)	Fracture Load (kips)	Arrest Load (kips)	Yield Stress (ksi)	Flow Stress (ksi)
			Charpy Ed/A	Maximum Em/A	Prop Ep/A								
H9	-30	22	177	79	98	3996.64	0.1562	4789.94	0.2306	4668.56	0	133	146
H12	-30	130	1047	381	666	3977.92	0.1549	5174.22	0.7027	3238.75	911.81	132	152
H11	-10	12	97	40	56	6873.73	0.1537	3939.64	0.1659	3932.31	261.18	129	130
H10	20	187	1507	382	1125	3907.16	0.1513	5156.97	0.71	n/a	n/a	130	151
H14	25	134	1080	364	716	3766.83	0.1525	5010.25	0.5942	3015.91	87.77	125	146
H16	75	142	1144	443	701	3602.79	0.1525	4881.83	0.8528	2628.86	656.61	120	141
H15	100	148	1192	350	842	3536.88	0.1537	4881.83	0.6966	n/a	n/a	118	140
H13	130	167	1346	351	994	3595.14	0.1525	4867.3	0.6978	n/a	n/a	120	141

Table 5-8 Instrumented Charpy Impact Test Results for Turkey Point Unit 3 ASTM Correlation Monitor Material Irradiated to a Fluence of 2.90 x 10^{19} n/cm^2 (E> 1.0 MeV)

Sample Number	Test Temp (°F)	Charpy Energy (ft-lb)	Normalized Energies (ft-lb/in^2)			Yield Load (kips)	Time to Yield (µsec)	Maximum Load (kips)	Time to Maximum (µsec)	Fracture Load (kips)	Arrest Load (kips)	Yield Stress (ksi)	Flow Stress (ksi)
			Charpy Ed/A	Maximum Em/A	Prop Ep/A								
R51	60	8	64	32	33	3311.69	0.144	3353.03	0.1513	3353.03	0	110	111
R50	100	14	113	46	67	3555.47	0.1525	3954.85	0.1842	3903.71	440.78	118	125
R49	150	27	218	116	101	3234.15	0.1427	4221.95	0.3123	4221.95	543.9	108	124
R55	200	38	306	151	155	3101.39	0.1525	4202.43	0.3916	4139.24	1489.93	103	122
R54	225	67	540	224	316	3137.86	0.1464	4417.77	0.5148	4085.04	2280.53	104	126
R56	250	65	524	195	328	3106.28	0.1476	4257.48	0.4734	n/a	n/a	103	123
R52	275	68	548	206	342	3237.98	0.1537	4569.82	0.4746	n/a	n/a	108	130
R53	325	69	556	193	363	3130.56	0.1574	4270.49	0.4734	n/a	n/a	104	123

Table 5-9 The Effect of 550°F Irradiation at 2.90 x 10^{19} n/cm^2 (E>1.0 MeV) on the Notch Toughness Properties of the Turkey Point Unit 3 Reactor Vessel Surveillance Capsule Materials

Material	Average 30 (ft-lb) Transition Temperature (°F)			Average 35 mil Lateral Expansion Temperature (°F)			Average 50 ft-lb Transition Temperature (°F)			Average Energy Absorption at Full Shear (ft-lb)		
	Unirradiated	Irradiated	ΔT	Unirradiated	Irradiated	ΔT	Unirradiated	Irradiated	ΔT	Unirradiated	Irradiated	ΔT
Lower Forging 123S266VA1	-63.3	9.14	72.44	-58.25	31.57	89.82	-35.44	27.95	63.4	148	162	14
Weld Metal	- 08	190.97	191.06	26 28	n/a	n/a	59.7	n/a	n/a	64.7	45	-19.7
HAZ Metal	-71.77	-45.77	26	-49.78	-20.61	29.17	-49 28	-30.55	18.72	177	158	-19
Correlation Material	30.1	156.96	126.86	48.11	224.5	176 38	74.58	202.03	127.45	67.5	67	-0.5

Table 5-10 Comparison of the Turkey Point Unit 3 Reactor Vessel Surveillance Capsule Charpy Impact Test Results with Regulatory Guide 1.99 Revision 2 Predictions

Material	Capsule	Fluence ($x 10^{19}$ n/cm^2)	30 ft-lb Transition Temperature Shift		Upper Shelf Energy Decrease	
			Predicted (°F)	Measured (°F)	Predicted (%)	Measured (%)
Intermediate Shell Forging Heat # 123P461VA1	T	0.739	33.85	11.48	17	0
	S	1.72	42.55	2.83	20	12
Lower Shell Forging Heat # 123S266VA1	S	1.72	58.65	48.55	20	18
	V	1.53	57.12	42.68	20	0
	X	2.90	65.43	72.44	24	0
Weld Metal	T	0.739	153.31	163.87	34	10
	V	1.53	187.66	180.77	39	26
	X	2.90	214.97	191.06	48	30
HAZ Metal	T	0.739	--	14.72	--	6
	V	1.53	--	-2.13	--	8
	X	2.90	--	26	--	11
Correlation Material	S	1.72	--	106.6	--	11
	T	0.739	--	86.66	--	0
	V	1.53	--	100.32	--	3
	X	2.90	--	126.86	--	1

Table 5-11 Tensile Properties for Turkey Point Unit 3 Reactor Vessel Material Irradiated to a fluence of 2.90 x 10^{19} n/cm^2 (E > 1.0 MeV)

Material	Sample Number	Test Temp. (°F)	0.2% Yield Strength (ksi)	Ultimate Strength (ksi)	Fracture Load (kip)	Fracture Stress (ksi)	Fracture Strength (ksi)	Uniform Elongation (%)	Total Elongation (%)	Reduction in Area (%)
Plate	S13	200	61.6	82.5	2.56	178.9	52.1	9.8	22.4	71
Plate	S14	550	63.2	88.3	3.15	152.8	64.2	10.2	19.9	58
Weld	W3	300	92.2	104.9	4.00	177.1	81.5	10.1	19.4	54
Weld	W4	550	87.1	104.2	4.00	172.8	81.5	9.3	18.3	53

LOWER SHELL FORGING 123S266VA-1 (TANG)

CVGRAPH 4 1 Hyperbolic Tangent Curve Printed at 113436 on 06-17-2002

Results

Curve	Fluence	USE	d-USE	USE	d-USE	T @ 30	d-T @ 30	T @ 50	d-T @ 50
1	0	2.19	0	148	0	-63.3	0	-35.44	0
2	0	2.19	0	122	-26	-14.74	48.55	4.2	39.65
3	0	2.19	0	166.5	18.5	-20.62	42.68	3.39	38.84
4	0	2.19	0	162	14	9.14	72.44	27.95	63.4

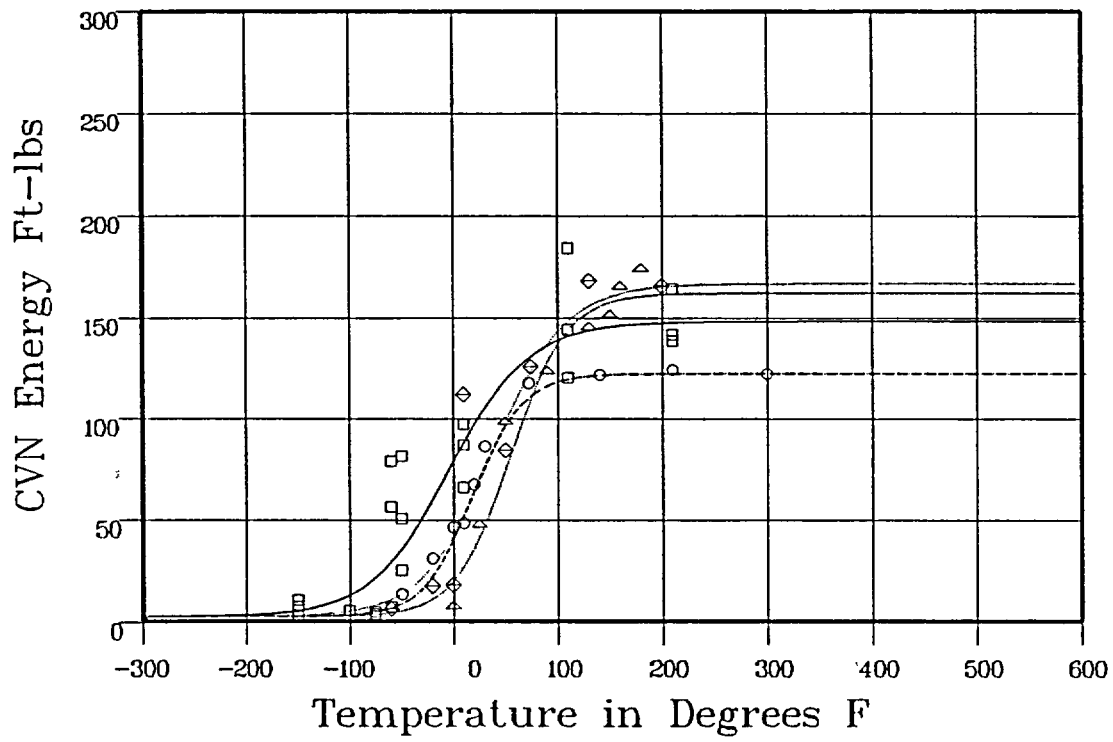

Curve Legend

1 ——— 2 ---------- 3 ——— 4 ———

Data Set(s) Plotted

Curve	Plant	Capsule	Material	Orl	Heat#
1	TP3	UNIRR	FORGING SA508 2	LT	123S266VA-1
2	TP3	S	FORGING SA508 2	LT	123S266VA-1
3	TP3	V	FORGING SA508 2	LT	123S266VA-1
4	TP3	X	FORGING SA508 2	LT	123S266VA-1

Figure 5-1 Charpy V-Notch Impact Energy vs. Temperature for Turkey Point Unit 3 Reactor Vessel Lower Forging 123S266VA1 (Tangential Orientation)

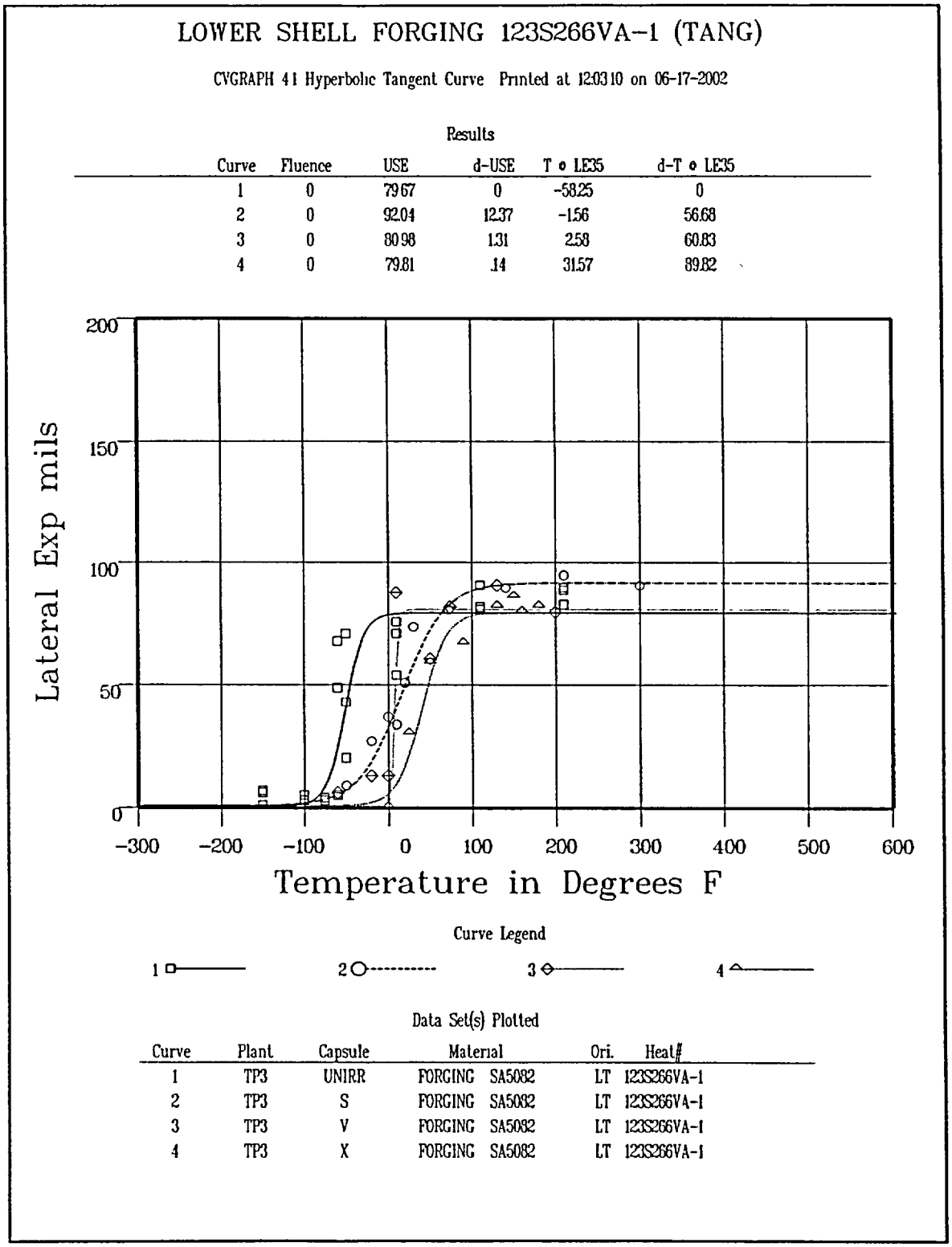

Figure 5-2 Charpy V-Notch Lateral Expansion vs. Temperature for Turkey Point Unit 3 Reactor Vessel Lower Forging 123S266VA1 (Tangential Orientation)

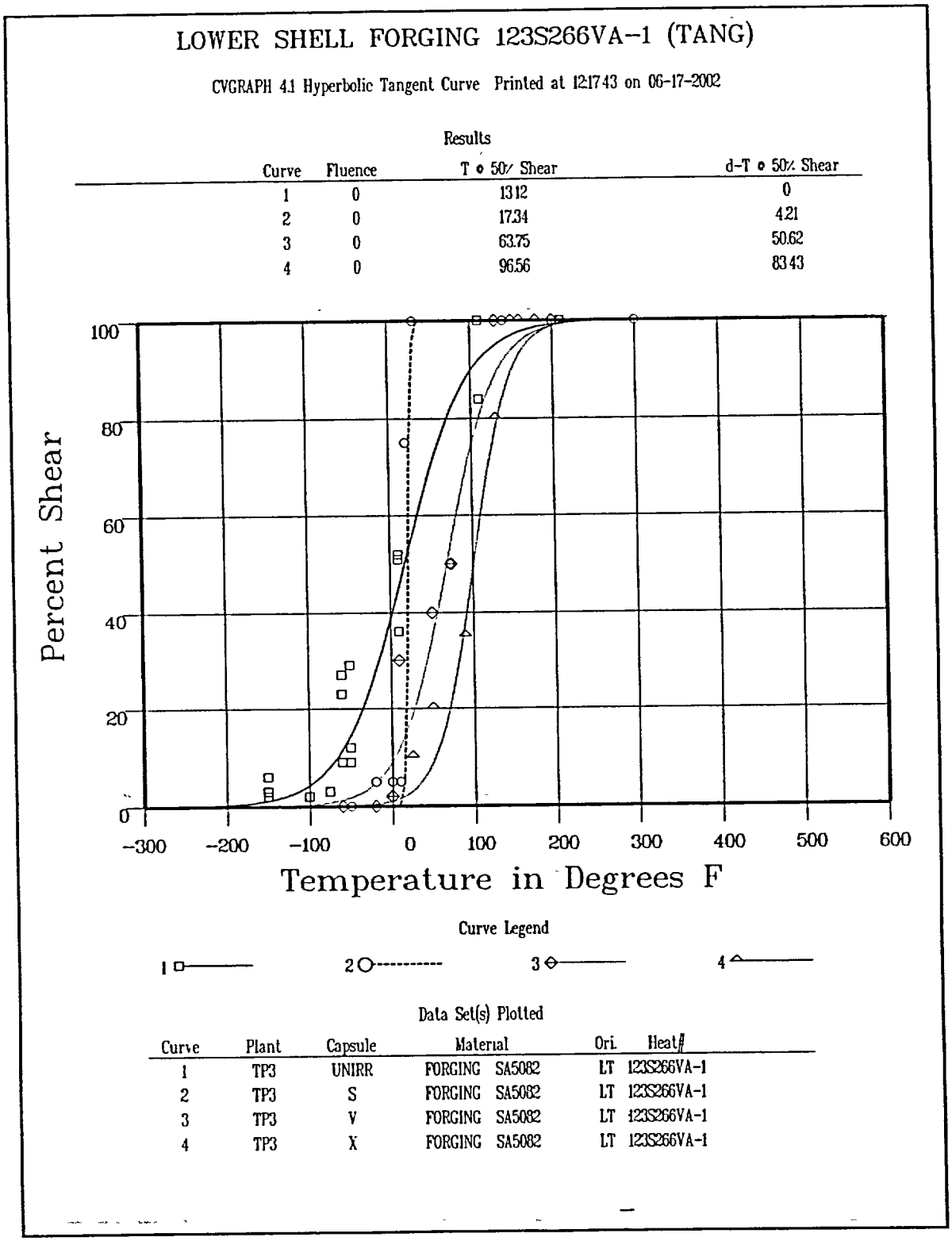

Figure 5-3 Charpy V-Notch Percent Shear vs. Temperature for Turkey Point Unit 3 Reactor Vessel Lower Forging 123S266VA1 (Tangential Orientation)

SURVEILLANCE PROGRAM WELD METAL

CVGRAPH 4 1 Hyperbolic Tangent Curve Printed at 11:23:09 on 06-19-2002

Results

Curve	Fluence	LSE	d-LSE	USE	d-USE	T o 30	d-T o 30	T o 50	d-T o 50
1	0	2.19	0	64.69	0	-.08	0	59.7	0
2	0	2.2	0	58.5	-6.19	163.78	163.87	244.99	185.28
3	0	2.2	0	47.79	-16.89	180.68	180.77		
4	0	2.2	0	45	-19.69	190.97	191.06		
5	0	2.2	0	42	-22.69	216.18	216.27		

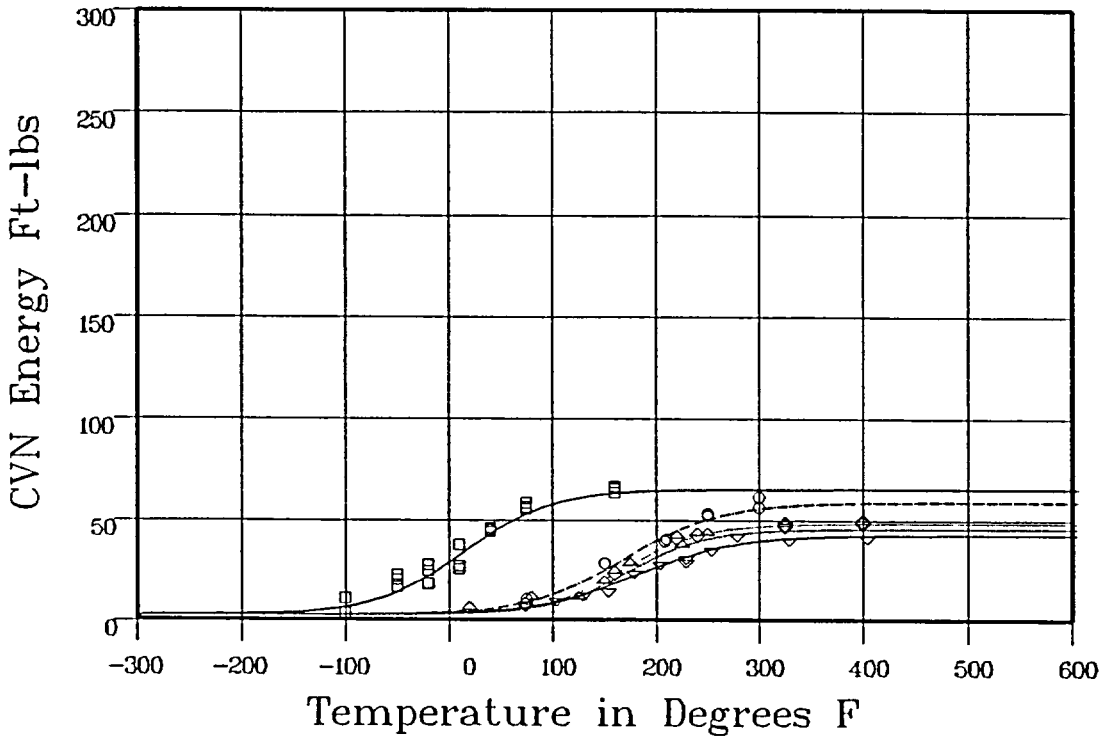

Curve Legend

1 ——— 2 ---------- 3 ——— 4 ——— 5 ———

Data Set(s) Plotted

Curve	Plant	Capsule	Material	Ori.	Heat#
1	TP3	UNIRR	WELD LINDE 80		71249
2	TP3	T	WELD LINDE 80		71249
3	TP3	V	WELD LINDE 80		71249
4	TP3	X	WELD LINDE 80		71249
5	TP3	A5	WELD LINDE 80	71249	FLUX LOT 8445

Figure 5-4 Charpy V-Notch Impact Energy vs. Temperature for Turkey Point Unit 3 Reactor Vessel Weld Metal

SURVEILLANCE PROGRAM WELD METAL

CVGRAPH 4.1 Hyperbolic Tangent Curve Printed at 10:35:19 on 06-25-2002

Results

Curve	Fluence	USE	d-USE	T @ LE35	d-T @ LE35
1	0	75.26	0	26.28	0
2	0	57.27	-17.98	243.44	217.15
3	0	45	-30.26	225.83	199.54
4	0	34.13	-41.12		
5	0	45.61	-29.64	262.89	236.6

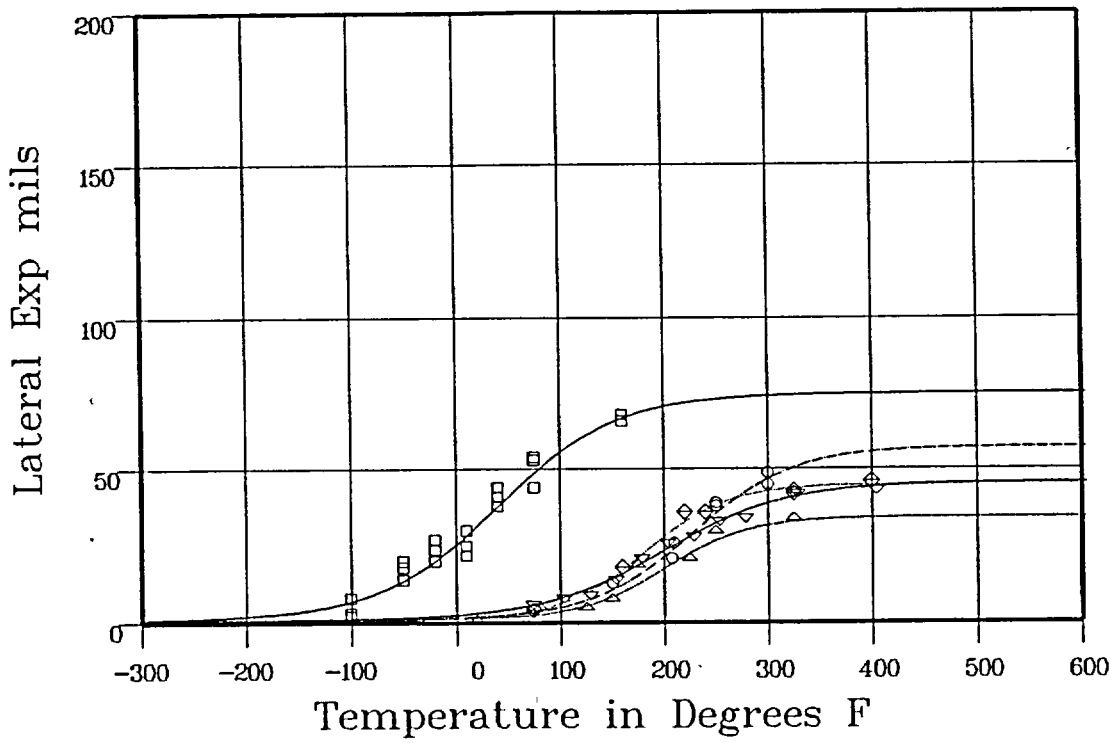

Curve Legend

1 □——— 2 ○---------- 3 ◇——— 4 △——— 5 ▽———

Data Set(s) Plotted

Curve	Plant	Capsule	Material	Ori.	Heat#
1	TP3	UNIRR	WELD LINDE 80		71249
2	TP3	T	WELD LINDE 80		71249
3	TP3	V	WELD LINDE 80		71249
4	TP3	X	WELD LINDE 80		71249
5	TP3	A5	WELD LINDE 80	71249 FLUX LOT 8445	

Figure 5-5 Charpy V-Notch Lateral Expansion vs. Temperature for Turkey Point Unit 3 Reactor Vessel Weld Metal

SURVEILLANCE PROGRAM WELD METAL

CVGRAPH 4.1 Hyperbolic Tangent Curve Printed at 10:43:00 on 06-25-2002

Results

Curve	Fluence	T @ 50% Shear	d-T @ 50% Shear
1	0	29.06	0
2	0	217.03	187.96
3	0	218.43	189.37
4	0	190.31	161.25
5	0	160.83	131.77

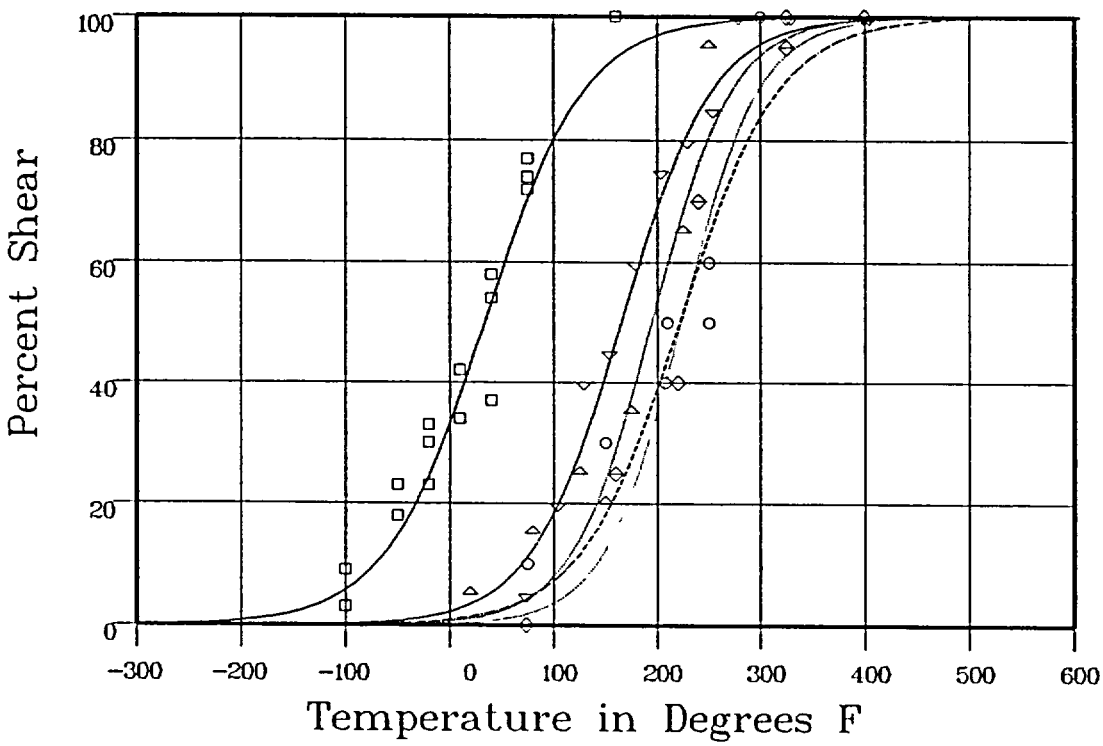

Curve Legend

1 2 3 4 5

Data Set(s) Plotted

Curve	Plant	Capsule	Material	Ori.	Heat#
1	TP3	UNIRR	WELD LINDE 80		71249
2	TP3	T	WELD LINDE 80		71249
3	TP3	V	WELD LINDE 80		71249
4	TP3	X	WELD LINDE 80		71249
5	TP3	A5	WELD LINDE 80	71249 FLUX LOT 8445	

Figure 5-6 Charpy V-Notch Percent Shear vs. Temperature for Turkey Point Unit 3 Reactor Vessel Weld Metal

HEAT AFFECTED ZONE

CVGRAPH 4.1 Hyperbolic Tangent Curve Printed at 09:13:55 on 06-18-2002

Results

Curve	Fluence	LSE	d-LSE	USE	d-USE	T o 30	d-T o 30	T o 50	d-T o 50
1	0	2.19	0	177	0	-71.77	0	-49.28	0
2	0	2.19	0	167	-10	-57.05	14.72	-55.67	-6.39
3	0	2.19	0	163	-14	-73.91	-2.13	-47.59	1.69
4	0	2.19	0	158	-19	-45.77	26	-30.55	18.72

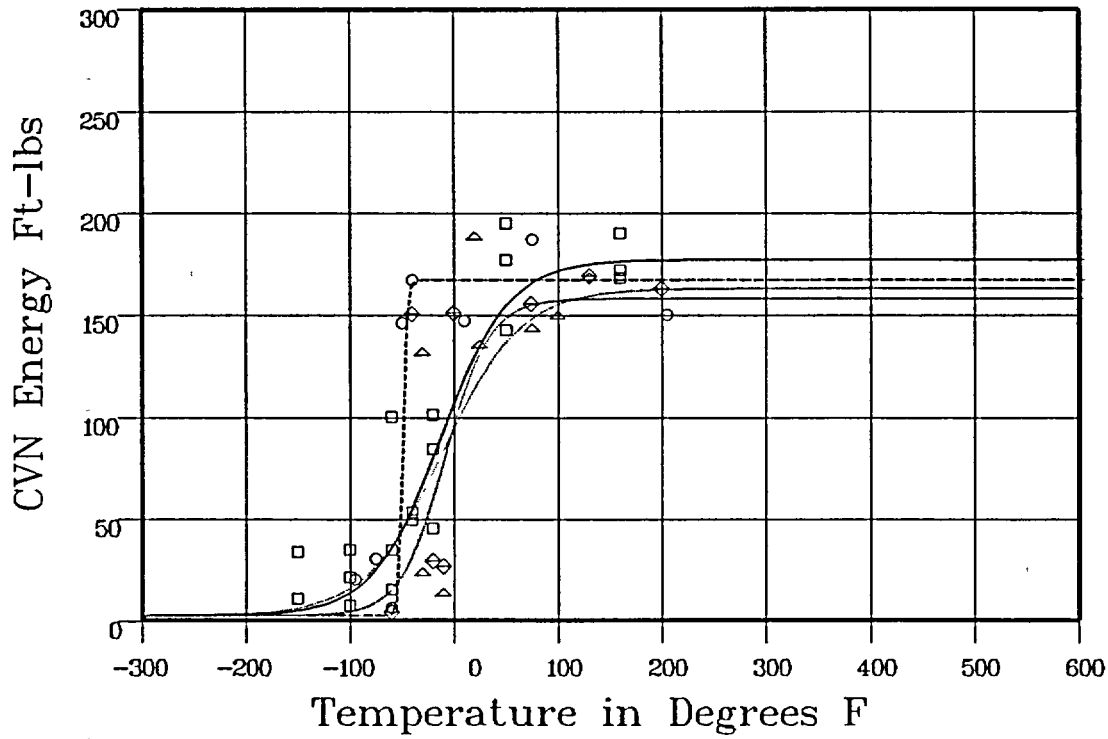

Curve Legend

1 □——— 2 ○---------- 3 ◇——— 4 △———

Data Set(s) Plotted

Curve	Plant	Capsule	Material	Ori	Heat#
1	TP3	UNIRR	HEAT AFFD ZONE		
2	TP3	T	HEAT AFFD ZONE		
3	TP3	V	HEAT AFFD ZONE		
4	TP3	X	HEAT AFFD ZONE		

Figure 5-7 Charpy V-Notch Impact Energy vs. Temperature for Turkey Point Unit 3 Reactor Vessel Weld Heat-Affected-Zone Metal

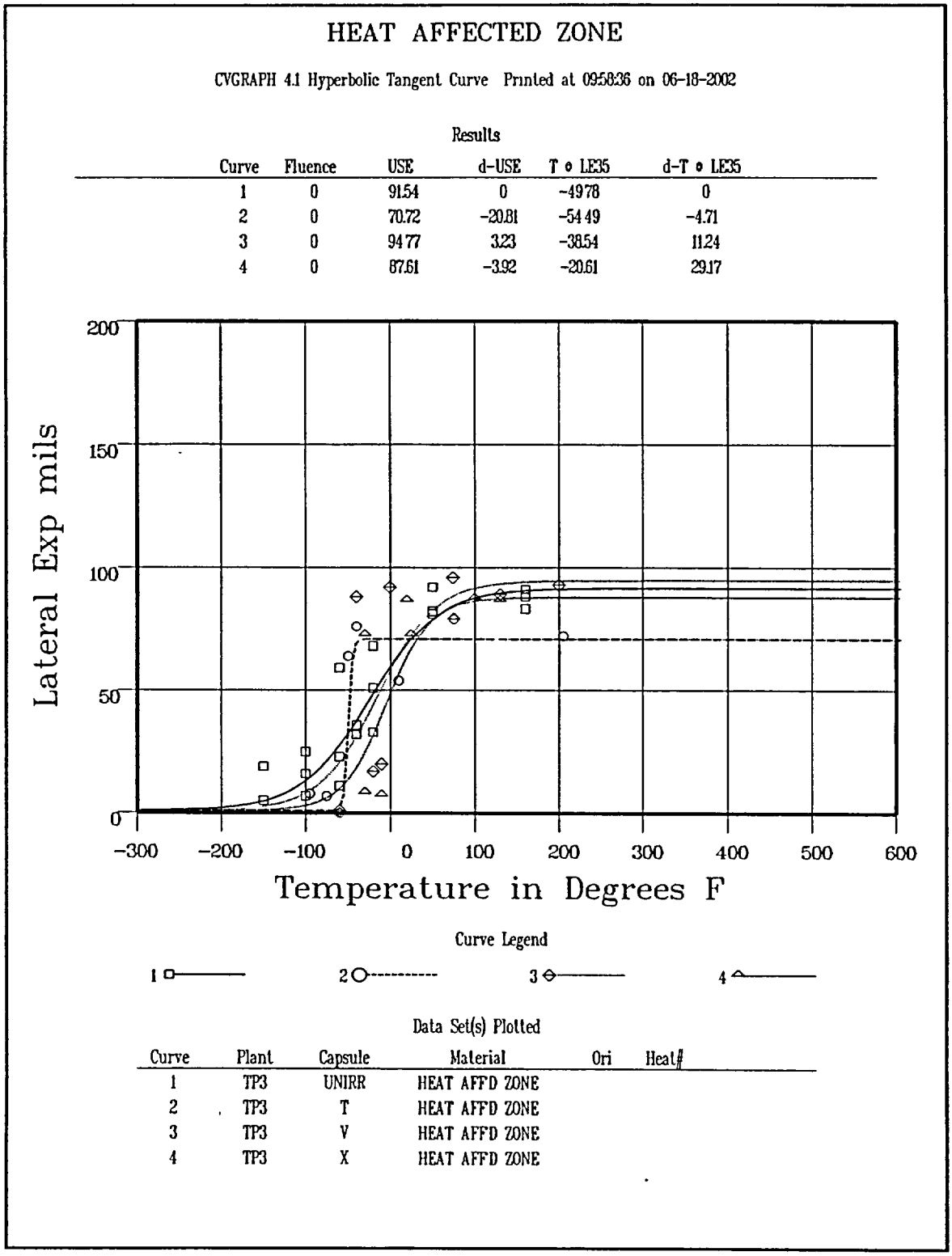

Figure 5-8 Charpy V-Notch Lateral Expansion vs. Temperature for Turkey Point Unit 3 Reactor Vessel Weld Heat-Affected-Zone Metal

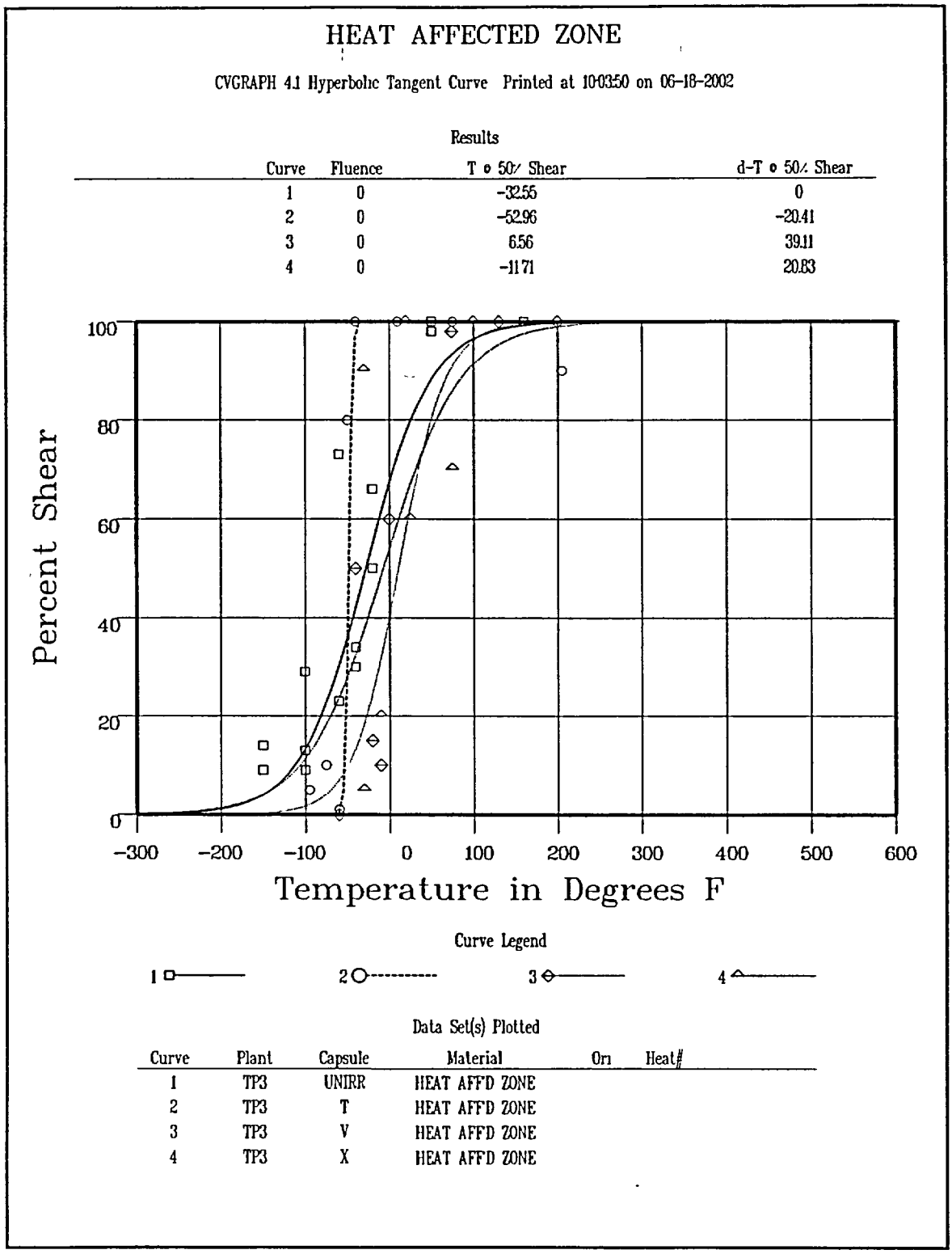

Figure 5-9 Charpy V-Notch Percent Shear vs. Temperature for Turkey Point Unit 3 Reactor Vessel Weld Heat-Affected-Zone Metal

STANDARD REFERENCE MATERIAL

CVGRAPH 41 Hyperbolic Tangent Curve Printed at 10:23:35 on 06-18-2002

Results

Curve	Fluence	LSE	d-LSE	USE	d-USE	T o 30	d-T o 30	T o 50	d-T o 50
1	0	2.19	0	67.5	0	30.1	0	74.58	0
2	0	2.2	0	60	-7.5	136.7	106.6	233.76	159.17
3	0	2.19	0	72	4.5	116.76	86.66	184.59	110.01
4	0	2.19	0	65.59	-1.9	130.42	100.32	191.64	117.06
5	0	2.19	0	67	-5	156.96	126.86	202.03	127.45

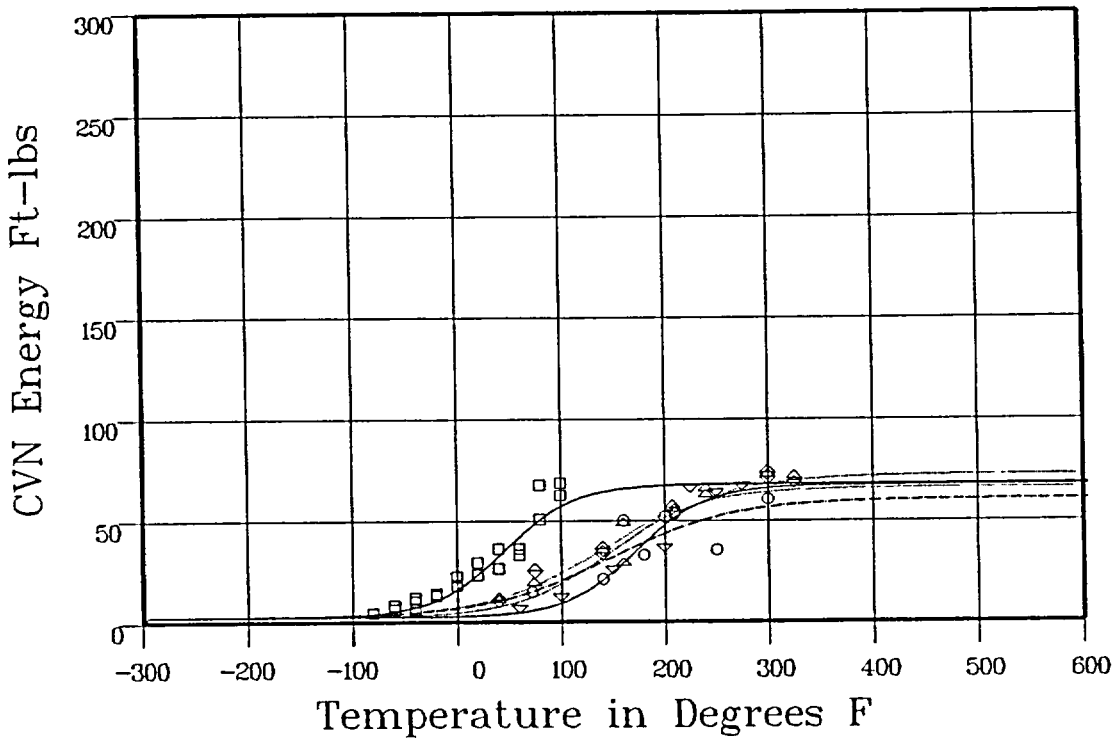

Curve Legend

1 □——— 2 ○---------- 3 ◇——— 4 △——— 5 ▽———

Data Set(s) Plotted

Curve	Plant	Capsule	Material	Ori	Heat#
1	TP3	UNIRR	SRM SA302B		
2	TP3	S	SRM SA302B		
3	TP3	T	SRM SA302B		
4	TP3	V	SRM SA302B		
5	TP3	X	SRM SA302B		

Figure 5-10 Charpy V-Notch Impact Energy vs. Temperature for Turkey Point Unit 3 ASTM Correlation Monitor Material

STANDARD REFERENCE MATERIAL

CVGRAPH 4.1 Hyperbolic Tangent Curve Printed at 10:36:08 on 06-18-2002

Results

Curve	Fluence	USE	d-USE	T @ LE35	d-T @ LE35
1	0	117.73	0	48.11	0
2	0	47.48	-70.25	168.11	120
3	0	57.49	-60.24	179.59	131.47
4	0	63.57	-54.16	163.3	115.19
5	0	182.37	64.63	224.5	176.38

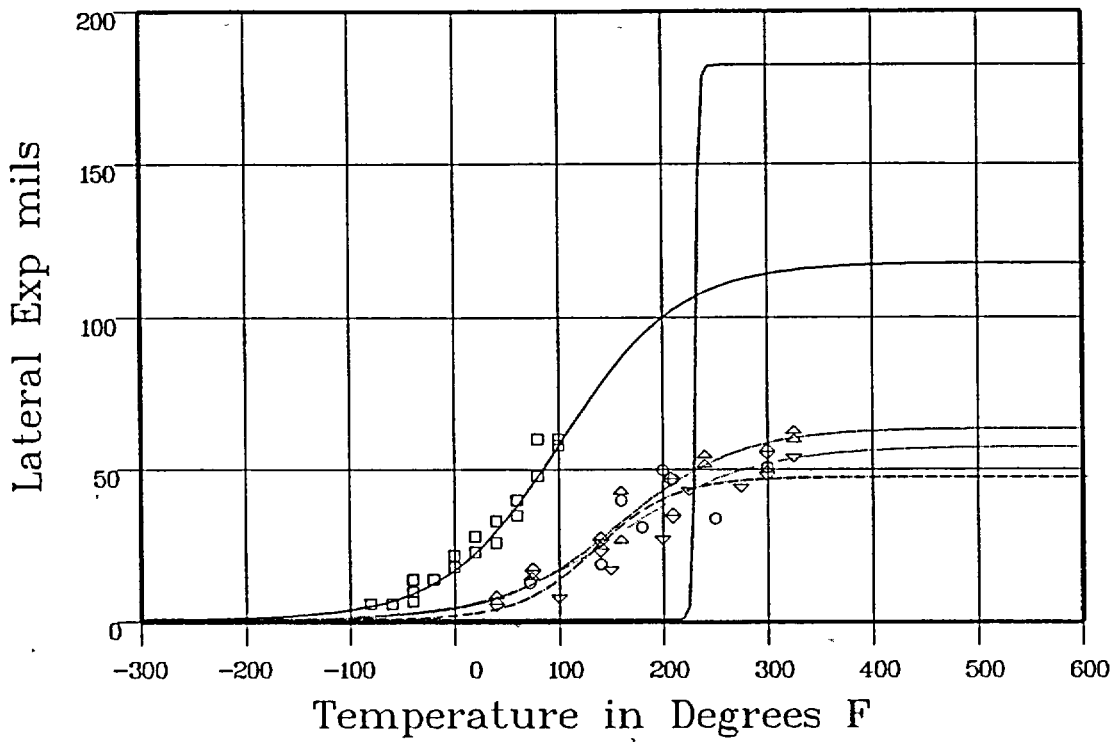

Curve Legend

1 □——— 2 ○---------- 3 ◇——— 4 △——— 5 ▽———

Data Set(s) Plotted

Curve	Plant	Capsule	Material	Ori.	Heat#
1	TP3	UNIRR	SRM SA302B		
2	TP3	S	SRM SA302B		
3	TP3	T	SRM SA302B		
4	TP3	V	SRM SA302B		
5	TP3	X	SRM SA302B		

Figure 5-11 Charpy V-Notch Lateral Expansion vs. Temperature for Turkey Point Unit 3 ASTM Correlation Monitor Material

STANDARD REFERENCE MATERIAL

CVGRAPH 4.1 Hyperbolic Tangent Curve Printed at 10:49:13 on 06-18-2002

Results

Curve	Fluence	T @ 50% Shear	d-T @ 50% Shear
1	0	43.12	0
2	0	171.38	128.26
3	0	178.12	135
4	0	163.47	120.35
5	0	170.5	127.38

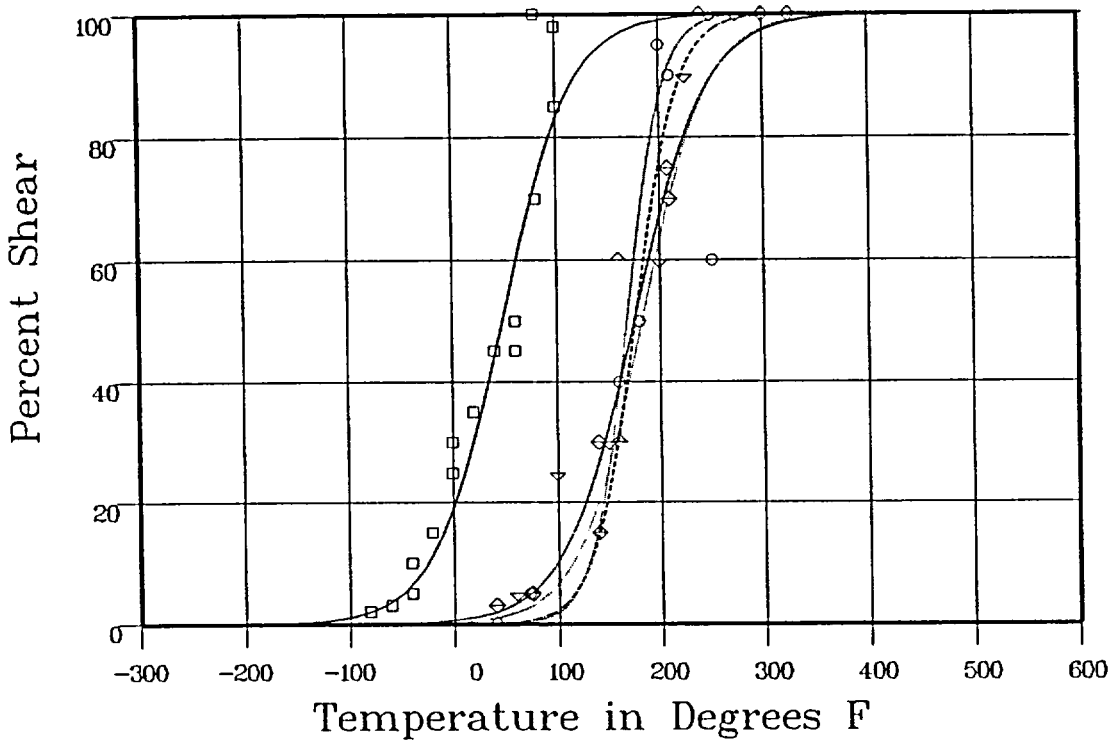

Curve Legend

1 2 3 4 5

Data Set(s) Plotted

Curve	Plant	Capsule	Material	Ori	Heat#
1	TP3	UNIRR	SRM SA302B		
2	TP3	S	SRM SA302B		
3	TP3	T	SRM SA302B		
4	TP3	V	SRM SA302B		
5	TP3	X	SRM SA302B		

Figure 5-12 Charpy V-Notch Percent Shear vs. Temperature for Turkey Point Unit 3 ASTM Correlation Monitor Material

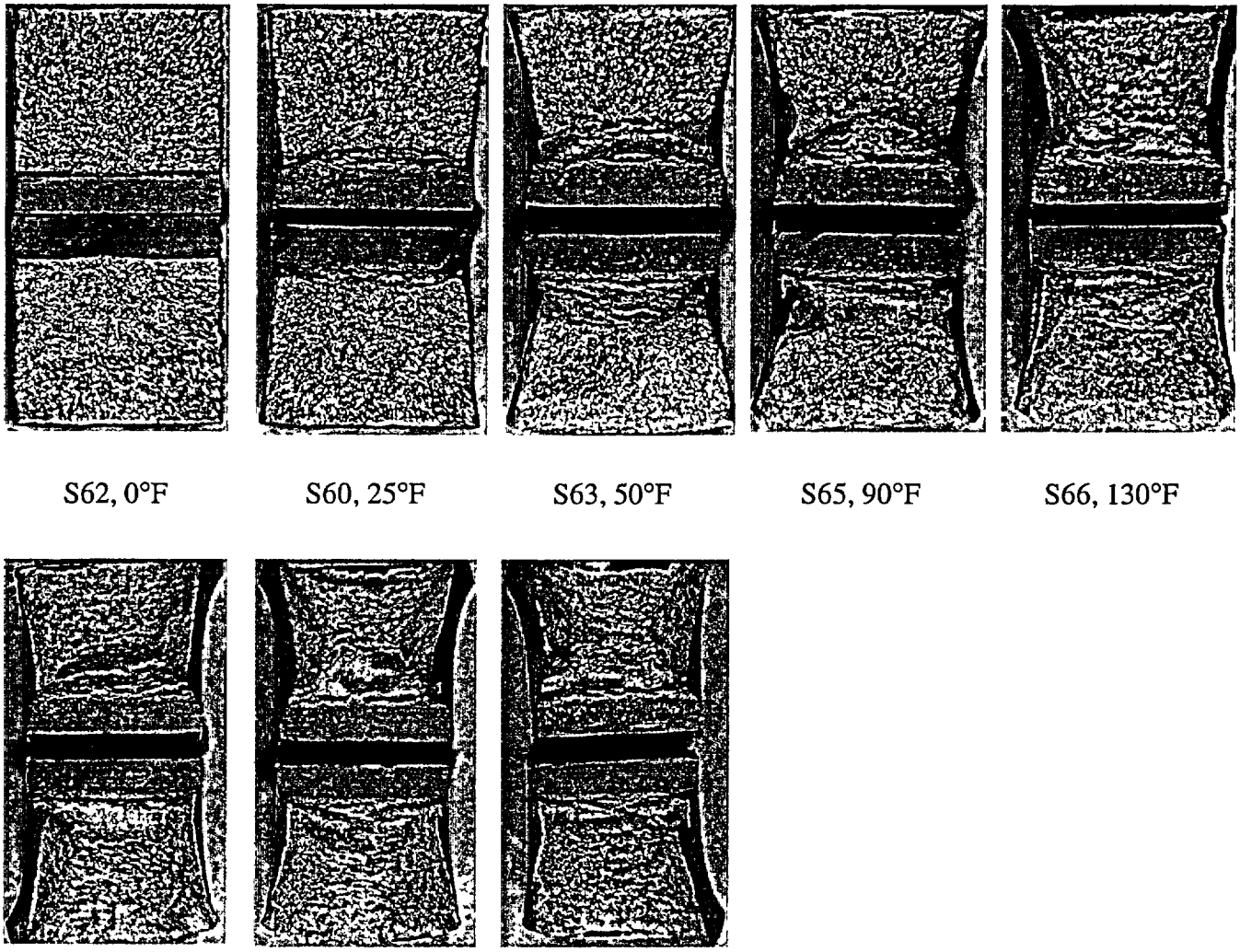

Figure 5-13 Charpy Impact Specimen Fracture Surfaces for Turkey Point Unit 3 Reactor Vessel Forging 123S266VA1 (Tangential Orientation)

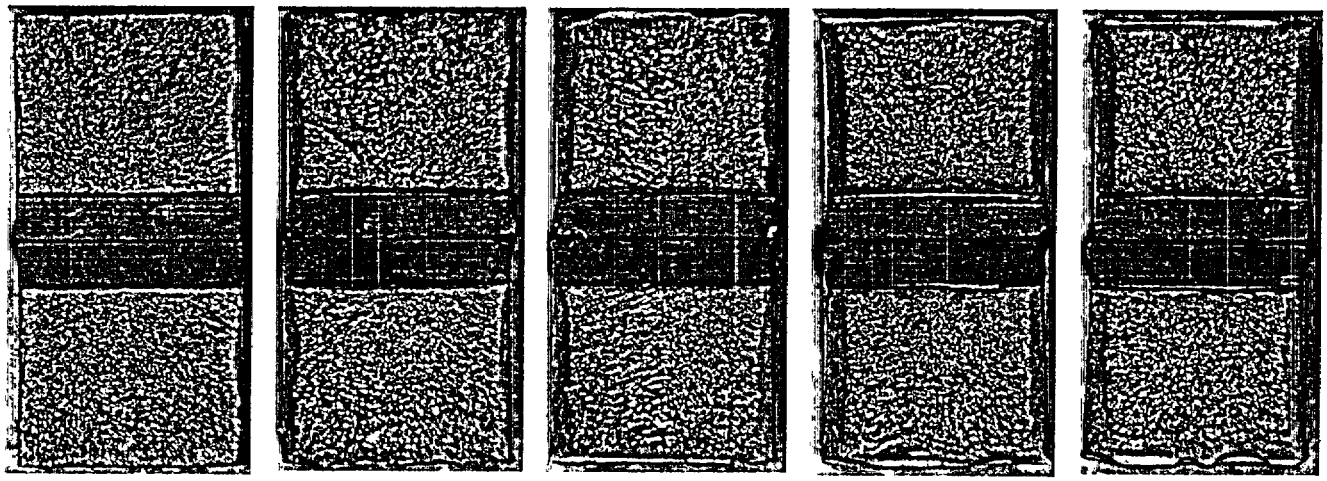

W13, 20°F W12, 80°F W10, 125°F W14, 150°F W11, 175°F

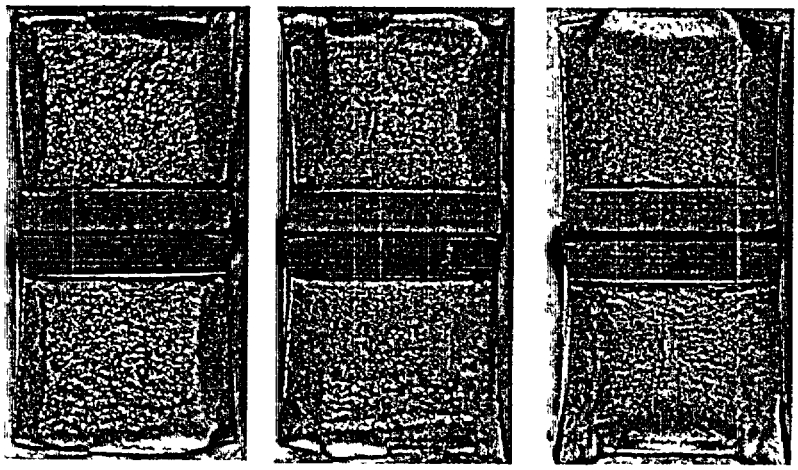

W16, 225°F W15, 250°F W9, 325°F

Figure 5-14 Charpy Impact Specimen Fracture Surfaces for Turkey Point Unit 3 Reactor Vessel Weld Metal

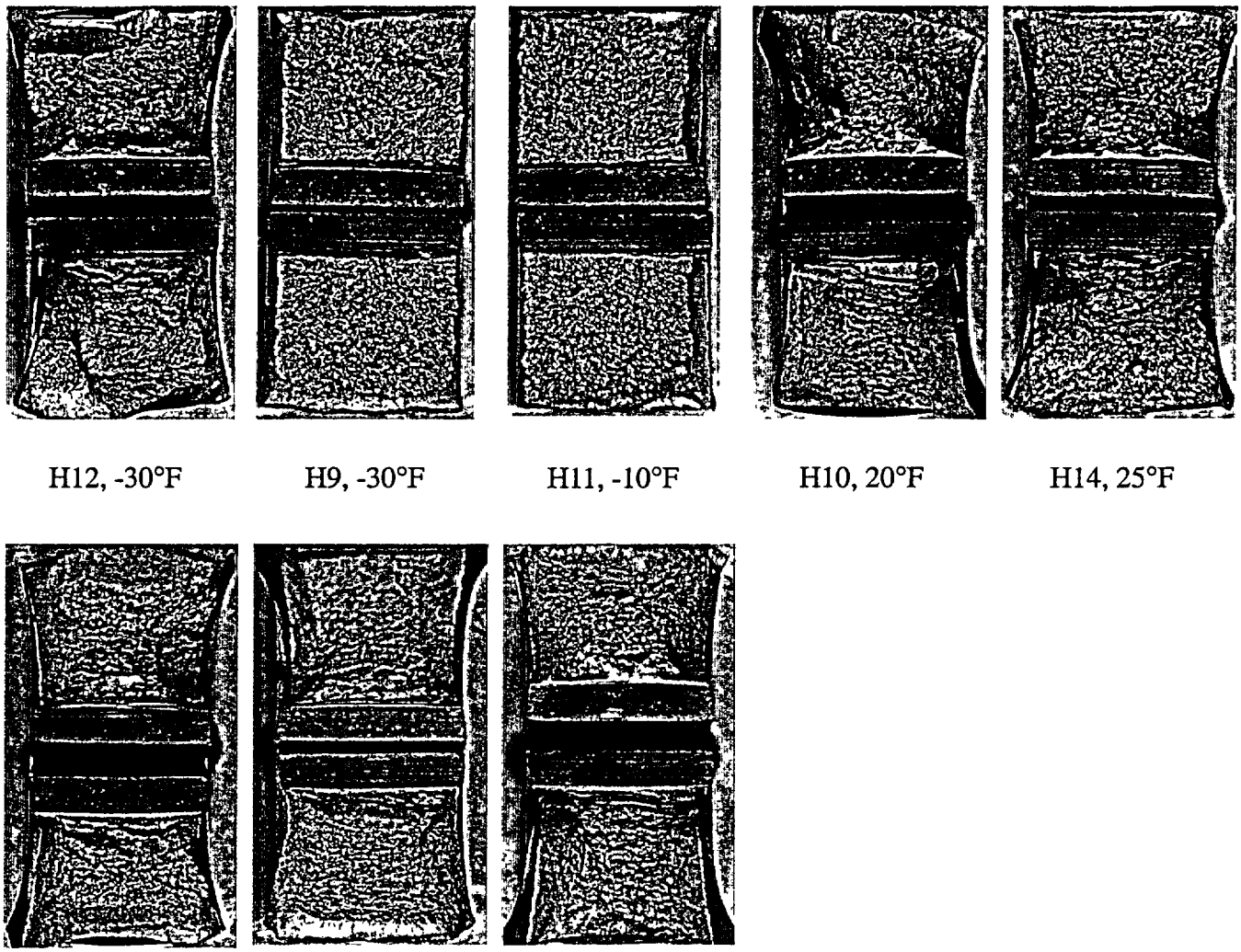

Figure 5-15 Charpy Impact Specimen Fracture Surfaces for Turkey Point Unit 3 Reactor Vessel Weld HAZ Metal

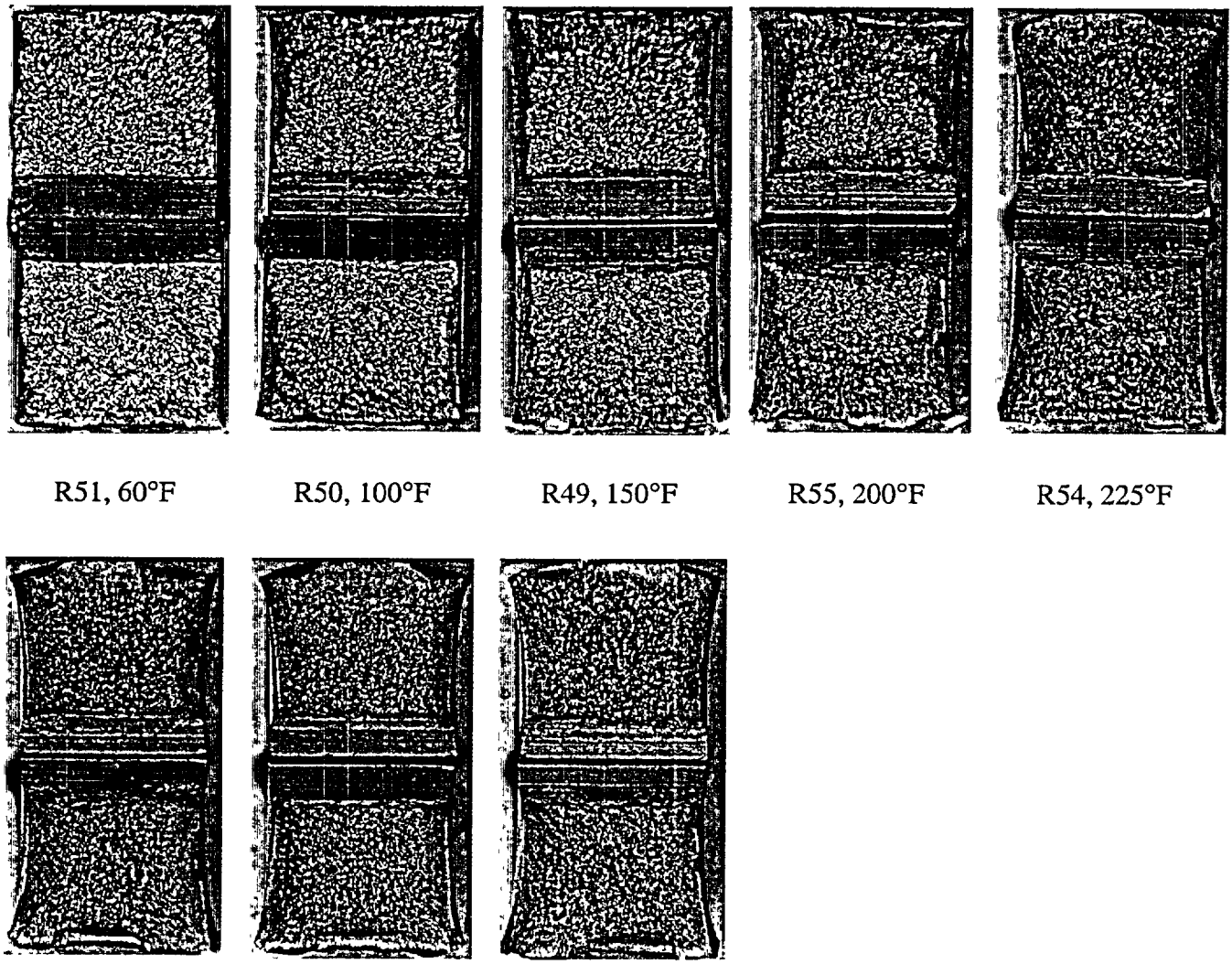

Figure 5-16 Charpy Impact Specimen Fracture Surfaces for ASTM Correlation Material

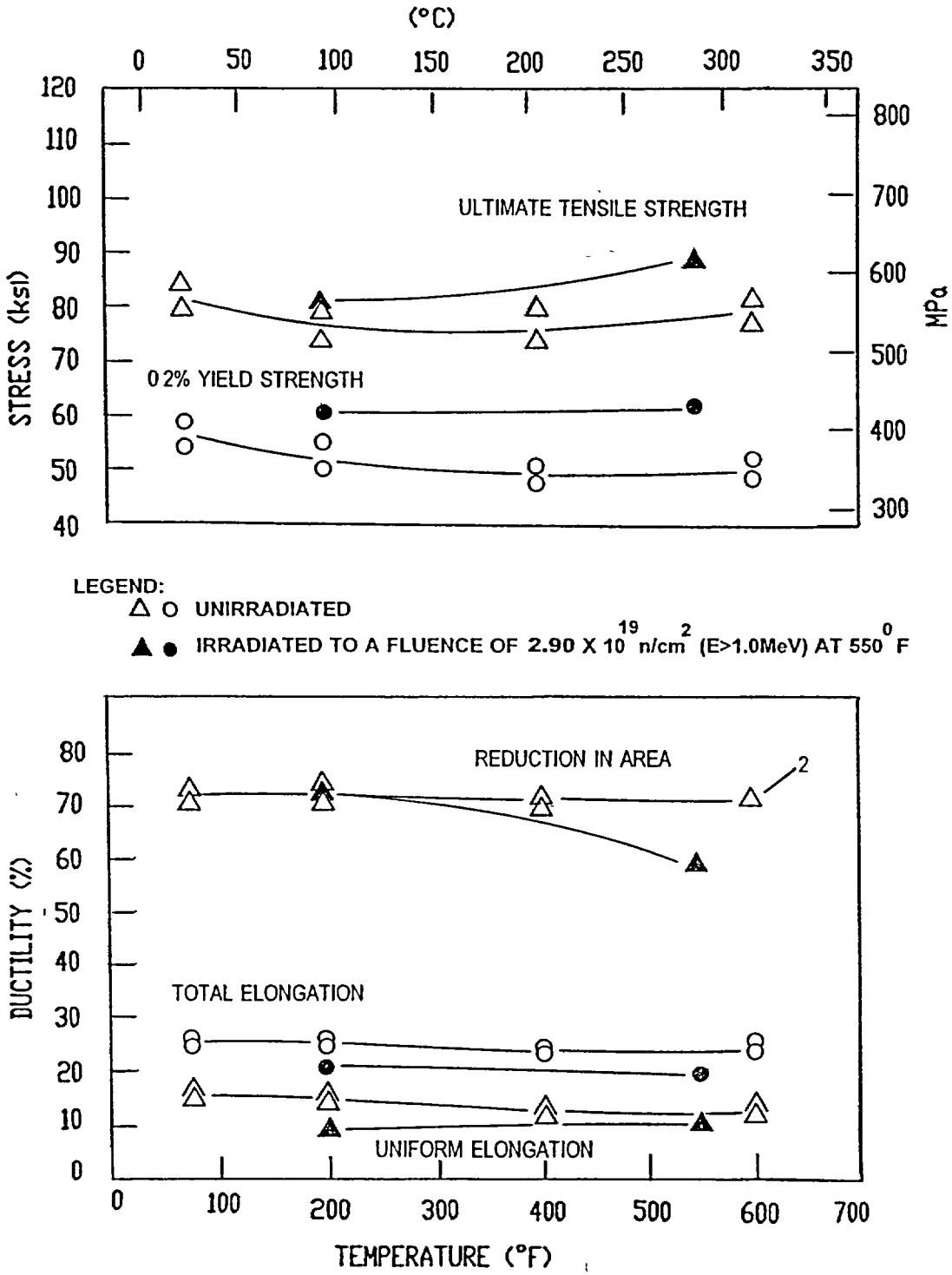

Figure 5-17 Tensile Properties for Turkey Point Unit 3 Reactor Vessel Shell Forging 123S266VA1 (Tangential Orientation)

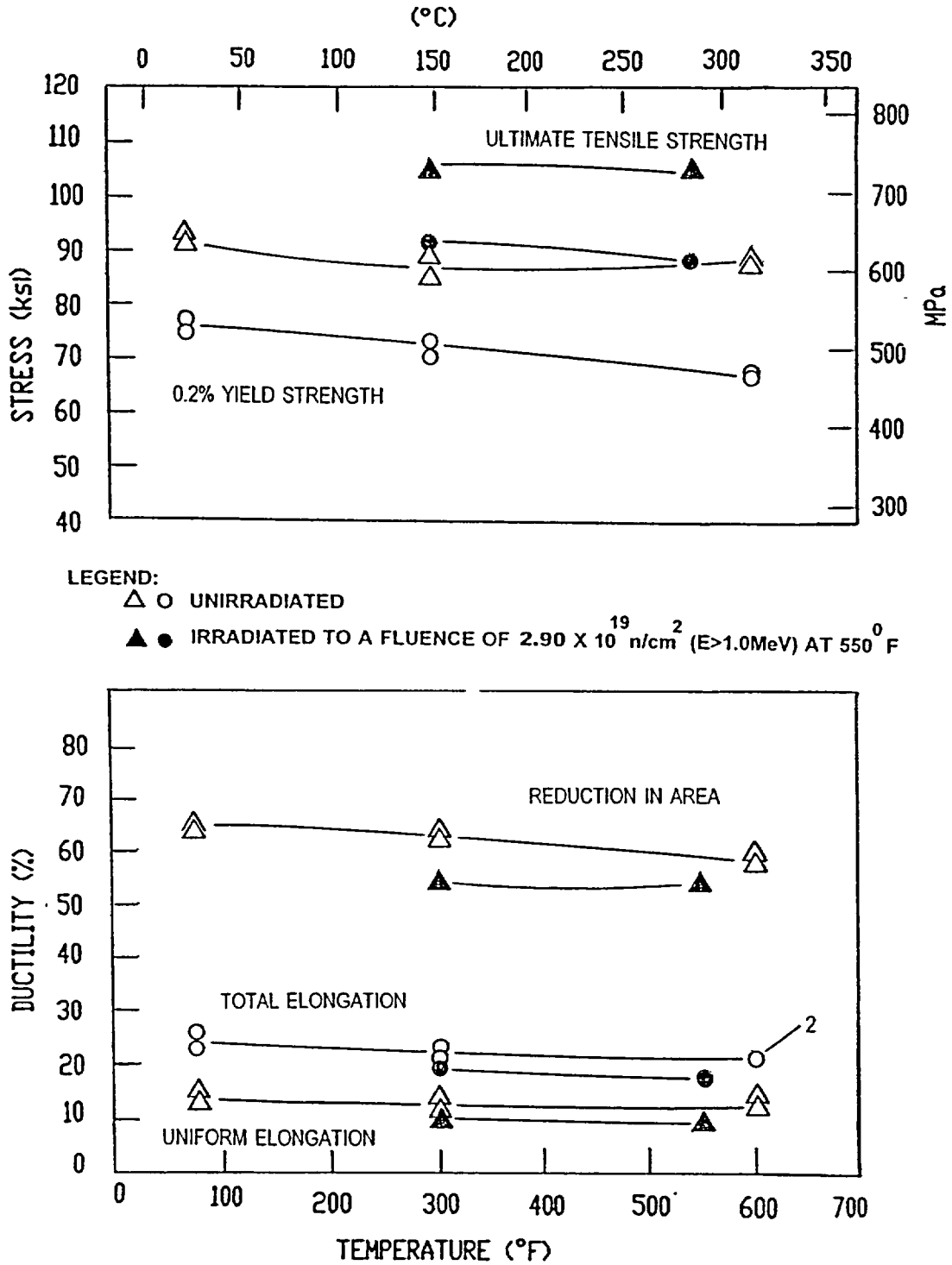

Figure 5-18 Tensile Properties for Turkey Point Unit 3 Reactor Vessel Weld Metal

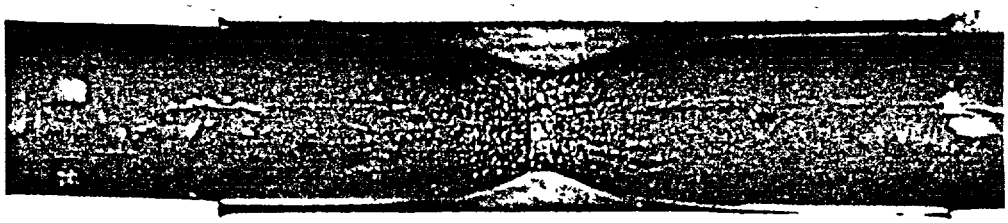

Specimen S13 Tested at 200°F

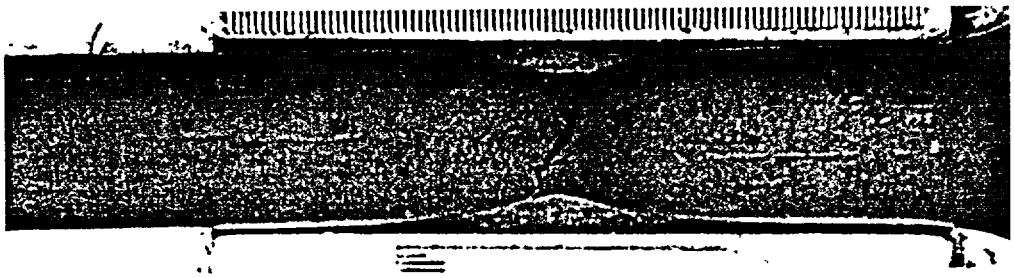

Specimen S14 Tested at 550°F

Figure 5-19 Fractured Tensile Specimens for Turkey Point Unit 3 Reactor Vessel Shell Forging 123S266VA1 (Tangential Orientation)

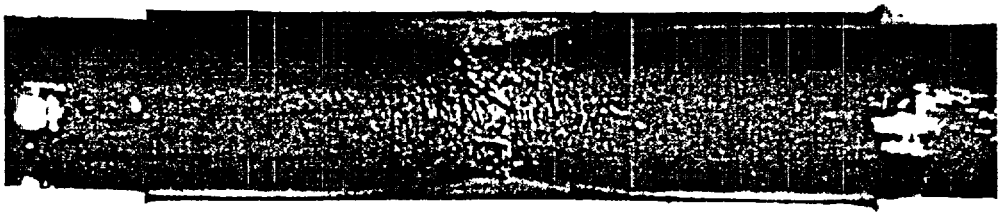

Specimen W3 Tested at 300°F

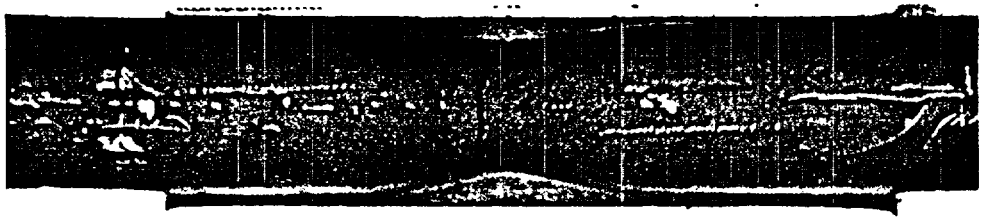

Specimen W4 Tested at 550°F

Figure 5-20 Fractured Tensile Specimens for Turkey Point Unit 3 Reactor Vessel Surveillance Weld Metal

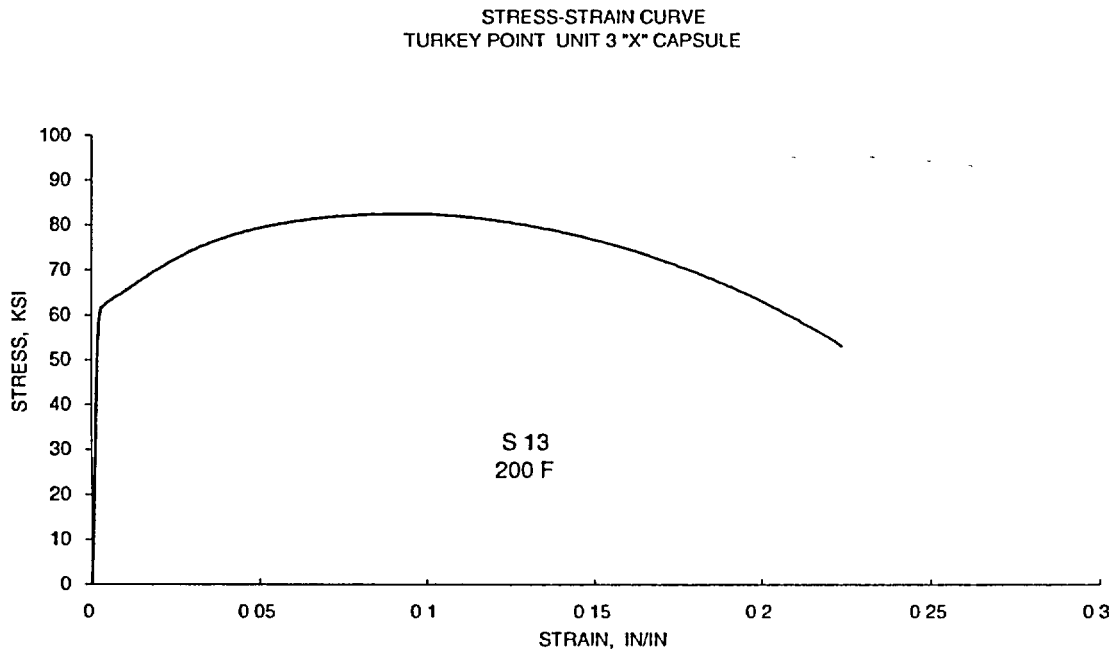

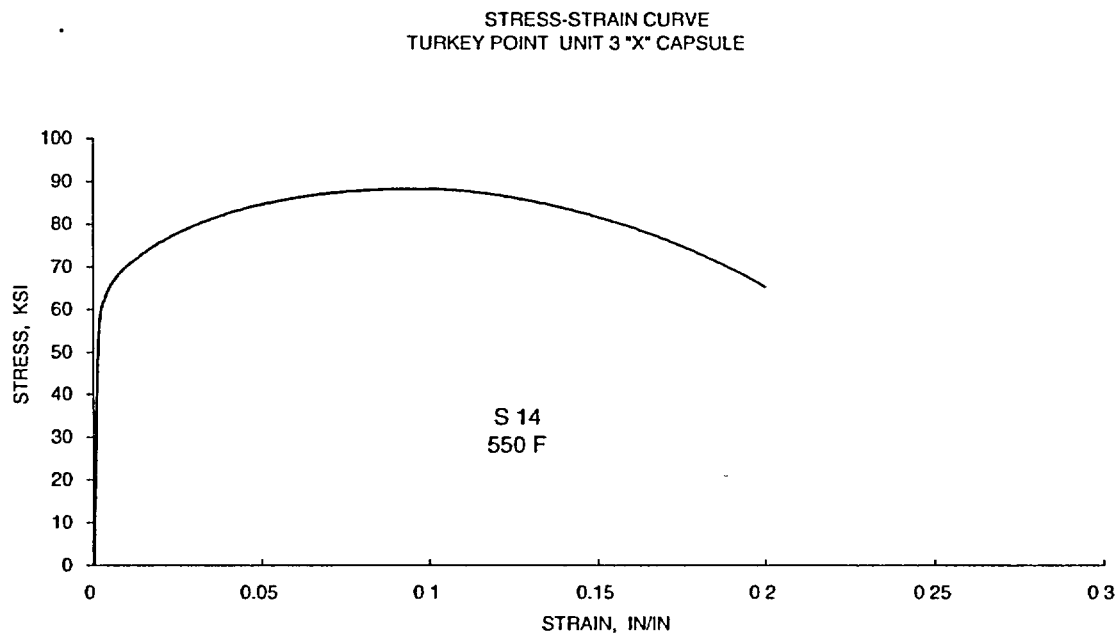

Figure 5-21 Engineering Stress-Strain Curves for Turkey Point Unit 3 Reactor Vessel Forging 123S266VA1, Tensile Specimens S13 and S14

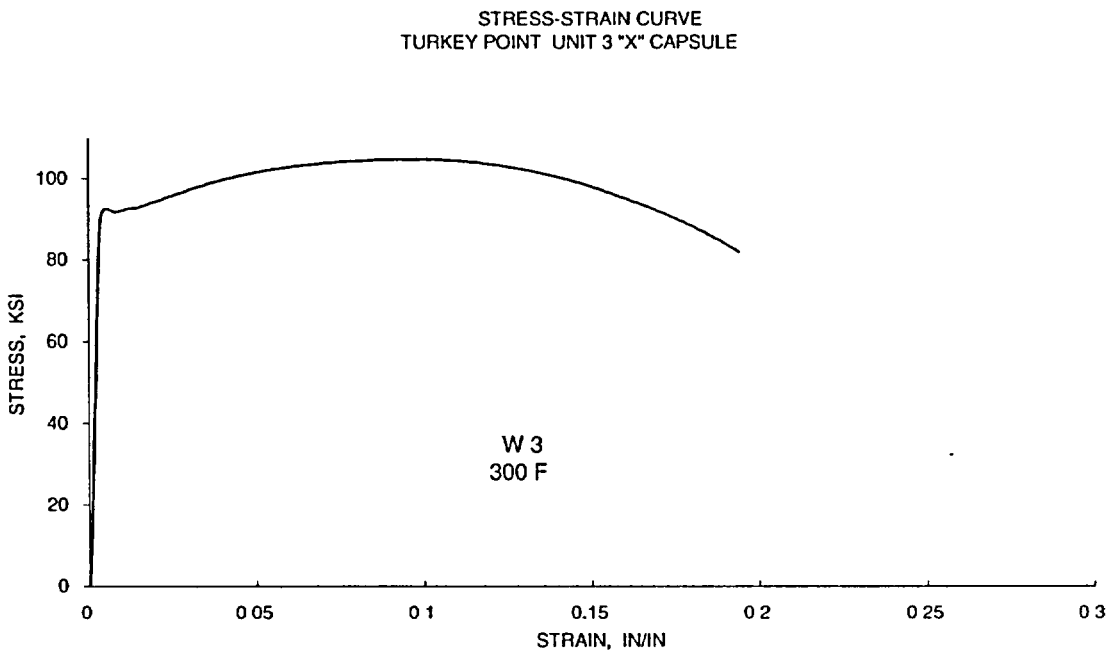

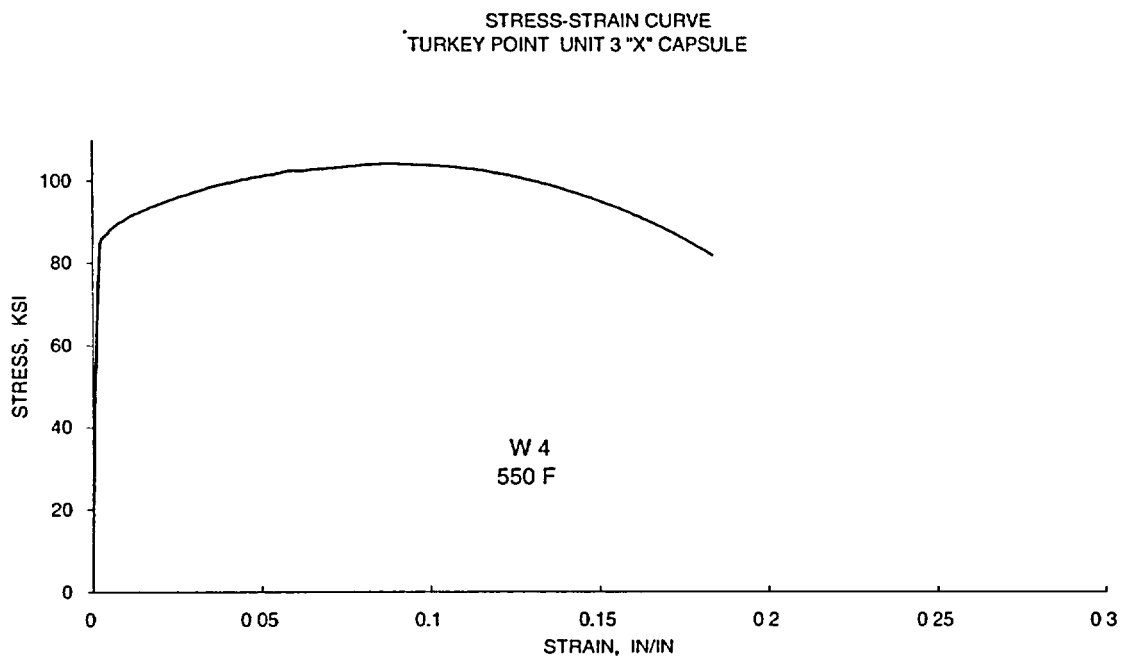

Figure 5-22 Engineering Stress-Strain Curves for Turkey Point Unit 3 Reactor Weld Metal, Tensile Specimens W3 and W4

6 RADIATION ANALYSIS AND NEUTRON DOSIMETRY

6.1 INTRODUCTION

This section describes a discrete ordinates S_n transport analysis performed for the Turkey Point Unit 3 reactor to determine the neutron radiation environment within the reactor pressure vessel and surveillance capsules. In this analysis, fast neutron exposure parameters in terms of fast neutron fluence (E > 1.0 MeV) and iron atom displacements (dpa) were established on a plant and fuel cycle specific basis. An evaluation of the most recent dosimetry sensor set from Capsule X, withdrawn at the end of the eighteenth plant operating cycle, is provided. In addition, to provide an up-to-date data base applicable to the Turkey Point Unit 3 reactor, sensor sets from previously withdrawn capsules (T, S, and V) were re-analyzed using the current dosimetry evaluation methodology. These dosimetry updates are presented in Appendix A of this report. Comparisons of the results from these dosimetry evaluations with the analytical predictions served to validate the plant specific neutron transport calculations. These validated calculations subsequently formed the basis for providing projections of the neutron exposure of the reactor pressure vessel for operating periods extending to 54 Effective Full Power Years (EFPY). These projections also account for a plant uprating, from 2200 MWt to 2300 MWt, which began during the fifteenth operating cycle.

The use of fast neutron fluence (E > 1.0 MeV) to correlate measured material property changes to the neutron exposure of the material has traditionally been accepted for the development of damage trend curves as well as for the implementation of trend curve data to assess the condition of the vessel. In recent years, however, it has been suggested that an exposure model that accounts for differences in neutron energy spectra between surveillance capsule locations and positions within the vessel wall could lead to an improvement in the uncertainties associated with damage trend curves and improved accuracy in the evaluation of damage gradients through the reactor vessel wall.

Because of this potential shift away from a threshold fluence toward an energy dependent damage function for data correlation, ASTM Standard Practice E853, "Analysis and Interpretation of Light-Water Reactor Surveillance Results," recommends reporting displacements per iron atom (dpa) along with fluence (E > 1.0 MeV) to provide a database for future reference. The energy dependent dpa function to be used for this evaluation is specified in ASTM Standard Practice E693, "Characterizing Neutron Exposures in Iron and Low Alloy Steels in Terms of Displacements per Atom." The application of the dpa parameter to the assessment of embrittlement gradients through the thickness of the reactor vessel wall has already been promulgated in Revision 2 to Regulatory Guide 1.99, "Radiation Embrittlement of Reactor Vessel Materials."

All of the calculations and dosimetry evaluations described in this section and in Appendix A were based on the latest available nuclear cross-section data derived from ENDF/B-VI and made use of the latest available calculational tools. Furthermore, the neutron transport and dosimetry evaluation methodologies follow the guidance and meet the requirements of Regulatory Guide 1.190, "Calculational and Dosimetry Methods for Determining Pressure Vessel Neutron Fluence."[14] Additionally, the methods used to develop the calculated pressure vessel fluence are consistent with the NRC approved methodology described in WCAP-14040-NP-A, "Methodology Used to Develop Cold Overpressure Mitigating System Setpoints and RCS Heatup and Cooldown Limit Curves," January 1996.[15] The specific calculational

methods applied are also consistent with those described in WCAP-15557, "Qualification of the Westinghouse Pressure Vessel Neutron Fluence Evaluation Methodology."[16]

6.2 Discrete Ordinates Analysis

A plan view of the Turkey Point Unit 3 reactor geometry at the core midplane is shown in Figure 4-1. Eight irradiation capsules attached to the thermal shield are included in the reactor design that constitutes the reactor vessel surveillance program. The capsules are located at azimuthal angles of 270° (0° from the core cardinal axes), 280° (10° from the core cardinal axes), 290° (20° from the core cardinal axes), 30° and 150° (30° from the core cardinal axes), and 40°, 50°, and 230° (40° from the core cardinal axes) as shown in Figure 4-1. The stainless steel specimen containers are 1-inch square by 56 inches in height. The containers are positioned axially such that the test specimens are centered on the core midplane, thus spanning the central 5 feet of the 12-foot high reactor core.

From a neutronic standpoint, the surveillance capsules and associated support structures are significant. The presence of these materials has a marked effect on both the spatial distribution of neutron flux and the neutron energy spectrum in the water annulus between the thermal shield and the reactor vessel. In order to determine the neutron environment at the test specimen location, the capsules themselves must be included in the analytical model.

In performing the fast neutron exposure evaluations for the Turkey Point Unit 3 reactor vessel and surveillance capsules, a series of fuel cycle specific forward transport calculations were carried out using the following three-dimensional flux synthesis technique:

$$\phi(r,\theta,z) = \phi(r,\theta) * \frac{\phi(r,z)}{\phi(r)}$$

where $\phi(r,\theta,z)$ is the synthesized three-dimensional neutron flux distribution, $\phi(r,\theta)$ is the transport solution in r,θ geometry, $\phi(r,z)$ is the two-dimensional solution for a cylindrical reactor model using the actual axial core power distribution, and $\phi(r)$ is the one-dimensional solution for a cylindrical reactor model using the same source per unit height as that used in the r,θ two-dimensional calculation. This synthesis procedure was carried out for each operating cycle at Turkey Point Unit 3.

For selected Turkey Point Unit 3 fuel cycles that utilized part-length absorber rods in fuel assemblies located on the core flats to suppress the vessel fluence, the multi-channel analysis form of the three-dimensional synthesis equation was used as promulgated in Regulatory Guide 1.190[14]. Specifically, the transport analyses for Cycles 9 through 19 of Turkey Point Unit 3 were based on the following equation:

$$\phi(r,\theta,z) = \phi_A(r,\theta) * \frac{\phi_A(r,z)}{\phi_A(r)} + \phi_B(r,\theta) * \frac{\phi_B(r,z)}{\phi_B(r)}$$

where the first term, denoted as channel "A", represents all assemblies in the core except for those containing part-length absorber rods, whereas the second term, referred to as channel "B" only represents the assemblies on the core flats that contain the part-length absorber rods.

For the Turkey Point Unit 3 transport calculations, the r,θ model depicted in Figure 6-1 was utilized since the reactor is octant symmetric. This r,θ model includes the core, the reactor internals, the thermal shield

-- including explicit representations of the surveillance capsules at 0°, 10°, 20°, 30°, and 40°, the pressure vessel cladding and vessel wall, the insulation external to the pressure vessel, and the primary biological shield wall. This model formed the basis for the calculated results and enabled making comparisons to the surveillance capsule dosimetry evaluations. In addition, maximum neutron exposures at the pressure vessel wall were derived based on a variant of this model in which the material composition of the surveillance capsules were redefined as downcomer water such that fast flux multipliers were determined and applied at selected azimuths along the vessel inner radius relative to the calculated results that were derived with the capsules present. In developing this analytical model, nominal design dimensions were employed for the various structural components. Likewise, water temperatures, and hence, coolant densities in the reactor core and downcomer regions of the reactor were taken to be representative of full power operating conditions. The coolant densities were treated on a fuel cycle specific basis. The reactor core itself was treated as a homogeneous mixture of fuel, cladding, water, and miscellaneous core structures such as fuel assembly grids, guide tubes, et cetera. The geometric mesh description of the r,θ reactor model consisted of 161 radial by 107 azimuthal intervals. Mesh sizes were chosen to assure that proper convergence of the inner iterations was achieved on a pointwise basis. The pointwise inner iteration flux convergence criterion utilized in the r,θ calculations was set at a value of 0.001.

The r,z model used for the Turkey Point Unit 3 calculations that is shown in Figure 6-2 extended radially from the centerline of the reactor core out to a location interior to the primary biological shield and over an axial span from an elevation 1-foot below the active fuel to approximately 1-foot above the active fuel. As in the case of the r,θ model, nominal design dimensions and full power coolant densities were employed in the calculations. In this case, the homogenous core region was treated as an equivalent cylinder with a volume equal to that of the active core zone. The stainless steel former plates located between the core baffle and core barrel regions were also explicitly included in the model. The r,z geometric mesh description of the reactor model consisted of 158 radial by 106 axial intervals. As in the case of the r,θ calculations, mesh sizes were chosen to assure that proper convergence of the inner iterations was achieved on a pointwise basis. The pointwise inner iteration flux convergence criterion utilized in the r,z calculations was also set at a value of 0.001.

The one-dimensional radial model used in the synthesis procedure consisted of the same 158 radial mesh intervals included in the r,z model. Thus, radial synthesis factors could be determined on a meshwise basis throughout the entire geometry.

The core power distributions used in the plant specific transport analysis were taken from the appropriate Turkey Point Unit 3 fuel cycle design reports as well as supplemental material provided by the utility. The data extracted from the design reports represented cycle dependent fuel assembly enrichments, burnups, and axial power distributions. This information was used to develop spatial and energy dependent core source distributions averaged over each individual fuel cycle. Therefore, the results from the neutron transport calculations provided data in terms of fuel cycle averaged neutron flux, which when multiplied by the appropriate fuel cycle length, generated the incremental fast neutron exposure for each fuel cycle. In constructing these core source distributions, the energy distribution of the source was based on an appropriate fission split for uranium and plutonium isotopes based on the initial enrichment and burnup history of individual fuel assemblies. From these assembly dependent fission splits, composite values of energy release per fission, neutron yield per fission, and fission spectrum were determined.

All of the transport calculations supporting this analysis were carried out using the DORT discrete ordinates code Version 3.1[17] and the BUGLE-96 cross-section library.[18] The BUGLE-96 library provides a 67 group coupled neutron-gamma ray cross-section data set produced specifically for light water reactor (LWR) applications. In these analyses, anisotropic scattering was treated with a P_5 legendre expansion and angular discretization was modeled with an S_{16} order of angular quadrature. Energy and space dependent core power distributions, as well as system operating temperatures, were treated on a fuel cycle specific basis.

Selected results from the neutron transport analyses are provided in Tables 6-1 through 6-7. In Table 6-1, the calculated exposure rates and integrated exposures, expressed in terms of both neutron fluence (E > 1.0 MeV) and dpa, are given at the radial and azimuthal center of the five azimuthally symmetric surveillance capsule positions (0°, 10°, 20°, 30°, and 40°). Also note that Table 6-1 presents calculated exposure rates and integrated exposures for Capsule X, which was irradiated at a 40° location during Cycles 1 through 11, and subsequently moved to a 0° location until it was removed from service at the end of Cycle 18. These results, representative of the axial midplane of the active core, establish the calculated exposure of the surveillance capsules withdrawn to date as well as projected into the future. Similar information is provided in Tables 6-2 and 6-3 for the reactor vessel inner radius. The vessel data given in Table 6-2 are representative of the axial location of the maximum neutron exposure at each of the four azimuthal locations, whereas comparable results that are summarized in Table 6-3 are maximum values taken at the intermediate shell course to lower shell course girth (circumferential) weld located approximately 22.8 inches below the core midplane. It is also important to note that the data for the vessel inner radius were taken at the clad/base metal interface, and thus, represent the maximum calculated exposure levels of the vessel forgings and welds.

Both calculated fluence (E > 1.0 MeV) and dpa data are provided in Table 6-1 through Table 6-3. These data tabulations include both plant and fuel cycle specific calculated neutron exposures at the end of the eighteenth operating fuel cycle as well as projections for the current operating fuel cycle, i.e., Cycle 19, and future projections to 32, 48, and 54 effective full power years (EFPY). The projections were based on the assumption that the radial power distribution from fuel cycle 7 (using the core octant most compatible with current core designs) was representative of future plant operation since the use of part-length absorbers in assemblies located on the core flats was conservatively assumed to be discontinued. All remaining core parameters were obtained from the current operating cycle 19 design. The future projections are also based on the current reactor power level of 2300 MWt.

Radial gradient information applicable to fast (E > 1.0 MeV) neutron fluence and dpa are given in Tables 6-4 and 6-5, respectively. The data, based on the cumulative integrated exposures from Cycles 1 through 19, are presented on a relative basis for each exposure parameter at several azimuthal locations. Exposure distributions through the vessel wall may be obtained by multiplying the calculated exposure at the vessel inner radius by the gradient data listed in Tables 6-4 and 6-5.

The calculated fast neutron exposures for the four surveillance capsules withdrawn from the Turkey Point Unit 3 reactor are provided in Table 6-6. These assigned neutron exposure levels are based on the plant and fuel cycle specific neutron transport calculations performed for the Turkey Point Unit 3 reactor.

Updated lead factors for the Turkey Point Unit 3 surveillance capsules are provided in Table 6-7. The capsule lead factor is defined as the ratio of the calculated fluence (E > 1.0 MeV) at the geometric center of the surveillance capsule to the corresponding maximum calculated fluence at the pressure vessel

clad/base metal interface. In Table 6-7, the lead factors for capsules that have been withdrawn from the reactor (T, S, V, and X) were based on the calculated fluence values for the irradiation period corresponding to the time of withdrawal for the individual capsules. For the capsules remaining in the reactor (U, Y, W, and Z), the lead factors correspond to the calculated fluence values at the end of Cycle 19, the current operating fuel cycle for Turkey Point Unit 3.

6.3 Neutron Dosimetry

The validity of the calculated neutron exposures previously reported in Section 6.2 is demonstrated by a direct comparison against the measured sensor reaction rates and via a least squares evaluation performed for each of the capsule dosimetry sets. However, since the neutron dosimetry measurement data merely serves to validate the calculated results, only the direct comparison of measured-to-calculated results for the most recent surveillance capsule removed from service is provided in this section of the report. For completeness, the assessment of all measured dosimetry removed to date, based on both direct and least squares evaluation comparisons, is documented in Appendix A.

The direct comparison of measured versus calculated fast neutron threshold reaction rates for the sensors from Capsule X, that was withdrawn from Turkey Point Unit 3 at the end of the eighteenth fuel cycle, is summarized below.

Reaction	Reaction Rates (rps/atom)		M/C
	Measured	Calculated	Ratio
$^{63}Cu(n,\alpha)^{60}Co$	3.36E-17	3.19E-17	1.05
$^{54}Fe(n,p)^{54}Mn$	3.16E-15	3.41E-15	0.93
$^{238}U(n,p)^{137}Cs$ (Cd)	1.36E-14	1.64E-14	0.83
$^{237}Np(n,f)^{137}Cs$ (Cd)	1.23E-13	1.23E-13	1.00
		Average:	0.95
		% Standard Deviation:	10.2

The measured-to-calculated (M/C) reaction rate ratios for the Capsule X threshold reactions range from 0.83 to 1.05, and the average M/C ratio is 0.95 ± 10.2% (1σ). This direct comparison falls well within the ± 20% criterion specified in Regulatory Guide 1.190; furthermore, it is consistent with the full set of comparisons given in Appendix A for all measured dosimetry removed to date from the Turkey Point Unit 3 reactor. As a result, these comparisons validate the current analytical results described in Section 6.2 and are deemed applicable for Turkey Point Unit 3.

6.4 Calculational Uncertainties

The uncertainty associated with the calculated neutron exposure of the Turkey Point Unit 3 surveillance capsule and reactor pressure vessel is based on the recommended approach provided in Regulatory Guide 1.190. In particular, the qualification of the methodology was carried out in the following four stages:

1 - Comparison of calculations with benchmark measurements from the Pool Critical Assembly (PCA) simulator at the Oak Ridge National Laboratory (ORNL).

2 - Comparisons of calculations with surveillance capsule and reactor cavity measurements from the H. B. Robinson power reactor benchmark experiment.

3 - An analytical sensitivity study addressing the uncertainty components resulting important input parameters applicable to the plant specific transport calculations used in the neutron exposure assessments.

4 - Comparisons of the plant specific calculations with all available dosimetry results from the Turkey Point Unit 3 surveillance program.

The first phase of the methods qualification (PCA comparisons) addressed the adequacy of basic transport calculation and dosimetry evaluation techniques and associated cross-sections. This phase, however, did not test the accuracy of commercial core neutron source calculations nor did it address uncertainties in operational or geometric variables that impact power reactor calculations. The second phase of the qualification (H. B. Robinson comparisons) addressed uncertainties in these additional areas that are primarily methods related and would tend to apply generically to all fast neutron exposure evaluations. The third phase of the qualification (analytical sensitivity study) identified the potential uncertainties introduced into the overall evaluation due to calculational methods approximations as well as to a lack of knowledge relative to various plant specific input parameters. The overall calculational uncertainty applicable to the Turkey Point Unit 3 analysis was established from results of these three phases of the methods qualification.

The fourth phase of the uncertainty assessment (comparisons with Turkey Point Unit 3 measurements) was used solely to demonstrate the validity of the transport calculations and to confirm the uncertainty estimates associated with the analytical results. The comparison was used only as a check and was not used in any way to modify the calculated surveillance capsule and pressure vessel neutron exposures previously described in Section 6.2. As such, the validation of the Turkey Point Unit 3 analytical model based on the measured plant dosimetry is completely described in Appendix A.

The following summarizes the uncertainties developed from the first three phases of the methodology qualification. Additional information pertinent to these evaluations is provided in Reference 3.

	Capsule	Vessel IR
PCA Comparisons	3%	3%
H. B. Robinson Comparisons	3%	3%
Analytical Sensitivity Studies	10%	11%
Additional Uncertainty for Factors not Explicitly Evaluated	5%	5%
Net Calculational Uncertainty	12%	13%

The net calculational uncertainty was determined by combining the individual components in quadrature. Therefore, the resultant uncertainty was random and no systematic bias was applied to the analytical results.

The plant specific measurement comparisons described in Appendix A support these uncertainty assessments for Turkey Point Unit 3.

Figure 6-1

Turkey Point Unit 3 r,θ Reactor Geometry at the Core Midplane

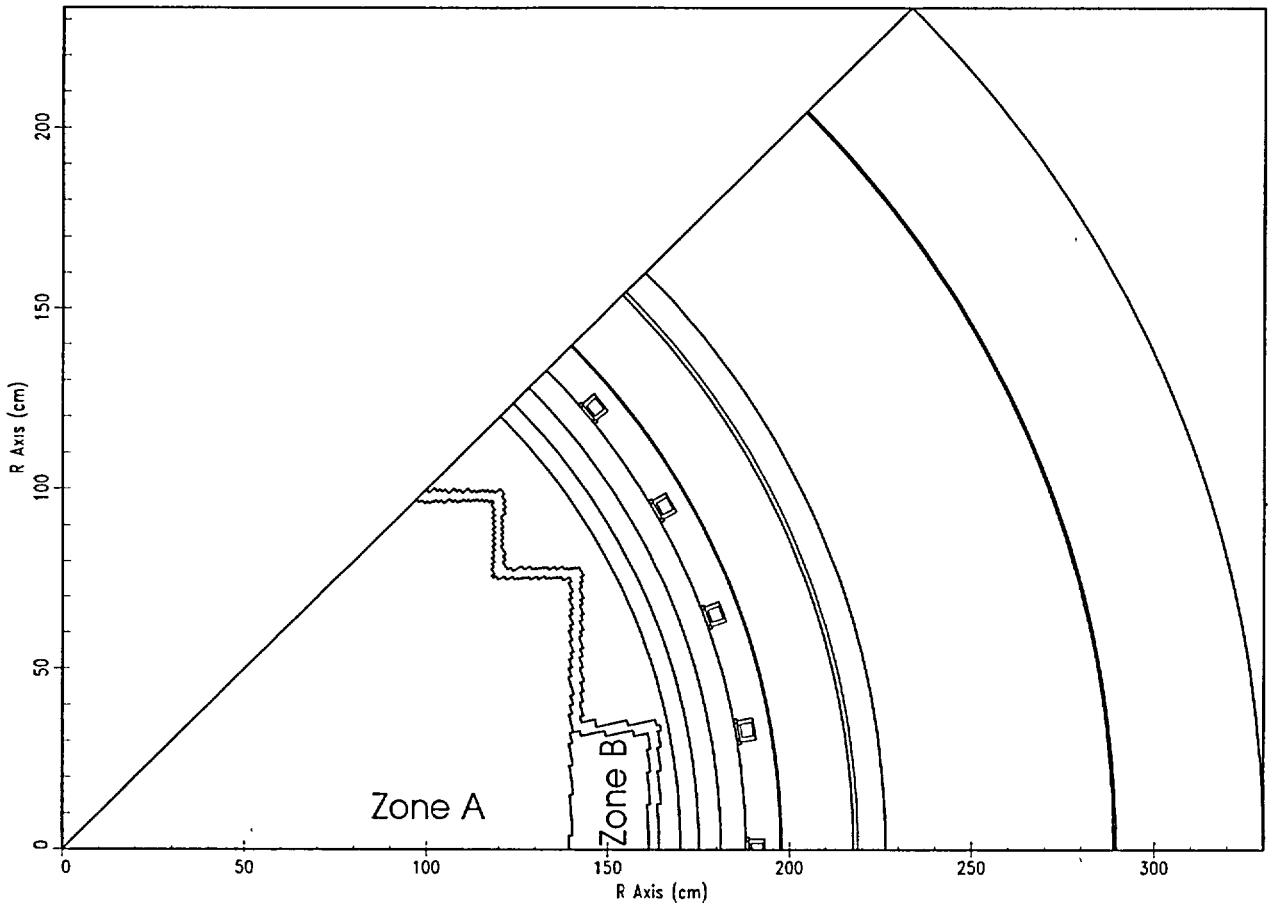

Note: For core reload designs that have part length absorber rods installed, Zone A represents the fuel assemblies that do not contain these rods and Zone B represents the fuel assemblies where these absorber rods are used

Figure 6-2

Turkey Point Unit 3 r,z Reactor Geometry

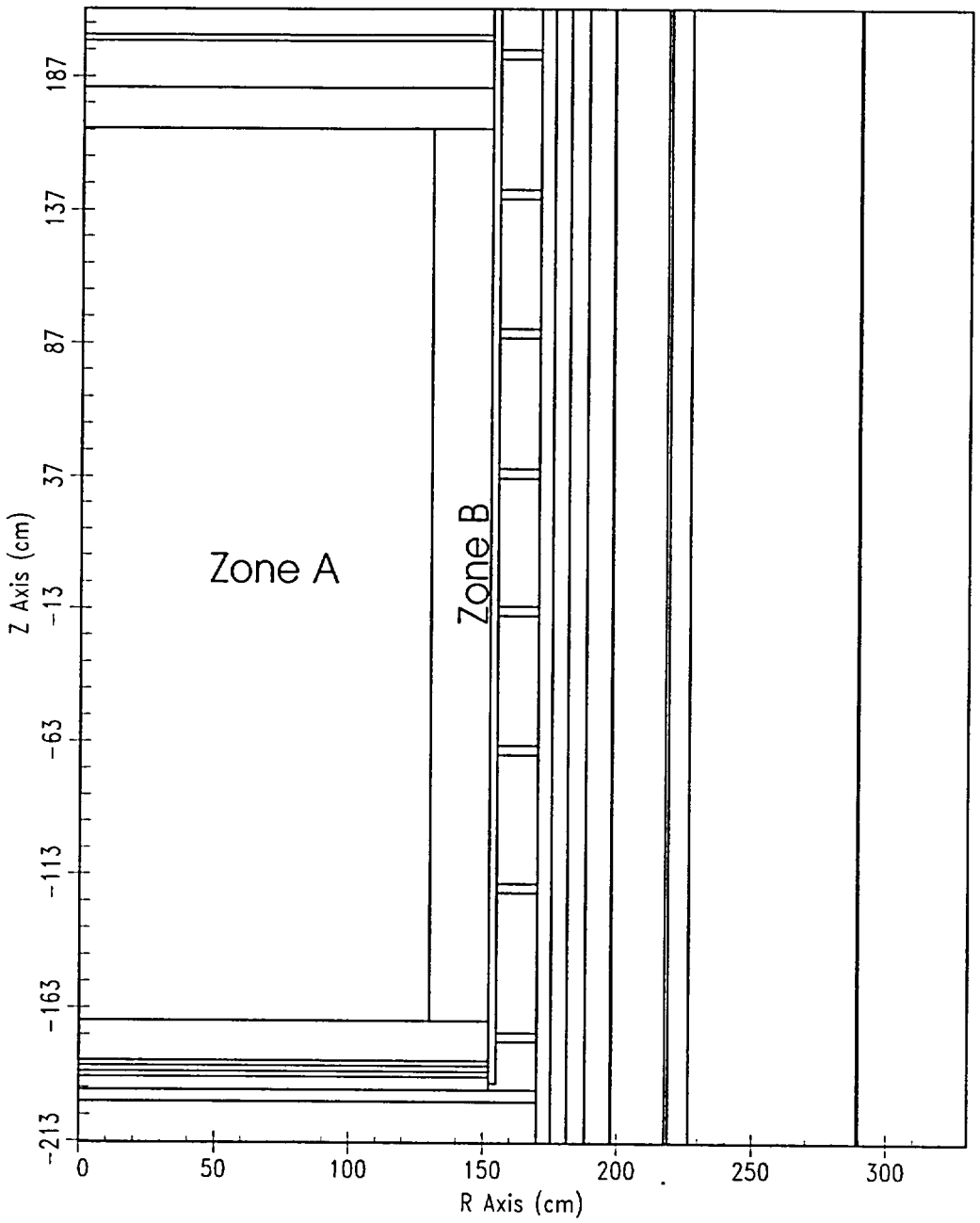

Note: For core reload designs that have part length absorber rods installed, Zone A represents the fuel assemblies that do not contain these rods and Zone B represents the fuel assemblies where these absorber rods are used.

Table 6-1

Calculated Neutron Exposure Rates And Integrated Exposures
At The Surveillance Capsule Center

Neutrons (E > 1.0 MeV)

Cycle	Cycle Length [EFPS]	Cumulative Irradiation Time [EFPS]	Cumulative Irradiation Time [EFPY]	Neutron Flux (E > 1.0 MeV) [n/cm^2-s]		
				0°	10°	20°
1	3.62E+07	3.62E+07	1.15	1.66E+11	1.16E+11	5.14E+10
2	2.45E+07	6.06E+07	1.92	1.61E+11	1.13E+11	4.88E+10
3	2.40E+07	8.46E+07	2.68	1.54E+11	1.19E+11	5.73E+10
4	2.46E+07	1.09E+08	3.46	1.56E+11	1.17E+11	4.91E+10
5	2.45E+07	1.34E+08	4.24	2.00E+11	1.41E+11	5.20E+10
6	1.59E+07	1.50E+08	4.74	1.85E+11	1.31E+11	4.81E+10
7	2.90E+07	1.79E+08	5.66	1.40E+11	9.88E+10	4.55E+10
8	4.30E+07	2.22E+08	7.03	1.47E+11	9.89E+10	4.56E+10
9	3.26E+07	2.54E+08	8.06	7.15E+10	5.72E+10	3.90E+10
10	3.95E+07	2.94E+08	9.31	6.84E+10	5.61E+10	3.80E+10
11	4.13E+07	3.35E+08	10.62	7.33E+10	5.76E+10	3.75E+10
12	3.91E+07	3.74E+08	11.86	7.16E+10	5.72E+10	3.77E+10
13	3.95E+07	4.14E+08	13.11	7.02E+10	5.47E+10	3.53E+10
14	3.93E+07	4.53E+08	14.36	7.46E+10	5.91E+10	3.90E+10
15	4.18E+07	4.95E+08	15.68	7.55E+10	5.89E+10	3.75E+10
16	4.38E+07	5.39E+08	17.07	7.71E+10	6.25E+10	4.53E+10
17	4.12E+07	5.80E+08	18.37	7.62E+10	5.81E+10	3.47E+10
18	4.65E+07	6.26E+08	19.85	6.64E+10	5.41E+10	4.04E+10
19 (Pjt.)	4.15E+07	6.68E+08	21.16	7.64E+10	5.92E+10	3.65E+10
Future	3.42E+08	1.01E+09	32.00	1.00E+11	8.30E+10	4.81E+10
Future	5.05E+08	1.51E+09	48.00	1.00E+11	8.30E+10	4.81E+10
Future	1.89E+08	1.70E+09	54.00	1.00E+11	8.30E+10	4.81E+10

Note: Neutron exposure values reported for the surveillance capsules are centered at the core midplane.

Table 6-1 cont'd

Calculated Neutron Exposure Rates And Integrated Exposures
At The Surveillance Capsule Center

Neutrons (E > 1.0 MeV)

Cycle	Cycle Length [EFPS]	Cumulative Irradiation Time [EFPS]	Cumulative Irradiation Time [EFPY]	Neutron Flux (E > 1.0 MeV) [n/cm^2-s]		
				30°	40°	40° → 0° (Cap. X*)
1	3.62E+07	3.62E+07	1.15	3.90E+10	2.59E+10	2.59E+10
2	2.45E+07	6.06E+07	1.92	3.66E+10	2.37E+10	2.37E+10
3	2.40E+07	8.46E+07	2.68	4.48E+10	3.03E+10	3.03E+10
4	2.46E+07	1.09E+08	3.46	3.49E+10	2.64E+10	2.64E+10
5	2.45E+07	1.34E+08	4.24	3.23E+10	2.07E+10	2.07E+10
6	1.59E+07	1.50E+08	4.74	2.96E+10	1.99E+10	1.99E+10
7	2.90E+07	1.79E+08	5.66	3.34E+10	2.27E+10	2.27E+10
8	4.30E+07	2.22E+08	7.03	3.29E+10	2.20E+10	2.20E+10
9	3.26E+07	2.54E+08	8.06	3.23E+10	2.35E+10	2.35E+10
10	3.95E+07	2.94E+08	9.31	2.99E+10	2.05E+10	2.05E+10
11	4.13E+07	3.35E+08	10.62	2.96E+10	1.98E+10	1.98E+10
12	3.91E+07	3.74E+08	11.86	3.00E+10	2.04E+10	7.16E+10
13	3.95E+07	4.14E+08	13.11	2.81E+10	2.05E+10	7.02E+10
14	3.93E+07	4.53E+08	14.36	3.14E+10	2.28E+10	7.46E+10
15	4.18E+07	4.95E+08	15.68	2.97E+10	2.07E+10	7.55E+10
16	4.38E+07	5.39E+08	17.07	3.57E+10	2.15E+10	7.71E+10
17	4.12E+07	5.80E+08	18.37	2.82E+10	1.92E+10	7.62E+10
18	4.65E+07	6.26E+08	19.85	3.25E+10	2.16E+10	6 64E+10
19 (Pjt.)	4.15E+07	6.68E+08	21.16	2.94E+10	2.02E+10	7.64E+10
Future	3.42E+08	1.01E+09	32.00	3.73E+10	2.52E+10	1.00E+11
Future	5.05E+08	1.51E+09	48.00	3.73E+10	2.52E+10	1 00E+11
Future	1 89E+08	1.70E+09	54.00	3.73E+10	2.52E+10	1.00E+11

Note: Neutron exposure values reported for the surveillance capsules are centered at the core midplane.

* Capsule X was irradiated at a 40° location during Cycles 1 through 11 followed by a 0° location during Cycles 12 through 18 when it was subsequently removed from service

Table 6-1 cont'd

Calculated Neutron Exposure Rates And Integrated Exposures
At The Surveillance Capsule Center

Neutrons (E > 1.0 MeV)

Cycle	Cycle Length [EFPS]	Cumulative Irradiation Time [EFPS]	Cumulative Irradiation Time [EFPY]	Neutron Fluence (E > 1.0 MeV) [n/cm^2]		
				0°	10°	20°
1	3.62E+07	3.62E+07	1.15	5.99E+18	4.21E+18	1.86E+18
2	2.45E+07	6.06E+07	1.92	9.92E+18	6.97E+18	3.05E+18
3	2.40E+07	8.46E+07	2.68	1.36E+19	9.84E+18	4.43E+18
4	2.46E+07	1.09E+08	3.46	1.75E+19	1.27E+19	5.64E+18
5	2.45E+07	1.34E+08	4.24	2.24E+19	1.62E+19	6.91E+18
6	1.59E+07	1.50E+08	4.74	2.53E+19	1.83E+19	7.68E+18
7	2.90E+07	1.79E+08	5.66	2.94E+19	2.11E+19	9.00E+18
8	4.30E+07	2.22E+08	7.03	3.57E+19	2.54E+19	1.10E+19
9	3.26E+07	2.54E+08	8.06	3.80E+19	2.73E+19	1.22E+19
10	3.95E+07	2.94E+08	9.31	4.07E+19	2.95E+19	1.37E+19
11	4.13E+07	3.35E+08	10.62	4.38E+19	3.19E+19	1.53E+19
12	3.91E+07	3.74E+08	11.86	4.66E+19	3.41E+19	1.68E+19
13	3.95E+07	4.14E+08	13.11	4.93E+19	3.63E+19	1.82E+19
14	3.93E+07	4.53E+08	14.36	5.23E+19	3.86E+19	1.97E+19
15	4.18E+07	4.95E+08	15.68	5.54E+19	4.10E+19	2.13E+19
16	4.38E+07	5.39E+08	17.07	5.88E+19	4.38E+19	2.32E+19
17	4.12E+07	5.80E+08	18.37	6.19E+19	4.62E+19	2.47E+19
18	4.65E+07	6.26E+08	19.85	6.50E+19	4.87E+19	2.65E+19
19 (Pjt.)	4.15E+07	6.68E+08	21.16	6.82E+19	5.11E+19	2.81E+19
Future	3.42E+08	1.01E+09	32.00	1.03E+20	7.95E+19	4.45E+19
Future	5.05E+08	1.51E+09	48.00	1.53E+20	1.21E+20	6.88E+19
Future	1.89E+08	1.70E+09	54.00	1.72E+20	1.37E+20	7.79E+19

Note. Neutron exposure values reported for the surveillance capsules are centered at the core midplane

Table 6-1 cont'd

Calculated Neutron Exposure Rates And Integrated Exposures
At The Surveillance Capsule Center

Neutrons (E > 1.0 MeV)

Cycle	Cycle Length [EFPS]	Cumulative Irradiation Time [EFPS]	Cumulative Irradiation Time [EFPY]	Neutron Fluence (E > 1.0 MeV) [n/cm^2]		
				30°	40°	40° → 0° (Cap. X*)
1	3.62E+07	3.62E+07	1.15	1.41E+18	9.36E+17	9.36E+17
2	2.45E+07	6.06E+07	1.92	2.31E+18	1.52E+18	1.52E+18
3	2.40E+07	8.46E+07	2.68	3.38E+18	2.24E+18	2.24E+18
4	2.46E+07	1.09E+08	3.46	4.24E+18	2.89E+18	2.89E+18
5	2.45E+07	1.34E+08	4.24	5.03E+18	3.40E+18	3.40E+18
6	1.59E+07	1.50E+08	4.74	5.50E+18	3.72E+18	3.72E+18
7	2.90E+07	1.79E+08	5.66	6.47E+18	4.38E+18	4.38E+18
8	4.30E+07	2.22E+08	7.03	7.89E+18	5.32E+18	5.32E+18
9	3.26E+07	2.54E+08	8.06	8.94E+18	6.09E+18	6.09E+18
10	3.95E+07	2.94E+08	9.31	1.01E+19	6.90E+18	6.90E+18
11	4.13E+07	3.35E+08	10.62	1.14E+19	7.72E+18	7.72E+18
12	3.91E+07	3.74E+08	11.86	1.25E+19	8.51E+18	1.05E+19
13	3.95E+07	4.14E+08	13.11	1.36E+19	9.33E+18	1.33E+19
14	3.93E+07	4.53E+08	14.36	1.49E+19	1.02E+19	1.62E+19
15	4.18E+07	4.95E+08	15.68	1.61E+19	1.11E+19	1.94E+19
16	4.38E+07	5.39E+08	17.07	1.77E+19	1.20E+19	2.27E+19
17	4.12E+07	5.80E+08	18.37	1.88E+19	1.28E+19	2.59E+19
18	4.65E+07	6.26E+08	19.85	2.03E+19	1.38E+19	2.90E+19
19 (Pjt.)	4.15E+07	6.68E+08	21.16	2.16E+19	1.47E+19	3.21E+19
Future	3.42E+08	1.01E+09	32.00	3.43E+19	2.33E+19	6.65E+19
Future	5.05E+08	1.51E+09	48.00	5.31E+19	3.60E+19	1.17E+20
Future	1.89E+08	1.70E+09	54.00	6.02E+19	4.08E+19	1.36E+20

Note: Neutron exposure values reported for the surveillance capsules are centered at the core midplane.

* Capsule X was irradiated at a 40° location during Cycles 1 through 11 followed by a 0° location during Cycles 12 through 18 when it was subsequently removed from service.

Table 6-1 cont'd

Calculated Neutron Exposure Rates And Integrated Exposures
At The Surveillance Capsule Center

IRON ATOM DISPLACEMENTS

Cycle	Cycle Length [EFPS]	Cumulative Irradiation Time [EFPS]	Cumulative Irradiation Time [EFPY]	Displacement Rate [dpa/s]		
				0°	10°	20°
1	3.62E+07	3.62E+07	1.15	2.80E-10	1.99E-10	8.41E-11
2	2.45E+07	6.06E+07	1.92	2.72E-10	1.93E-10	8.00E-11
3	2.40E+07	8.46E+07	2.68	2.61E-10	2.03E-10	9.38E-11
4	2.46E+07	1.09E+08	3.46	2.64E-10	2.00E-10	8.04E-11
5	2.45E+07	1.34E+08	4.24	3.38E-10	2.41E-10	8.53E-11
6	1.59E+07	1.50E+08	4.74	3.14E-10	2.24E-10	7.88E-11
7	2.90E+07	1.79E+08	5.66	2.37E-10	1.68E-10	7.44E-11
8	4.30E+07	2.22E+08	7.03	2.47E-10	1.68E-10	7.46E-11
9	3.26E+07	2.54E+08	8.06	1.20E-10	9.68E-11	6.35E-11
10	3.95E+07	2.94E+08	9.31	1.15E-10	9.49E-11	6.18E-11
11	4.13E+07	3.35E+08	10.62	1.23E-10	9.75E-11	6.11E-11
12	3.91E+07	3.74E+08	11.86	1.20E-10	9.67E-11	6.14E-11
13	3.95E+07	4.14E+08	13.11	1.18E-10	9.25E-11	5.74E-11
14	3.93E+07	4.53E+08	14.36	1.25E-10	9.99E-11	6.35E-11
15	4.18E+07	4.95E+08	15.68	1.27E-10	9.96E-11	6.11E-11
16	4.38E+07	5.39E+08	17.07	1.30E-10	1.06E-10	7.37E-11
17	4.12E+07	5.80E+08	18.37	1.28E-10	9.83E-11	5.65E-11
18	4.65E+07	6.26E+08	19.85	1.12E-10	9.14E-11	6.57E-11
19 (Pjt.)	4.15E+07	6.68E+08	21.16	1.28E-10	1.00E-10	5.94E-11
Future	3.42E+08	1.01E+09	32.00	1.69E-10	1.41E-10	7.84E-11
Future	5.05E+08	1.51E+09	48.00	1.69E-10	1.41E-10	7.84E-11
Future	1.89E+08	1.70E+09	54.00	1.69E-10	1.41E-10	7.84E-11

Note: Neutron exposure values reported for the surveillance capsules are centered at the core midplane.

Table 6-1 cont'd

Calculated Neutron Exposure Rates And Integrated Exposures
At The Surveillance Capsule Center

IRON ATOM DISPLACEMENTS

Cycle	Cycle Length [EFPS]	Cumulative Irradiation Time [EFPS]	Cumulative Irradiation Time [EFPY]	Displacement Rate [dpa/s]		
				30°	40°	40° → 0° (Cap. X*)
1	3.62E+07	3.62E+07	1.15	6.40E-11	4.20E-11	4.20E-11
2	2.45E+07	6.06E+07	1.92	6.00E-11	3.84E-11	3.84E-11
3	2.40E+07	8.46E+07	2.68	7.35E-11	4.90E-11	4.90E-11
4	2.46E+07	1.09E+08	3.46	5.70E-11	4.27E-11	4.27E-11
5	2.45E+07	1.34E+08	4.24	5.29E-11	3.35E-11	3.35E-11
6	1.59E+07	1.50E+08	4.74	4.84E-11	3.22E-11	3.22E-11
7	2.90E+07	1.79E+08	5.66	5.47E-11	3.67E-11	3.67E-11
8	4.30E+07	2.22E+08	7.03	5.39E-11	3.57E-11	3.57E-11
9	3.26E+07	2.54E+08	8.06	5.29E-11	3.80E-11	3.80E-11
10	3.95E+07	2.94E+08	9.31	4.88E-11	3.31E-11	3.31E-11
11	4.13E+07	3.35E+08	10.62	4.84E-11	3.20E-11	3.20E-11
12	3.91E+07	3.74E+08	11.86	4.91E-11	3.29E-11	1.20E-10
13	3.95E+07	4.14E+08	13.11	4.60E-11	3.32E-11	1.18E-10
14	3.93E+07	4.53E+08	14.36	5.13E-11	3.68E-11	1.25E-10
15	4.18E+07	4.95E+08	15.68	4.86E-11	3.35E-11	1.27E-10
16	4.38E+07	5.39E+08	17.07	5.84E-11	3.48E-11	1.30E-10
17	4.12E+07	5.80E+08	18.37	4.60E-11	3.10E-11	1.28E-10
18	4.65E+07	6.26E+08	19.85	5.31E-11	3.49E-11	1.12E-10
19 (Pjt.)	4.15E+07	6.68E+08	21.16	4.80E-11	3.27E-11	1.28E-10
Future	3.42E+08	1.01E+09	32.00	6.10E-11	4.08E-11	1.69E-10
Future	5.05E+08	1.51E+09	48.00	6.10E-11	4.08E-11	1.69E-10
Future	1.89E+08	1.70E+09	54.00	6.10E-11	4.08E-11	1.69E-10

Note: Neutron exposure values reported for the surveillance capsules are centered at the core midplane.

* Capsule X was irradiated at a 40° location during Cycles 1 through 11 followed by a 0° location during Cycles 12 through 18 when it was subsequently removed from service

Table 6-1 cont'd

Calculated Neutron Exposure Rates And Integrated Exposures
At The Surveillance Capsule Center

IRON ATOM DISPLACEMENTS

Cycle	Cycle Length [EFPS]	Cumulative Irradiation Time [EFPS]	Cumulative Irradiation Time [EFPY]	Displacements [dpa]		
				0°	10°	20°
1	3.62E+07	3.62E+07	1.15	1.01E-02	7.18E-03	3.04E-03
2	2.45E+07	6.06E+07	1.92	1.68E-02	1.19E-02	5.00E-03
3	2.40E+07	8.46E+07	2.68	2.31E-02	1.68E-02	7.25E-03
4	2.46E+07	1.09E+08	3.46	2.96E-02	2.17E-02	9.23E-03
5	2.45E+07	1.34E+08	4.24	3.79E-02	2.76E-02	1.13E-02
6	1.59E+07	1.50E+08	4.74	4.28E-02	3.12E-02	1.26E-02
7	2.90E+07	1.79E+08	5.66	4.97E-02	3.61E-02	1.47E-02
8	4.30E+07	2.22E+08	7.03	6.04E-02	4.33E-02	1.79E-02
9	3.26E+07	2.54E+08	8.06	6.43E-02	4.65E-02	2.00E-02
10	3.95E+07	2.94E+08	9.31	6.88E-02	5.02E-02	2.25E-02
11	4.13E+07	3.35E+08	10.62	7.39E-02	5.42E-02	2.50E-02
12	3.91E+07	3.74E+08	11.86	7.86E-02	5.80E-02	2.74E-02
13	3.95E+07	4.14E+08	13.11	8.33E-02	6.17E-02	2.97E-02
14	3.93E+07	4.53E+08	14.36	8.82E-02	6.56E-02	3.21E-02
15	4.18E+07	4.95E+08	15.68	9.35E-02	6.97E-02	3.47E-02
16	4.38E+07	5.39E+08	17.07	9.92E-02	7.44E-02	3.79E-02
17	4.12E+07	5.80E+08	18.37	1.05E-01	7.84E-02	4.03E-02
18	4.65E+07	6.26E+08	19.85	1.10E-01	8.27E-02	4.33E-02
19 (Pjt.)	4.15E+07	6.68E+08	21.16	1.15E-01	8.68E-02	4.58E-02
Future	3.42E+08	1.01E+09	32.00	1.73E-01	1.35E-01	7.26E-02
Future	5.05E+08	1.51E+09	48.00	2.58E-01	2.06E-01	1.12E-01
Future	1.89E+08	1.70E+09	54.00	2.90E-01	2.33E-01	1.27E-01

Note. Neutron exposure values reported for the surveillance capsules are centered at the core midplane.

Table 6-1 cont'd

Calculated Neutron Exposure Rates And Integrated Exposures
At The Surveillance Capsule Center

IRON ATOM DISPLACEMENTS

Cycle	Cycle Length [EFPS]	Cumulative Irradiation Time [EFPS]	Cumulative Irradiation Time [EFPY]	Displacements [dpa]		
				30°	40°	40° → 0° (Cap. X*)
1	3.62E+07	3.62E+07	1.15	2.31E-03	1.52E-03	1.52E-03
2	2.45E+07	6.06E+07	1.92	3.78E-03	2.46E-03	2.46E-03
3	2.40E+07	8.46E+07	2.68	5.55E-03	3.63E-03	3.63E-03
4	2.46E+07	1.09E+08	3.46	6.95E-03	4.69E-03	4.69E-03
5	2.45E+07	1.34E+08	4.24	8.25E-03	5.51E-03	5 51E-03
6	1.59E+07	1.50E+08	4.74	9.02E-03	6.02E-03	6.02E-03
7	2.90E+07	1.79E+08	5.66	1.06E-02	7.08E-03	7.08E-03
8	4.30E+07	2.22E+08	7.03	1.29E-02	8.62E-03	8.62E-03
9	3.26E+07	2.54E+08	8.06	1.47E-02	9.86E-03	9.86E-03
10	3.95E+07	2.94E+08	9.31	1.66E-02	1.12E-02	1.12E-02
11	4.13E+07	3.35E+08	10.62	1.86E-02	1.25E-02	1.25E-02
12	3.91E+07	3.74E+08	11.86	2.05E-02	1.38E-02	1.72E-02
13	3.95E+07	4.14E+08	13.11	2.23E-02	1.51E-02	2.19E-02
14	3.93E+07	4.53E+08	14.36	2.43E-02	1.65E-02	2.68E-02
15	4.18E+07	4.95E+08	15.68	2.64E-02	1.79E-02	3.21E-02
16	4.38E+07	5.39E+08	17.07	2.89E-02	1.95E-02	3.78E-02
17	4.12E+07	5.80E+08	18.37	3.08E-02	2.07E-02	4.30E-02
18	4.65E+07	6.26E+08	19.85	3.33E-02	2.24E-02	4.82E-02
19 (Pjt.)	4.15E+07	6.68E+08	21.16	3.53E-02	2.37E-02	5.36E-02
Future	3.42E+08	1.01E+09	32.00	5.61E-02	3.77E-02	1.11E-01
Future	5.05E+08	1.51E+09	48.00	8.69E-02	5.82E-02	1.97E-01
Future	1.89E+08	1.70E+09	54.00	9.85E-02	6.60E-02	2.29E-01

Note: Neutron exposure values reported for the surveillance capsules are centered at the core midplane.

* Capsule X was irradiated at a 40° location during Cycles 1 through 11 followed by a 0° location during Cycles 12 through 18 when it was subsequently removed from service.

Table 6-2

Calculated Azimuthal Variation Of Maximum Exposure Rates
And Integrated Exposures At The Reactor Vessel
Clad/Base Metal Interface

Cycle	Cycle Length [EFPS]	Cumulative Irradiation Time [EFPS]	Cumulative Irradiation Time [EFPY]	Neutron Flux (E > 1.0 MeV) [n/cm^2-s]			
				0°	15°	30°	45°
1	3.62E+07	3.62E+07	1.15	6.07E+10	2.78E+10	1.55E+10	1.01E+10
2	2.45E+07	6.06E+07	1.92	5.93E+10	2.70E+10	1.46E+10	9.29E+09
3	2.40E+07	8.46E+07	2.68	5.66E+10	2.94E+10	1.75E+10	1.17E+10
4	2.46E+07	1.09E+08	3.46	5.68E+10	2.76E+10	1.38E+10	1.03E+10
5	2.45E+07	1.34E+08	4.24	7.19E+10	3.14E+10	1.28E+10	7.98E+09
6	1.59E+07	1.50E+08	4.74	6.66E+10	2.91E+10	1.17E+10	7.73E+09
7	2.90E+07	1.79E+08	5.66	5.09E+10	2.41E+10	1.32E+10	8.87E+09
8	4.30E+07	2.22E+08	7.03	5.27E+10	2.41E+10	1.30E+10	8.55E+09
9	3.26E+07	2.54E+08	8.06	3.23E+10	1.88E+10	1.27E+10	9.20E+09
10	3.95E+07	2.94E+08	9.31	3.10E+10	1.87E+10	1.19E+10	8.03E+09
11	4.13E+07	3.35E+08	10.62	3.31E+10	1.86E+10	1.21E+10	7.97E+09
12	3.91E+07	3.74E+08	11.86	3.24E+10	1.86E+10	1.18E+10	7.91E+09
13	3.95E+07	4.14E+08	13.11	3.17E+10	1.78E+10	1.13E+10	8.13E+09
14	3.93E+07	4.53E+08	14.36	3.35E+10	1.92E+10	1.24E+10	8.93E+09
15	4.18E+07	4.95E+08	15.68	3.41E+10	1.89E+10	1.18E+10	8.09E+09
16	4.38E+07	5.39E+08	17.07	3.49E+10	2.13E+10	1.41E+10	8.22E+09
17	4.12E+07	5.80E+08	18.37	3.42E+10	1.80E+10	1.11E+10	7.44E+09
18	4.65E+07	6.26E+08	19.85	2.99E+10	1.86E+10	1.28E+10	8.35E+09
19 (Pjt.)	4.15E+07	6.68E+08	21.16	3.43E+10	1.86E+10	1.16E+10	7.84E+09
Future	3.42E+08	1.01E+09	32.00	3.71E+10	2.28E+10	1.47E+10	9.81E+09
Future	5.05E+08	1.51E+09	48.00	3.71E+10	2.28E+10	1.47E+10	9.81E+09
Future	1.89E+08	1.70E+09	54.00	3.71E+10	2.28E+10	1.47E+10	9.81E+09

Table 6-2 cont'd

Calculated Azimuthal Variation Of Maximum Exposure Rates
And Integrated Exposures At The Reactor Vessel
Clad/Base Metal Interface

Cycle	Cycle Length [EFPS]	Cumulative Irradiation Time [EFPS]	Cumulative Irradiation Time [EFPY]	Neutron Fluence (E > 1.0 MeV) [n/cm^2]			
				0°	15°	30°	45°
1	3.62E+07	3.62E+07	1.15	2.19E+18	1.01E+18	5.59E+17	3.65E+17
2	2.45E+07	6.06E+07	1.92	3.64E+18	1.66E+18	9.17E+17	5.90E+17
3	2.40E+07	8.46E+07	2.68	5.00E+18	2.37E+18	1.34E+18	8.71E+17
4	2.46E+07	1.09E+08	3.46	6.40E+18	3.04E+18	1.68E+18	1.13E+18
5	2.45E+07	1.34E+08	4.24	8.17E+18	3.80E+18	1.99E+18	1.32E+18
6	1.59E+07	1.50E+08	4.74	9.22E+18	4.27E+18	2.18E+18	1.44E+18
7	2.90E+07	1.79E+08	5.66	1.07E+19	4.96E+18	2.56E+18	1.70E+18
8	4.30E+07	2.22E+08	7.03	1.30E+19	5.97E+18	3.12E+18	2.05E+18
9	3.26E+07	2.54E+08	8.06	1.40E+19	6.53E+18	3.53E+18	2.35E+18
10	3.95E+07	2.94E+08	9.31	1.53E+19	7.22E+18	4.00E+18	2.66E+18
11	4.13E+07	3.35E+08	10.62	1.66E+19	7.95E+18	4.50E+18	2.98E+18
12	3.91E+07	3.74E+08	11.86	1.79E+19	8.64E+18	4.96E+18	3.29E+18
13	3.95E+07	4.14E+08	13.11	1.91E+19	9.33E+18	5.41E+18	3.61E+18
14	3.93E+07	4.53E+08	14.36	2.05E+19	1.01E+19	5.90E+18	3.96E+18
15	4.18E+07	4.95E+08	15.68	2.19E+19	1.09E+19	6.39E+18	4.29E+18
16	4.38E+07	5.39E+08	17.07	2.34E+19	1.18E+19	7.00E+18	4.65E+18
17	4.12E+07	5.80E+08	18.37	2.48E+19	1.25E+19	7.46E+18	4.96E+18
18	4.65E+07	6.26E+08	19.85	2.62E+19	1.34E+19	8.05E+18	5.35E+18
19 (Pjt.)	4.15E+07	6.68E+08	21.16	2.76E+19	1.42E+19	8.54E+18	5.67E+18
Future	3.42E+08	1.01E+09	32.00	4.03E+19	2.19E+19	1.35E+19	9.03E+18
Future	5.05E+08	1.51E+09	48.00	5.91E+19	3.33E+19	2.09E+19	1.40E+19
Future	1.89E+08	1.70E+09	54.00	6.61E+19	3.76E+19	2.37E+19	1.58E+19

Table 6-2 cont'd

Calculated Azimuthal Variation Of Fast Neutron Exposure Rates
And Iron Atom Displacement Rates At The Reactor Vessel
Clad/Base Metal Interface

Cycle	Cycle Length [EFPS]	Cumulative Irradiation Time [EFPS]	Cumulative Irradiation Time [EFPY]	Iron Atom Displacement Rate [dpa/s]			
				0°	15°	30°	45°
1	3.62E+07	3.62E+07	1.15	1.05E-10	4.63E-11	2.63E-11	1.66E-11
2	2.45E+07	6.06E+07	1.92	1.02E-10	4.49E-11	2.49E-11	1.52E-11
3	2.40E+07	8.46E+07	2.68	9.74E-11	4.88E-11	2.98E-11	1.91E-11
4	2.46E+07	1.09E+08	3.46	9.79E-11	4.59E-11	2.35E-11	1.69E-11
5	2.45E+07	1.34E+08	4.24	1.24E-10	5.22E-11	2.18E-11	1.31E-11
6	1.59E+07	1.50E+08	4.74	1.15E-10	4.85E-11	2.01E-11	1.27E-11
7	2.90E+07	1.79E+08	5.66	8.77E-11	4.00E-11	2.25E-11	1.45E-11
8	4.30E+07	2.22E+08	7.03	9.08E-11	4.00E-11	2.21E-11	1.40E-11
9	3.26E+07	2.54E+08	8.06	5.56E-11	3.10E-11	2.15E-11	1.50E-11
10	3.95E+07	2.94E+08	9.31	5.33E-11	3.08E-11	2.01E-11	1.31E-11
11	4.13E+07	3.35E+08	10.62	5.69E-11	3.07E-11	2.04E-11	1.30E-11
12	3.91E+07	3.74E+08	11.86	5.56E-11	3.07E-11	2.00E-11	1.29E-11
13	3.95E+07	4.14E+08	13.11	5.45E-11	2.94E-11	1.91E-11	1.33E-11
14	3.93E+07	4.53E+08	14.36	5.76E-11	3.17E-11	2.10E-11	1.46E-11
15	4.18E+07	4.95E+08	15.68	5.85E-11	3.12E-11	1.99E-11	1.32E-11
16	4.38E+07	5.39E+08	17.07	6.00E-11	3.51E-11	2.39E-11	1.35E-11
17	4.12E+07	5.80E+08	18.37	5.88E-11	2.98E-11	1.88E-11	1.22E-11
18	4.65E+07	6.26E+08	19.85	5.14E-11	3.06E-11	2.16E-11	1.36E-11
19 (Pjt.)	4.15E+07	6.68E+08	21.16	5.89E-11	3.07E-11	1.96E-11	1.28E-11
Future	3.42E+08	1.01E+09	32.00	6.39E-11	3.76E-11	2.49E-11	1.60E-11
Future	5.05E+08	1.51E+09	48.00	6.39E-11	3.76E-11	2.49E-11	1.60E-11
Future	1.89E+08	1.70E+09	54.00	6.39E-11	3.76E-11	2.49E-11	1.60E-11

Table 6-2 cont'd

Calculated Azimuthal Variation Of Maximum Exposure Rates
And Integrated Exposures At The Reactor Vessel
Clad/Base Metal Interface

Cycle	Cycle Length [EFPS]	Cumulative Irradiation Time [EFPS]	Cumulative Irradiation Time [EFPY]	Iron Atom Displacements [dpa]			
				0°	15°	30°	45°
1	3.62E+07	3.62E+07	1.15	3.78E-03	1.67E-03	9.51E-04	5.99E-04
2	2.45E+07	6.06E+07	1.92	6.28E-03	2.76E-03	1.56E-03	9.67E-04
3	2.40E+07	8.46E+07	2.68	8.62E-03	3.93E-03	2.28E-03	1.43E-03
4	2.46E+07	1.09E+08	3.46	1.10E-02	5.06E-03	2.85E-03	1.84E-03
5	2.45E+07	1.34E+08	4.24	1.41E-02	6.32E-03	3.39E-03	2.16E-03
6	1.59E+07	1.50E+08	4.74	1.59E-02	7.09E-03	3.71E-03	2.36E-03
7	2.90E+07	1.79E+08	5.66	1.84E-02	8.25E-03	4.36E-03	2.78E-03
8	4.30E+07	2.22E+08	7.03	2.23E-02	9.92E-03	5.31E-03	3.37E-03
9	3.26E+07	2.54E+08	8 06	2.42E-02	1.08E-02	6.01E-03	3.85E-03
10	3.95E+07	2.94E+08	9.31	2.63E-02	1.20E-02	6.81E-03	4.36E-03
11	4.13E+07	3.35E+08	10.62	2.86E-02	1.32E-02	7.65E-03	4.88E-03
12	3.91E+07	3.74E+08	11.86	3.08E-02	1.43E-02	8.43E-03	5.39E-03
13	3.95E+07	4.14E+08	13.11	3.29E-02	1.55E-02	9.19E-03	5.90E-03
14	3.93E+07	4.53E+08	14.36	3.52E-02	1.67E-02	1.00E-02	6.47E-03
15	4.18E+07	4.95E+08	15.68	3.77E-02	1.80E-02	1.08E-02	7.03E-03
16	4.38E+07	5.39E+08	17.07	4.03E-02	1.95E-02	1.19E-02	7.61E-03
17	4.12E+07	5.80E+08	18.37	4.27E-02	2.08E-02	1.27E-02	8.11E-03
18	4 65E+07	6.26E+08	19.85	4.51E-02	2.22E-02	1.37E-02	8.75E-03
19 (Pjt.)	4.15E+07	6.68E+08	21.16	4.75E-02	2.35E-02	1.45E-02	9.28E-03
Future	3.42E+08	1.01E+09	32.00	6.94E-02	3.62E-02	2.30E-02	1.48E-02
Future	5.05E+08	1.51E+09	48.00	1.02E-01	5.50E-02	3.55E-02	2.29E-02
Future	1.89E+08	1.70E+09	54.00	1.14E-01	6.21E-02	4.02E-02	2.59E-02

Table 6-3

Calculated Azimuthal Variation Of Maximum Exposure Rates
And Integrated Exposures At The Intermediate Shell Course to Lower Shell Course Girth Weld
Clad/Base Metal Interface

Cycle	Cycle Length [EFPS]	Cumulative Irradiation Time [EFPS]	Cumulative Irradiation Time [EFPY]	Neutron Flux (E > 1.0 MeV) [n/cm^2-s]			
				0°	15°	30°	45°
1	3.62E+07	3.62E+07	1.15	5.90E+10	2.71E+10	1.50E+10	9.84E+09
2	2.45E+07	6.06E+07	1.92	5.75E+10	2.62E+10	1.42E+10	9.01E+09
3	2.40E+07	8.46E+07	2.68	5.46E+10	2.84E+10	1.69E+10	1.13E+10
4	2.46E+07	1.09E+08	3.46	5.52E+10	2.68E+10	1.34E+10	1.00E+10
5	2.45E+07	1.34E+08	4.24	6.84E+10	2.98E+10	1.22E+10	7.59E+09
6	1.59E+07	1.50E+08	4.74	6.45E+10	2.82E+10	1.14E+10	7.49E+09
7	2.90E+07	1.79E+08	5.66	4.96E+10	2.35E+10	1.29E+10	8.64E+09
8	4.30E+07	2.22E+08	7.03	4.86E+10	2.22E+10	1.20E+10	7.88E+09
9	3.26E+07	2.54E+08	8.06	2.08E+10	1.50E+10	1.22E+10	8.88E+09
10	3.95E+07	2.94E+08	9.31	1.99E+10	1.46E+10	1.11E+10	7.58E+09
11	4.13E+07	3.35E+08	10.62	2.14E+10	1.50E+10	1.15E+10	7.59E+09
12	3.91E+07	3.74E+08	11.86	2.09E+10	1.49E+10	1.15E+10	7.70E+09
13	3.95E+07	4.14E+08	13.11	2.05E+10	1.42E+10	1.08E+10	7.86E+09
14	3.93E+07	4.53E+08	14.36	2.17E+10	1.52E+10	1.17E+10	8.44E+09
15	4.18E+07	4.95E+08	15.68	2.18E+10	1.48E+10	1.11E+10	7.67E+09
16	4.38E+07	5.39E+08	17.07	2.24E+10	1.69E+10	1.33E+10	7.82E+09
17	4.12E+07	5.80E+08	18.37	2.21E+10	1.41E+10	1.06E+10	7.13E+09
18	4.65E+07	6.26E+08	19.85	1.94E+10	1.51E+10	1.23E+10	8.05E+09
19 (Pjt.)	4.15E+07	6.68E+08	21.16	2.22E+10	1.46E+10	1.10E+10	7.49E+09
Future	3.42E+08	1.01E+09	32.00	3.55E+10	2.18E+10	1.40E+10	9.38E+09
Future	5.05E+08	1.51E+09	48.00	3.55E+10	2.18E+10	1.40E+10	9.38E+09
Future	1.89E+08	1.70E+09	54.00	3.55E+10	2.18E+10	1.40E+10	9.38E+09

Table 6-3 cont'd

Calculated Azimuthal Variation Of Maximum Exposure Rates
And Integrated Exposures At The Intermediate Shell Course to Lower Shell Course Girth Weld
Clad/Base Metal Interface

Cycle	Cycle Length [EFPS]	Cumulative Irradiation Time [EFPS]	Cumulative Irradiation Time [EFPY]	Neutron Fluence (E > 1.0 MeV) [n/cm^2]			
				0°	15°	30°	45°
1	3.62E+07	3.62E+07	1.15	2.13E+18	9.79E+17	5.44E+17	3.56E+17
2	2.45E+07	6.06E+07	1.92	3.54E+18	1.62E+18	8.90E+17	5.76E+17
3	2.40E+07	8.46E+07	2.68	4.85E+18	2.30E+18	1.30E+18	8.47E+17
4	2.46E+07	1.09E+08	3.46	6.21E+18	2.96E+18	1.63E+18	1.09E+18
5	2.45E+07	1.34E+08	4.24	7.89E+18	3.69E+18	1.93E+18	1.28E+18
6	1.59E+07	1.50E+08	4.74	8.91E+18	4.14E+18	2.11E+18	1.40E+18
7	2.90E+07	1.79E+08	5.66	1.04E+19	4.82E+18	2.48E+18	1.65E+18
8	4.30E+07	2.22E+08	7.03	1.24E+19	5.78E+18	2.99E+18	1.99E+18
9	3.26E+07	2.54E+08	8.06	1.31E+19	6.27E+18	3.39E+18	2.28E+18
10	3.95E+07	2.94E+08	9.31	1.39E+19	6.85E+18	3.83E+18	2.58E+18
11	4.13E+07	3.35E+08	10.62	1.48E+19	7.47E+18	4.31E+18	2.89E+18
12	3.91E+07	3.74E+08	11.86	1.56E+19	8.05E+18	4.76E+18	3.19E+18
13	3.95E+07	4.14E+08	13.11	1.64E+19	8.61E+18	5.18E+18	3.50E+18
14	3.93E+07	4.53E+08	14.36	1.73E+19	9.20E+18	5.64E+18	3.84E+18
15	4.18E+07	4.95E+08	15.68	1.82E+19	9.82E+18	6.11E+18	4.16E+18
16	4.38E+07	5.39E+08	17.07	1.92E+19	1.06E+19	6 69E+18	4.50E+18
17	4.12E+07	5.80E+08	18.37	2.01E+19	1.11E+19	7.12E+18	4.79E+18
18	4.65E+07	6.26E+08	19.85	2.10E+19	1.19E+19	7.69E+18	5.17E+18
19 (Pjt.)	4.15E+07	6.68E+08	21.16	2.19E+19	1.25E+19	8.15E+18	5.48E+18
Future	3.42E+08	1.01E+09	32.00	3.40E+19	1.99E+19	1.29E+19	8.68E+18
Future	5.05E+08	1.51E+09	48.00	5.20E+19	3.09E+19	2.00E+19	1.34E+19
Future	1.89E+08	1.70E+09	54.00	5.87E+19	3.50E+19	2.27E+19	1.52E+19

Table 6-3 cont'd

Calculated Azimuthal Variation Of Fast Neutron Exposure Rates
And Integrated Exposures At The Intermediate Shell Course to Lower Shell Course Girth Weld
Clad/Base Metal Interface

Cycle	Cycle Length [EFPS]	Cumulative Irradiation Time [EFPS]	Cumulative Irradiation Time [EFPY]	Iron Atom Displacement Rate [dpa/s]			
				0°	15°	30°	45°
1	3.62E+07	3.62E+07	1.15	1.02E-10	4.52E-11	2.57E-11	1.62E-11
2	2.45E+07	6.06E+07	1.92	9.95E-11	4.37E-11	2.42E-11	1.48E-11
3	2.40E+07	8.46E+07	2.68	9.44E-11	4.73E-11	2.89E-11	1.85E-11
4	2.46E+07	1.09E+08	3.46	9.54E-11	4.47E-11	2.29E-11	1.65E-11
5	2.45E+07	1.34E+08	4.24	1.18E-10	4.98E-11	2.08E-11	1.25E-11
6	1.59E+07	1.50E+08	4.74	1.12E-10	4.71E-11	1.95E-11	1.24E-11
7	2.90E+07	1.79E+08	5.66	8.58E-11	3.92E-11	2.20E-11	1.42E-11
8	4.30E+07	2.22E+08	7.03	8.40E-11	3.70E-11	2.04E-11	1.30E-11
9	3.26E+07	2.54E+08	8.06	3.59E-11	2.48E-11	2.07E-11	1.45E-11
10	3.95E+07	2.94E+08	9.31	3.45E-11	2.42E-11	1.89E-11	1.24E-11
11	4.13E+07	3.35E+08	10.62	3.70E-11	2.48E-11	1.95E-11	1.24E-11
12	3.91E+07	3.74E+08	11.86	3.61E-11	2.46E-11	1.95E-11	1.26E-11
13	3.95E+07	4.14E+08	13.11	3.55E-11	2.34E-11	1.84E-11	1.29E-11
14	3.93E+07	4.53E+08	14.36	3.75E-11	2.51E-11	1.99E-11	1.38E-11
15	4.18E+07	4.95E+08	15.68	3.77E-11	2.45E-11	1.89E-11	1.26E-11
16	4.38E+07	5.39E+08	17.07	3.87E-11	2.79E-11	2.26E-11	1.29E-11
17	4.12E+07	5.80E+08	18.37	3.82E-11	2.33E-11	1.80E-11	1.17E-11
18	4.65E+07	6.26E+08	19.85	3.36E-11	2.49E-11	2.08E-11	1.32E-11
19 (Pjt.)	4.15E+07	6.68E+08	21.16	3.84E-11	2.42E-11	1.87E-11	1.23E-11
Future	3.42E+08	1.01E+09	32.00	6.13E-11	3.61E-11	2.38E-11	1.54E-11
Future	5.05E+08	1.51E+09	48.00	6.13E-11	3.61E-11	2.38E-11	1.54E-11
Future	1.89E+08	1.70E+09	54.00	6.13E-11	3.61E-11	2.38E-11	1.54E-11

Table 6-3 cont'd

Calculated Azimuthal Variation Of Maximum Exposure Rates
And Integrated Exposures At The Intermediate Shell Course to Lower Shell Course Girth Weld
Clad/Base Metal Interface

Cycle	Cycle Length [EFPS]	Cumulative Irradiation Time [EFPS]	Cumulative Irradiation Time [EFPY]	Iron Atom Displacements [dpa]			
				0°	15°	30°	45°
1	3.62E+07	3.62E+07	1.15	3.69E-03	1.63E-03	9.29E-04	5.85E-04
2	2.45E+07	6.06E+07	1.92	6.13E-03	2.70E-03	1.52E-03	9.48E-04
3	2.40E+07	8.46E+07	2.68	8.39E-03	3.84E-03	2.22E-03	1.39E-03
4	2.46E+07	1.09E+08	3.46	1.07E-02	4.94E-03	2.78E-03	1.80E-03
5	2.45E+07	1.34E+08	4.24	1.36E-02	6.16E-03	3.29E-03	2.11E-03
6	1.59E+07	1.50E+08	4.74	1.54E-02	6.91E-03	3.60E-03	2.30E-03
7	2.90E+07	1.79E+08	5.66	1.79E-02	8.05E-03	4.24E-03	2.71E-03
8	4.30E+07	2.22E+08	7.03	2.15E-02	9.64E-03	5.12E-03	3.27E-03
9	3.26E+07	2.54E+08	8.06	2.27E-02	1.04E-02	5.79E-03	3.75E-03
10	3.95E+07	2.94E+08	9.31	2.41E-02	1.14E-02	6.54E-03	4.24E-03
11	4.13E+07	3.35E+08	10.62	2.56E-02	1.24E-02	7.34E-03	4.75E-03
12	3.91E+07	3.74E+08	11.86	2.70E-02	1.34E-02	8.11E-03	5.24E-03
13	3.95E+07	4.14E+08	13.11	2.84E-02	1.43E-02	8.83E-03	5.75E-03
14	3.93E+07	4.53E+08	14.36	2.99E-02	1.53E-02	9.61E-03	6.29E-03
15	4.18E+07	4.95E+08	15.68	3.14E-02	1.63E-02	1.04E-02	6.82E-03
16	4.38E+07	5.39E+08	17.07	3.31E-02	1.75E-02	1.14E-02	7.38E-03
17	4.12E+07	5.80E+08	18.37	3.47E-02	1.85E-02	1.21E-02	7.86E-03
18	4.65E+07	6.26E+08	19.85	3.63E-02	1.97E-02	1.31E-02	8.47E-03
19 (Pjt.)	4.15E+07	6.68E+08	21.16	3.79E-02	2.07E-02	1.39E-02	8.98E-03
Future	3.42E+08	1.01E+09	32.00	5.88E-02	3.30E-02	2.20E-02	1.42E-02
Future	5.05E+08	1.51E+09	48.00	8.98E-02	5.12E-02	3.41E-02	2.20E-02
Future	1.89E+08	1.70E+09	54.00	1.01E-01	5.80E-02	3.86E-02	2.49E-02

Table 6-4

Relative Radial Distribution Of Neutron Fluence (E > 1.0 MeV)
Within The Reactor Vessel Wall

RADIUS (cm)	AZIMUTHAL ANGLE			
	0°	15°	30°	45°
197.881	1.000	1.000	1.000	1.000
202.802	0.591	0.596	0.600	0.595
207.724	0.308	0.311	0.318	0.311
212.645	0.152	0.155	0.161	0.158
217.566	0.064	0.069	0.076	0.079

Note:
Base Metal Inner Radius = 197.881 cm
Base Metal 1/4T = 202.802 cm
Base Metal 1/2T = 207.724 cm
Base Metal 3/4T = 212.645 cm
Base Metal Outer Radius = 217.566 cm

Table 6-5

Relative Radial Distribution Of Iron Atom Displacements (dpa)
Within The Reactor Vessel Wall

RADIUS (cm)	AZIMUTHAL ANGLE			
	0°	15°	30°	45°
197.881	1.000	1.000	1.000	1.000
202.802	0.678	0.696	0.692	0.691
207.724	0.430	0.451	0.452	0.453
212.645	0.256	0.280	0.287	0.296
217.566	0.120	0.145	0.164	0.187

Note:
Base Metal Inner Radius = 197.881 cm
Base Metal 1/4T = 202.802 cm
Base Metal 1/2T = 207.724 cm
Base Metal 3/4T = 212.645 cm
Base Metal Outer Radius = 217.566 cm

Table 6-6

Calculated Fast Neutron Exposure of Surveillance Capsules
Withdrawn from Turkey Point Unit 3

Capsule	Irradiation Time [EFPY]	Fluence (E > 1.0 MeV) [n/cm^2]	Iron Displacements [dpa]
T	1.15	5.99E+18	1.01E-02
S	3.46	1.27E+19	2.17E-02
V	8.06	1.22E+19	2.00E-02
X	19.85	2.90E+19	4.82E-02

Table 6-7

Calculated Surveillance Capsule Lead Factors

Capsule ID And Location	Status	Lead Factor
T (0°)	Withdrawn EOC 1	2.73
S (10°)	Withdrawn EOC 4	1.99
V (20°)	Withdrawn EOC 9	0.87
X (40° Ψ 0°)	Withdrawn EOC 18	1.11
U (30°)	In Reactor	0.78
Y (30°)	In Reactor	0.78
W (40°)	In Reactor	0.53
Z (40°)	In Reactor	0.53

Notes: (1) Capsule X was irradiated at a 40° location for Cycles 1 through 11, and at a 0° location during Cycles 12 through 18, after which it was removed from service.
(2) Lead factors for capsules remaining in the reactor are based on cycle specific exposure calculations through the current operating fuel reload, i.e., Cycle 19.

7 SURVEILLANCE CAPSULE REMOVAL SCHEDULE

The following surveillance capsule removal schedule meets the requirements of ASTM E185-82 and is recommended for future capsules to be removed from the Turkey Point Unit 3 and Unit 4 reactor vessels.

Table 7-1

Turkey Point Unit 3 and Unit 4 Reactor Vessel Surveillance Capsule Withdrawal Schedule

Capsule	Withdrawal EFPY[(a)]	Fluence (n/cm^2)
T3	1.15	7.39×10^{18} (b)
T4	1.17	7.08×10^{18} (b)
S3	3.46	1.72×10^{19} (b)
S4	3.41	1.43×10^{19} (b)
V3	8.06	1.53×10^{19} (b)
X3	19.85	2.90×10^{19} (b)
X4	35[(c)]	5.91×10^{19} (c)
U3	Standby	--
Y3	Standby	--
W3	Standby	--
Z3	Standby	--
U4	Standby	--
V4	Standby	--
Y4	Standby	--
W4	Standby	--
Z4	Standby	--

Notes

(a) Effective Full Power Years (EFPY) from plant startup.

(b) Plant Specific Evaluation

(c) Capsule X4 will reach a fluence of 5.91×10^{19} at 35 EFPY (peak EOL vessel fluence).

8 REFERENCES

1. WCAP-7656, "*Florida Power and Light Co. Turkey Point Unit No. 3 Reactor Vessel Radiation Surveillance Program*," S. E. Yanichko, May 1971.

2. Code of Federal Regulations, 10CFR50, Appendix G, *Fracture Toughness Requirements*, U.S. Nuclear Regulatory Commission, Washington, D.C.

3. Regulatory Guide 1.99, Revision 2, May 1988, *Radiation Embrittlement of Reactor Vessel Materials*

4. Section XI of the ASME Boiler and Pressure Vessel Code, Appendix G, *Fracture Toughness Criteria for Protection Against Failure*

5. ASTM E208, *Standard Test Method for Conducting Drop-Weight Test to Determine Nil-Ductility Transition Temperature of Ferritic Steels*, in ASTM Standards, Section 3, American Society for Testing and Materials, Philadelphia, PA.

6. ASTM E185-82, *Standard Practice for Conducting Surveillance Tests for Light-Water Cooled Nuclear Power Reactor Vessels*, E706 (IF), in ASTM Standards, Section 3, American Society for Testing and Materials, Philadelphia, PA, 1993.

7. WCAP-15092 Revision 3, "Turkey Point Units 3 and 4 WOG Reactor Vessel 60-Year Evaluaion Minigroup Heatup and Cooldown Limit Curves for Normal Operation" T. J. Laubham and J. H. Ledger, May 2000.

8. ASTM E23-98, Standard Test Method for Notched Bar Impact Testing of Metallic Materials.

9. ASTM A370-97a, Standard Test Methods and Definitions for Mechanical Testing of Steel Products

10. ASTM E8-99, Standard Test Methods for Tension Testing of Metallic Materials

11. ASTM E21-92 (1998), Standard Test Methods for Elevated Temperature Tension Tests of Metallic Materials

12. ASTM E83-93, Standard Practice for Verification and Classification of Extensometers

13. ASTM Designation E185-66, Surveillance Tests on Structural Materials in Nuclear Reactors

14. Regulatory Guide RG-1.190, "Calculational and Dosimetry Methods for Determining Pressure Vessel Neutron Fluence," U. S. Nuclear Regulatory Commission, Office of Nuclear Regulatory Research, March 2001.

15. WCAP-14040-NP-A, Revision 2, "Methodology Used to Develop Cold Overpressure Mitigating System Setpoints and RCS Heatup and Cooldown Limit Curves," January 1996.

16. WCAP-15557, Revision 0, "Qualification of the Westinghouse Pressure Vessel Neutron Fluence Evaluation Methodology," August 2000.

17. RSICC Computer Code Collection CCC-650, "DOORS 3.1, One, Two- and Three-Dimensional Discrete Ordinates Neutron/Photon Transport Code System," August 1996.

18. RSIC Data Library Collection DLC-185, "BUGLE-96, Coupled 47 Neutron, 20 Gamma-Ray Group Cross Section Library Derived from ENDF/B-VI for LWR Shielding and Pressure Vessel Dosimetry Applications," March 1996.

19. BAW-2312, Revision 1 "Low Upper-Shelf Toughness Fracture Mechanics Analysis of Reactor Vessels of Turkey Point Units 3 and 4 for Extended Life Through 48 Effective Full Power Years" (FTI Document No. 77-2312-01) transmitted by letter FTI-00-3072 dated 12/18/2000 to E. Thompson.

20. Licensing Letter L-85-66, J. W. Williams to D. G. Eisenhut "Turkey Point Units 3 and 4 Proposed License Amendment, Reactor Plant Surveillance Material Program" dated 2/8/1985.

21. NRC letter dated 4/22/1985, Safety Evaluation by NRR Related to Amendment No. 112 to Facility Operating License No. DPR-31 and Amendment No. 106 to Facility Operating License No. DPR-41, D. G. Macdonald to J. W. Williams

APPENDIX A

VALIDATION OF THE RADIATION TRANSPORT MODELS BASED ON NEUTRON DOSIMETRY MEASUREMENTS

A.1 Neutron Dosimetry

Comparisons of measured dosimetry results to both the calculated and least squares adjusted values for all surveillance capsules withdrawn from service to date at Turkey Point Unit 3 are described herein. The sensor sets from these capsules have been analyzed in accordance with the current dosimetry evaluation methodology described in Regulatory Guide 1.190, "Calculational and Dosimetry Methods for Determining Pressure Vessel Neutron Fluence."[A-1] One of the main purposes for presenting this material is to demonstrate that the overall measurements agree with the calculated and least squares adjusted values to within ± 20% as specified by Regulatory Guide 1.190, thus serving to validate the calculated neutron exposures previously reported in Section 6.2 of this report. This information may also be useful in the future, in particular, as least squares adjustment techniques become accepted in the regulatory environment.

A.1.1 Sensor Reaction Rate Determinations

In this section, the results of the evaluations of the four neutron sensor sets withdrawn to date as a part of the Turkey Point Unit 3 Reactor Vessel Materials Surveillance Program are presented. The capsule designation, location within the reactor, and time of withdrawal of each of these dosimetry sets were as follows:

Capsule ID	Azimuthal Location	Withdrawal Time	Irradiation Time [EFPY]
T	0°	End of Cycle 1	1.15
S	10°	End of Cycle 4	3.46
V	20°	End of Cycle 9	8.06
X*	40° → 0°	End of Cycle 18	19.85

* Capsule X was irradiated at a 40° location during Cycles 1 through 11 followed by irradiation at a 0° location during Cycles 12 through 18 when it was subsequently removed from service.

The azimuthal locations included in the above tabulation represent the first octant equivalent azimuthal angle of the geometric center of the respective surveillance capsules.

The passive neutron sensors included in the evaluations of Surveillance Capsules T, S, V, and X are summarized as follows:

Sensor Material	Reaction Of Interest	Capsule T	Capsule S	Capsule V	Capsule X
Copper	$^{63}Cu(n,\alpha)^{60}Co$	X	X	X	X
Iron	$^{54}Fe(n,p)^{54}Mn$	X	X	X	X
Nickel	$^{58}Ni(n,p)^{58}Co$	X	N/A	N/A	N/A
Uranium-238	$^{238}U(n,f)^{137}Cs$	X	N/A	X	X
Neptunium-237	$^{237}Np(n,f)^{137}Cs$	X	N/A	X	X
Cobalt-Aluminum*	$^{59}Co(n,\gamma)^{60}Co$	N/A	X	X	X

* The cobalt-aluminum measurements for this plant include both bare wire and cadmium-covered sensors.

The copper, iron, nickel, and cobalt-aluminum monitors, in wire form, were placed in holes drilled in spacers at several radial locations within the test specimen array. As a result, gradient corrections were applied to these measured reaction rates in order to index all of the sensor measurements to the radial center of the respective surveillance capsules. Since the cadmium-shielded uranium and neptunium fission monitors were accommodated within the dosimeter block centered at the radial, azimuthal, and axial center of the material test specimen array, gradient corrections were not required for the fission monitor reaction rates. Pertinent physical and nuclear characteristics of the passive neutron sensors are listed in Table A-1.

The use of passive monitors such as those listed above does not yield a direct measure of the energy dependent neutron flux at the point of interest. Rather, the activation or fission process is a measure of the integrated effect that the time and energy dependent neutron flux has on the target material over the course of the irradiation period. An accurate assessment of the average neutron flux level incident on the various monitors may be derived from the activation measurements only if the irradiation parameters are well known. In particular, the following variables are of interest:

- the measured specific activity of each monitor,
- the physical characteristics of each monitor,
- the operating history of the reactor,
- the energy response of each monitor, and
- the neutron energy spectrum at the monitor location.

The radiometric counting of the neutron sensors from Capsule T was carried out at the Westinghouse Analytical Services Laboratory at the Waltz Mill Site.[A-2] The radiometric counting of the sensors from Capsules S and V were performed by the Southwest Research Institute.[A-3 and A-4] The radiometric counting of the sensors from Capsule X was completed at the Antech Analytical Laboratory, also located at the Waltz Mill Site. In all cases, the radiometric counting followed established ASTM procedures. Following sample preparation and weighing, the specific activity of each sensor was determined by means of a high-resolution gamma spectrometer. For the copper, iron, nickel, and cobalt-aluminum sensors, these analyses were performed by direct counting of each of the individual samples. In the case of the uranium and neptunium fission sensors, the analyses were carried out by direct counting preceded by dissolution and chemical separation of cesium from the sensor material.

It is worthwhile noting that the majority of measured reaction rates for Capsules S and V were determined to be statistically different than similar measurement data obtained from the Westinghouse 3-loop, thermal-shield reactor plant database for 10° and 20° surveillance capsules. In addition, Reference A-5 documents that detector calibration problems existed at the laboratory that performed the Capsule S counting reported in Reference A-3. Furthermore, Reference A-4 states that the counting "data is inconclusive for computing fluence rate" for all Capsule V dosimetry measurements except for iron. As a result, the Capsule S and V measurements were not utilized in the least squares adjustment calculation for these capsules.

The irradiation history of the reactor over the irradiation periods experienced by Capsules T, S, V, and X was based on the reported monthly power generation of Turkey Point Unit 3 from initial reactor startup through the end of the dosimetry evaluation period. For the sensor sets utilized in the surveillance capsules, the half-lives of the product isotopes are long enough that a monthly histogram describing reactor operation has proven to be an adequate representation for use in radioactive decay corrections for the reactions of interest in the exposure evaluations. The irradiation history applicable to Capsules T, S, V, and X is given in Table A-2.

Having the measured specific activities, the physical characteristics of the sensors, and the operating history of the reactor, reaction rates referenced to full-power operation were determined from the following equation:

$$R = \frac{A}{N_0 \, F \, Y \, \Sigma \, \frac{P_j}{P_{ref}} \, C_j \, [1 - e^{-\lambda t_j}] \, [e^{-\lambda t_d}]}$$

where:

R	=	Reaction rate averaged over the irradiation period and referenced to operation at a core power level of P_{ref} (rps/nucleus).
A	=	Measured specific activity (dps/gm).
N_0	=	Number of target element atoms per gram of sensor.
F	=	Weight fraction of the target isotope in the sensor material.
Y	=	Number of product atoms produced per reaction.
P_j	=	Average core power level during irradiation period j (MW).
P_{ref}	=	Maximum or reference power level of the reactor (MW).
C_j	=	Calculated ratio of $\phi(E > 1.0 \text{ MeV})$ during irradiation period j to the time weighted average $\phi(E > 1.0 \text{ MeV})$ over the entire irradiation period.
λ	=	Decay constant of the product isotope (1/sec).
t_j	=	Length of irradiation period j (sec).
t_d	=	Decay time following irradiation period j (sec).

and the summation is carried out over the total number of monthly intervals comprising the irradiation period.

In the equation describing the reaction rate calculation, the ratio $[P_j]/[P_{ref}]$ accounts for month-by-month variation of reactor core power level within any given fuel cycle as well as over multiple fuel cycles. The ratio C_j, which was calculated for each fuel cycle using the transport methodology discussed in Section 6.2, accounts for the change in sensor reaction rates caused by variations in flux level induced by changes in core spatial power distributions from fuel cycle to fuel cycle. For a single-cycle irradiation, C_j is normally taken to be 1.0. However, for multiple-cycle irradiations, particularly those employing low leakage fuel management, the additional C_j term should be employed. The impact of changing flux levels for constant power operation can be quite significant for sensor sets that have been irradiated for many cycles in a reactor that has transitioned from non-low leakage to low leakage fuel management or for sensor sets contained in surveillance capsules that have been moved from one capsule location to another.

The fuel cycle specific neutron flux values along with the computed values for C_j are listed in Table A-3. These flux values represent the cycle dependent results at the radial and azimuthal center of the respective capsules at the axial elevation of the active fuel midplane.

Prior to using the measured reaction rates in the least-squares evaluations of the dosimetry sensor sets, additional corrections were made to the ^{238}U measurements to account for the presence of ^{235}U impurities in the sensors as well as to adjust for the build-in of plutonium isotopes over the course of the irradiation. Corrections were also made to the ^{238}U and ^{237}Np sensor reaction rates to account for gamma ray induced fission reactions that occurred over the course of the capsule irradiations. The correction factors applied to the Turkey Point Unit 3 fission sensor reaction rates are summarized as follows:

Correction	Capsule T	Capsule S*	Capsule V*	Capsule X
^{235}U Impurity/Pu Build-in	0.861	N/A	0.837	0.780
^{238}U(γ,f)	0.959	N/A	0.960	0.957
Net ^{238}U Correction	0.826	N/A	0.804	0.746
^{237}Np(γ,f)	0.985	N/A	0.984	0.982

* Type I capsules (e.g., S) do not contain ^{238}U and ^{237}Np sensors whereas Type II capsules (e.g., T, V, and X) contain fission monitors. As a result, the aforementioned corrections are not applicable to Type I capsules. Also recognize that most of the Capsule S and V measured reaction rates were determined to be statistically different than the corresponding data obtained from the Westinghouse 3-loop, thermal-shield plant database for 10° and 20° surveillance capsules. This is consistent with historical documentation that describes detector calibration problems at the Southwest Research Institute laboratory that analyzed Capsule S (see Reference A-5) and a statement in the Southwest Research Institute dosimetry analysis report for Capsule V that suggests the counting "data is inconclusive for computing fluence rate" for all measured results except for iron (see Reference A-4). Therefore, the Capsule S and V measurement results were not used in the subsequent least squares adjustment calculation involving these capsules.

These factors were applied in a multiplicative fashion to the decay corrected uranium and neptunium fission sensor reaction rates.

Results of the sensor reaction rate determinations for Capsules T, S, V, and X are given in Table A-4. In Table A-4, the measured specific activities, decay corrected saturated specific activities, and computed reaction rates for each sensor indexed to the radial center of the capsule are listed. The fission sensor reaction rates are listed both with and without the applied corrections for ^{238}U impurities, plutonium build-in, and gamma ray induced fission effects.

A.1.2 Least Squares Evaluation of Sensor Sets

Least squares adjustment methods provide the capability of combining the measurement data with the corresponding neutron transport calculations resulting in a Best Estimate neutron energy spectrum with associated uncertainties. Best Estimates for key exposure parameters such as $\phi(E > 1.0\ \text{MeV})$ or dpa/s along with their uncertainties are then easily obtained from the adjusted spectrum. In general, the least squares methods, as applied to surveillance capsule dosimetry evaluations, act to reconcile the measured sensor reaction rate data, dosimetry reaction cross-sections, and the calculated neutron energy spectrum within their respective uncertainties. For example,

$$R_i \pm \delta_{R_i} = \sum_g (\sigma_{ig} \pm \delta_{\sigma_{ig}})(\phi_g \pm \delta_{\phi_g})$$

relates a set of measured reaction rates, R_i, to a single neutron spectrum, ϕ_g, through the multigroup dosimeter reaction cross-section, σ_{ig}, each with an uncertainty δ. The primary objective of the least squares evaluation is to produce unbiased estimates of the neutron exposure parameters at the location of the measurement.

For the least squares evaluation of the Turkey Point Unit 3 surveillance capsule dosimetry, the FERRET code[A-6] was employed to combine the results of the plant specific neutron transport calculations and sensor set reaction rate measurements to determine best-estimate values of exposure parameters

(ϕ(E > 1.0 MeV) and dpa) along with associated uncertainties for the four in-vessel capsules withdrawn to date.

The application of the least squares methodology requires the following input:

1 - The calculated neutron energy spectrum and associated uncertainties at the measurement location.
2 - The measured reaction rates and associated uncertainty for each sensor contained in the multiple foil set.
3 - The energy dependent dosimetry reaction cross-sections and associated uncertainties for each sensor contained in the multiple foil sensor set.

For the Turkey Point Unit 3 application, the calculated neutron spectrum was obtained from the results of plant specific neutron transport calculations described in Section 6.2 of this report. The sensor reaction rates were derived from the measured specific activities using the procedures described in Section A.1.1. The dosimetry reaction cross-sections and uncertainties were obtained from the SNLRML dosimetry cross-section library[A-7]. The SNLRML library is an evaluated dosimetry reaction cross-section compilation recommended for use in LWR evaluations by ASTM Standard E1018, "Application of ASTM Evaluated Cross-Section Data File, Matrix E 706 (IIB)".

The uncertainties associated with the measured reaction rates, dosimetry cross-sections, and calculated neutron spectrum were input to the least squares procedure in the form of variances and covariances. The assignment of the input uncertainties followed the guidance provided in ASTM Standard E 944, "Application of Neutron Spectrum Adjustment Methods in Reactor Surveillance."

The following provides a summary of the uncertainties associated with the least squares evaluation of the Turkey Point Unit 3 surveillance capsule sensor sets.

Reaction Rate Uncertainties

The overall uncertainty associated with the measured reaction rates includes components due to the basic measurement process, irradiation history corrections, and corrections for competing reactions. A high level of accuracy in the reaction rate determinations is assured by utilizing laboratory procedures that conform to the ASTM National Consensus Standards for reaction rate determinations for each sensor type.

After combining all of these uncertainty components, the sensor reaction rates derived from the counting and data evaluation procedures were assigned the following net uncertainties for input to the least squares evaluation:

Reaction	Uncertainty
$^{63}Cu(n,\alpha)^{60}Co$	5%
$^{54}Fe(n,p)^{54}Mn$	5%
$^{58}Ni(n,p)^{58}Co$	5%
$^{238}U(n,f)^{137}Cs$	10%
$^{237}Np(n,f)^{137}Cs$	10%
$^{59}Co(n,\gamma)^{60}Co$	5%

These uncertainties are given at the 1σ level.

Dosimetry Cross-Section Uncertainties

The reaction rate cross-sections used in the least squares evaluations were taken from the SNLRML library. This data library provides reaction cross-sections and associated uncertainties, including covariances, for 66 dosimetry sensors in common use. Both cross-sections and uncertainties are provided in a fine multigroup structure for use in least squares adjustment applications. These cross-sections were compiled from the most recent cross-section evaluations and they have been tested with respect to their accuracy and consistency for least squares evaluations. Further, the library has been empirically tested for use in fission spectra determination as well as in the fluence and energy characterization of 14 MeV neutron sources.

For sensors included in the Turkey Point Unit 3 surveillance program, the following uncertainties in the fission spectrum averaged cross-sections are provided in the SNLRML documentation package.

Reaction	Uncertainty
$^{63}Cu(n,\alpha)^{60}Co$	4.08-4.16%
$^{54}Fe(n,p)^{54}Mn$	3.05-3.11%
$^{58}Ni(n,p)^{58}Co$	4.49-4.56%
$^{238}U(n,f)^{137}Cs$	0.54-0.64%
$^{237}Np(n,f)^{137}Cs$	10.32-10.97%
$^{59}Co(n,\gamma)^{60}Co$	0.79-3.59%

These tabulated ranges provide an indication of the dosimetry cross-section uncertainties associated with the sensor sets used in LWR irradiations.

Calculated Neutron Spectrum

The neutron spectra input to the least squares adjustment procedure were obtained directly from the results of plant specific transport calculations for each surveillance capsule irradiation period and location. The spectrum for each capsule was input in an absolute sense (rather than as simply a relative spectral shape). Therefore, within the constraints of the assigned uncertainties, the calculated data were treated equally with the measurements.

While the uncertainties associated with the reaction rates were obtained from the measurement procedures and counting benchmarks and the dosimetry cross-section uncertainties were supplied directly with the SNLRML library, the uncertainty matrix for the calculated spectrum was constructed from the following relationship:

$$M_{gg'} = R_n^2 + R_g * R_{g'} * P_{gg'}$$

where R_n specifies an overall fractional normalization uncertainty and the fractional uncertainties R_g and $R_{g'}$ specify additional random groupwise uncertainties that are correlated with a correlation matrix given by:

$$P_{gg'} = [1 - \theta]\delta_{gg'} + \theta e^{-H}$$

where

$$H = \frac{(g - g')^2}{2\gamma^2}$$

The first term in the correlation matrix equation specifies purely random uncertainties, while the second term describes the short-range correlations over a group range γ (θ specifies the strength of the latter term). The value of δ is 1.0 when g = g', and is 0.0 otherwise.

The set of parameters defining the input covariance matrix for the Turkey Point Unit 3 calculated spectra was as follows:

Flux Normalization Uncertainty (R_n) 15%

Flux Group Uncertainties (R_g, $R_{g'}$)
- (E > 0.0055 MeV) 15%
- (0.68 eV < E < 0.0055 MeV) 29%
- (E < 0.68 eV) 52%

Short Range Correlation (θ)
- (E > 0.0055 MeV) 0.9
- (0.68 eV < E < 0.0055 MeV) 0.5
- (E < 0.68 eV) 0.5

Flux Group Correlation Range (γ)
- (E > 0.0055 MeV) 6
- (0.68 eV < E < 0.0055 MeV) 3
- (E < 0.68 eV) 2

A.1.3 Comparisons of Measurements and Calculations

Results of the least squares evaluations of the dosimetry from the Turkey Point Unit 3 surveillance capsules withdrawn to date are provided in Tables A-5 and A-6. In Table A-5, measured, calculated, and best-estimate values for sensor reaction rates are given for each capsule. Also provided in this tabulation are ratios of the measured reaction rates to both the calculated and least squares adjusted reaction rates.

These ratios of M/C and M/BE illustrate the consistency of the fit of the calculated neutron energy spectra to the measured reaction rates both before and after adjustment. In Table A-6, comparison of the calculated and best estimate values of neutron flux (E > 1.0 MeV) and iron atom displacement rate are tabulated along with the BE/C ratios observed for each of the capsules.

The data comparisons provided in Tables A-5 and A-6 show that the adjustments to the calculated spectra are relatively small and well within the assigned uncertainties for the calculated spectra, measured sensor reaction rates, and dosimetry reaction cross-sections. Further, these results indicate that the use of the least squares evaluation results in a reduction in the uncertainties associated with the exposure of the surveillance capsules. From Section 6.4 of this report, it may be noted that the uncertainty associated with the unadjusted calculation of neutron fluence (E > 1.0 MeV) and iron atom displacements at the surveillance capsule locations is specified as 12% at the 1σ level. From Table A-6, it is noted that the corresponding uncertainties associated with the least squares adjusted exposure parameters have been reduced to 6% for neutron flux (E > 1.0 MeV) and 7% for iron atom displacement rate. Again, the uncertainties from the least squares evaluation are at the 1σ level.

Further comparisons of the measurement results with calculations are given in Tables A-7 and A-8. These comparisons are given on two levels. In Table A-7, calculations of individual threshold sensor

reaction rates are compared directly with the corresponding measurements. These threshold reaction rate comparisons provide a good evaluation of the accuracy of the fast neutron portion of the calculated energy spectra. In Table A-8, calculations of fast neutron exposure rates in terms of $\phi(E > 1.0\ MeV)$ and dpa/s are compared with the best estimate results obtained from the least squares evaluation of the capsule dosimetry results. These two levels of comparison yield consistent and similar results with all measurement-to-calculation comparisons falling well within the 20% limits specified as the acceptance criteria in Regulatory Guide 1.190.

In the case of the direct comparison of measured and calculated sensor reaction rates, the M/C comparisons for fast neutron reactions range from 0.83–1.35 for the 9 samples included in the data set. The overall average M/C ratio for the entire set of Turkey Point Unit 3 data is 1.10 with an associated standard deviation of 14.7%.

In the comparisons of best estimate and calculated fast neutron exposure parameters, the corresponding BE/C comparisons for the capsule data sets range from 0.92–1.16 for neutron flux ($E > 1.0$ MeV) and from 0.91 to 1.13 for iron atom displacement rate. The overall average BE/C ratios for neutron flux ($E > 1.0$ MeV) and iron atom displacement rate are 1.04 with a standard deviation of 16.5% and 1.02 with a standard deviation of 15.5%, respectively.

Based on these comparisons, it is concluded that the calculated fast neutron exposures provided in Section 6.2 of this report are validated for use in the assessment of the condition of the materials comprising the beltline region of the Turkey Point Unit 3 reactor pressure vessel.

Table A-1

Nuclear Parameters Used In The Evaluation Of Neutron Sensors

Monitor Material	Reaction of Interest	Target Atom Fraction	90% Response Range (MEV)	Product Half-life	Fission Yield (%)
Copper	^{63}Cu (n,α)	0.6917	4.9 – 11.8	5.271 y	
Iron	^{54}Fe (n,p)	0.0585	2.1 – 8.3	312.3 d	
Nickel	^{58}Ni (n,p)	0.6808	1.5 – 8.1	70.82 d	
Uranium-238	^{238}U (n,f)	0.9996	1.2 – 6.7	30.07 y	6.02
Neptunium-237	^{237}Np (n,f)	1.0000	0.4 – 3.5	30.07 y	6.17
Cobalt-Aluminum	^{59}Co (n,γ)	0.0015	non-threshold	5.271 y	

Notes: The 90% response range is defined such that, in the neutron spectrum characteristic of the Turkey Point Unit 3 surveillance capsules, approximately 90% of the sensor response is due to neutrons in the energy range specified with approximately 5% of the total response due to neutrons with energies below the lower limit and 5% of the total response due to neutrons with energies above the upper limit.

The counting results determined by the Southwest Research Institute for the ^{59}Co (n,γ) reactions from Capsules S and V were reported based on the weight of Co in the sample rather than the total weight of the dosimeter material. As a result, the target atom fraction used in the ^{59}Co (n,γ) analysis of Capsules S and V was set to unity.

Table A-2

Monthly Thermal Generation During The First Eighteen Fuel Cycles
Of The Turkey Point Unit 3 Reactor
(Reactor Power of 2200 MWt through October 11, 1996, and 2300 MWt thereafter)

Year	Month	Thermal Generation (MWt-hr)	Year	Month	Thermal Generation (MWt-hr)	Year	Month	Thermal Generation (MWt-hr)
1972	11	93785	1976	1	1540335	1979	1	707
1972	12	191555	1976	2	1177919	1979	2	0
1973	1	508292	1976	3	1340004	1979	3	0
1973	2	847407	1976	4	1529615	1979	4	449651
1973	3	745477	1976	5	1277770	1979	5	1299648
1973	4	759432	1976	6	1085183	1979	6	811321
1973	5	1154965	1976	7	1629884	1979	7	1556985
1973	6	1304071	1976	8	1012048	1979	8	1329137
1973	7	1053495	1976	9	1525830	1979	9	1440462
1973	8	726401	1976	10	1614699	1979	10	1242241
1973	9	1101797	1976	11	684046	1979	11	1569305
1973	10	799316	1976	12	0	1979	12	2229
1973	11	1141315	1977	1	512809	1980	1	0
1973	12	540365	1977	2	1395687	1980	2	1033604
1974	1	1198875	1977	3	1629974	1980	3	1612394
1974	2	930609	1977	4	1244675	1980	4	1513229
1974	3	915164	1977	5	1599328	1980	5	1458855
1974	4	1422477	1977	6	1543264	1980	6	1566925
1974	5	1494789	1977	7	1387483	1980	7	1612271
1974	6	1072047	1977	8	1626729	1980	8	1613090
1974	7	1453392	1977	9	1391626	1980	9	1558594
1974	8	1550349	1977	10	1628892	1980	10	257027
1974	9	948103	1977	11	1084071	1980	11	1192309
1974	10	138875	1977	12	0	1980	12	1285346
1974	11	0	1978	1	0	1981	1	1560412
1974	12	587671	1978	2	521921	1981	2	1464865
1975	1	1590161	1978	3	1420093	1981	3	0
1975	2	1404960	1978	4	1537183	1981	4	0
1975	3	1245352	1978	5	1449975	1981	5	0
1975	4	1457721	1978	6	1443357	1981	6	0
1975	5	1511021	1978	7	1405115	1981	7	0
1975	6	1564961	1978	8	1209429	1981	8	0
1975	7	1281697	1978	9	1492193	1981	9	0
1975	8	1565298	1978	10	1479800	1981	10	0
1975	9	1506518	1978	11	1481730	1981	11	0
1975	10	1238155	1978	12	1551960	1981	12	0
1975	11	0						
1975	12	264818						

Table A-2 cont'd

Monthly Thermal Generation During The First Eighteen Fuel Cycles
Of The Turkey Point Unit 3 Reactor
(Reactor Power of 2200 MWt through October 11, 1996, and 2300 MWt thereafter)

Year	Month	Thermal Generation (MWt-hr)	Year	Month	Thermal Generation (MWt-hr)	Year	Month	Thermal Generation (MWt-hr)
1982	1	0	1985	1	1410411	1988	1	518370
1982	2	0	1985	2	1429004	1988	2	370671
1982	3	0	1985	3	1468951	1988	3	888882
1982	4	905576	1985	4	0	1988	4	1557479
1982	5	1476098	1985	5	0	1988	5	1638874
1982	6	1538557	1985	6	0	1988	6	1546625
1982	7	1067596	1985	7	232394	1988	7	1625539
1982	8	1237180	1985	8	1524164	1988	8	1621379
1982	9	1534227	1985	9	1575804	1988	9	1574465
1982	10	1640558	1985	10	906410	1988	10	46931
1982	11	1201773	1985	11	1226293	1988	11	0
1982	12	1618792	1985	12	1302579	1988	12	0
1983	1	1506295	1986	1	1066580	1989	1	0
1983	2	1365136	1986	2	1349846	1989	2	932196
1983	3	1615637	1986	3	212780	1989	3	1461857
1983	4	1586657	1986	4	1108434	1989	4	0
1983	5	1588610	1986	5	1568694	1989	5	0
1983	6	1577299	1986	6	1497417	1989	6	247865
1983	7	1627091	1986	7	737454	1989	7	1611920
1983	8	1631788	1986	8	975435	1989	8	1554544
1983	9	1531474	1986	9	1512236	1989	9	1457916
1983	10	40693	1986	10	1643601	1989	10	1461571
1983	11	0	1986	11	1577530	1989	11	1565712
1983	12	0	1986	12	1389881	1989	12	1547473
1984	1	1049166	1987	1	1215136	1990	1	1638267
1984	2	943756	1987	2	1234335	1990	2	152915
1984	3	1516127	1987	3	312127	1990	3	0
1984	4	1303305	1987	4	0	1990	4	0
1984	5	994815	1987	5	0	1990	5	0
1984	6	1520181	1987	6	0	1990	6	805329
1984	7	1386143	1987	7	0	1990	7	1607741
1984	8	1535986	1987	8	0	1990	8	1613090
1984	9	1562568	1987	9	69494	1990	9	1559480
1984	10	1619414	1987	10	0	1990	10	1630270
1984	11	1577093	1987	11	0	1990	11	1580537
1984	12	632365	1987	12	127764	1990	12	609211

Table A-2 cont'd

Monthly Thermal Generation During The First Eighteen Fuel Cycles
Of The Turkey Point Unit 3 Reactor
(Reactor Power of 2200 MWt through October 11, 1996, and 2300 MWt thereafter)

Year	Month	Thermal Generation (MWt-hr)	Year	Month	Thermal Generation (MWt-hr)	Year	Month	Thermal Generation (MWt-hr)
1991	1	0	1994	1	1583340	1997	1	1581388
1991	2	0	1994	2	1390840	1997	2	1536699
1991	3	0	1994	3	1637020	1997	3	55821
1991	4	0	1994	4	133320	1997	4	651475
1991	5	0	1994	5	401478	1997	5	1707980
1991	6	0	1994	6	1520860	1997	6	1653585
1991	7	0	1994	7	1592118	1997	7	1477428
1991	8	0	1994	8	1634380	1997	8	1655793
1991	9	0	1994	9	1543300	1997	9	1653263
1991	10	1215537	1994	10	1638780	1997	10	1709889
1991	11	1483685	1994	11	1574760	1997	11	1617245
1991	12	1639202	1994	12	1375880	1997	12	1708256
1992	1	1558758	1995	1	1615460	1998	1	1707773
1992	2	1414833	1995	2	1475540	1998	2	1308539
1992	3	1422730	1995	3	1598520	1998	3	1708394
1992	4	1198455	1995	4	1471140	1998	4	1650825
1992	5	912262	1995	5	1628660	1998	5	1666603
1992	6	1384481	1995	6	1537800	1998	6	1653401
1992	7	1420554	1995	7	1634820	1998	7	1679943
1992	8	840627	1995	8	1620960	1998	8	1707957
1992	9	0	1995	9	134200	1998	9	1047259
1992	10	0	1995	10	933900	1998	10	64009
1992	11	0	1995	11	1575200	1998	11	1628653
1992	12	1184161	1995	12	1634820	1998	12	1707727
1993	1	1272201	1996	1	1631740	1999	1	1707819
1993	2	1476438	1996	2	998580	1999	2	1516114
1993	3	1557074	1996	3	1531860	1999	3	1708348
1993	4	1579380	1996	4	1574606	1999	4	1650549
1993	5	1635920	1996	5	1632246	1999	5	1651561
1993	6	1547898	1996	6	1538328	1999	6	1563425
1993	7	1595000	1996	7	1632444	1999	7	1708325
1993	8	1637020	1996	8	1576146	1999	8	1708118
1993	9	1520200	1996	9	1387012	1999	9	1602410
1993	10	1188638	1996	10	1652661	1999	10	1709015
1993	11	1583120	1996	11	1651745	1999	11	1541276
1993	12	1636580	1996	12	1704231	1999	12	1707612

Table A-2 cont'd

Monthly Thermal Generation During The First Eighteen Fuel Cycles
Of The Turkey Point Unit 3 Reactor
(Reactor Power of 2200 MWt through October 11, 1996, and 2300 MWt thereafter)

Year	Month	Thermal Generation (MWt-hr)	Year	Month	Thermal Generation (MWt-hr)	Year	Month	Thermal Generation (MWt-hr)
2000	1	1708601	2000	8	1708003	2001	3	1662463
2000	2	1432210	2000	9	1652619	2001	4	1651101
2000	3	213900	2000	10	1710533	2001	5	1667178
2000	4	1651285	2000	11	1614508	2001	6	1653125
2000	5	1700988	2000	12	1708049	2001	7	1656966
2000	6	1607884	2001	1	1708072	2001	8	1320200
2000	7	1708670	2001	2	1542794	2001	9	1557376

Table A-3

Calculated C_j Factors at the Surveillance Capsule Center
Core Midplane Elevation

Fuel Cycle	ϕ(E > 1.0 MeV) [n/cm^2-s]				C_j			
	Capsule T	Capsule S	Capsule V	Capsule X*	T	S	V	X*
1	1.66E+11	1.16E+11	5.14E+10	2.59E+10	1.000	1.000	1.068	0.560
2		1.13E+11	4.88E+10	2.37E+10		0.970	1.016	0.512
3		1.19E+11	5.73E+10	3.03E+10		1.024	1.191	0.655
4		1.17E+11	4.91E+10	2.64E+10		1.008	1.021	0.571
5			5.20E+10	2.07E+10			1.082	0.447
6			4.81E+10	1.99E+10			1.000	0.430
7			4.55E+10	2.27E+10			0.946	0.491
8			4.56E+10	2.20E+10			0.949	0.476
9			3.90E+10	2.35E+10			0.812	0.509
10				2.05E+10				0.443
11				1.98E+10				0.427
12				7.16E+10				1 548
13				7.02E+10				1.518
14				7.46E+10				1.612
15				7.55E+10				1.632
16				7.71E+10				1.666
17				7.62E+10				1.646
18				6.64E+10				1.435
Average	1.66E+11	1.16E+11	4.81E+10	4.63E+10	1.000	1.000	1.000	1.000

*Note: Cj factors based on the ratio of the cycle specific fast (E > 1.0 MeV) neutron flux divided by the average flux over the total irradiation period were deemed unsuitable for Capsule X since reaction rates did not vary by constant values as a function of azimuthal position for this capsule. To a large extent, this was due to moving Capsule X from a 40° to 0° location following the eleventh fuel cycle. As a result of this observation, the Cj terms that were utilized in the final Capsule X analysis were based on the individual reaction rates determined from the synthesized transport calculations. The final Cj terms for Capsule X, which are based on individual reaction rates, are reported on the next page of this table.

Table A-3 cont'd

Calculated C_j Factors at the Surveillance Capsule Center
Core Midplane Elevation
(Capsule X only)

Fuel Cycle	Capsule X Reaction Rates [rps/atom]					
	^{63}Cu (n,α)	^{54}Fe (n,p)	^{238}U (n,f)	^{237}Np (n,f)	^{59}Co (n,γ)	^{59}Co (n,γ) Cd
1	2.27E-17	2.18E-15	9.55E-15	6.60E-14	9.57E-13	4.88E-13
2	2.10E-17	2.01E-15	8.75E-15	6.03E-14	8.76E-13	4.46E-13
3	2.65E-17	2.55E-15	1.12E-14	7.71E-14	1.12E-12	5.71E-13
4	2.34E-17	2.23E-15	9.75E-15	6.72E-14	9.71E-13	4.95E-13
5	1.93E-17	1.79E-15	7.68E-15	5.24E-14	7.55E-13	3.84E-13
6	1.86E-17	1.72E-15	7.40E-15	5.05E-14	7.27E-13	3.70E-13
7	2.09E-17	1.95E-15	8.42E-15	5.76E-14	8.29E-13	4.22E-13
8	2.03E-17	1.90E-15	8.18E-15	5.59E-14	8.04E-13	4.10E-13
9	2.15E-17	2.02E-15	8.73E-15	5.97E-14	8.55E-13	4.36E-13
10	1.91E-17	1.77E-15	7.62E-15	5.19E-14	7.40E-13	3.78E-13
11	1.84E-17	1.71E-15	7.35E-15	5.01E-14	7.18E-13	3.66E-13
12	4.37E-17	5.03E-15	2.50E-14	1.92E-13	3.24E-12	1.68E-12
13	4.30E-17	4.94E-15	2.45E-14	1.89E-13	3.18E-12	1.65E-12
14	4.58E-17	5.25E-15	2.60E-14	2.00E-13	3.36E-12	1.74E-12
15	4.59E-17	5.30E-15	2.63E-14	2.03E-13	3.42E-12	1.77E-12
16	4.69E-17	5.41E-15	2.69E-14	2.07E-13	3.49E-12	1.81E-12
17	4.66E-17	5.36E-15	2.66E-14	2.04E-13	3.44E-12	1.78E-12
18	4.08E-17	4.67E-15	2.32E-14	1.78E-13	3.00E-12	1.56E-12
Average	3.19E-17	3.44E-15	1.64E-14	1.22E-13	1.99E-12	1.03E-12

Fuel Cycle	Capsule X C_j					
	^{63}Cu (n,α)	^{54}Fe (n,p)	^{238}U (n,f)	^{237}Np (n,f)	^{59}Co (n,γ)	^{59}Co (n,γ) Cd
1	0.711	0.634	0.582	0.539	0.482	0.476
2	0.659	0.583	0.533	0.493	0.441	0.435
3	0.830	0.741	0.681	0.630	0.564	0.557
4	0.732	0.649	0.594	0.549	0.489	0.483
5	0.605	0.520	0.468	0.428	0.380	0.375
6	0.581	0.500	0.451	0.413	0.366	0.361
7	0.653	0.567	0.513	0.471	0.418	0.412
8	0.636	0.552	0.499	0.457	0.405	0.399
9	0.674	0.587	0.532	0.488	0.431	0.425
10	0.598	0.515	0.464	0.424	0.373	0.369
11	0.576	0.497	0.448	0.410	0.362	0.357
12	1.367	1.462	1.523	1.571	1.634	1.639
13	1.346	1.437	1.495	1.540	1.599	1.605
14	1.433	1.527	1.587	1.634	1.694	1.701
15	1.438	1.540	1.605	1.656	1.721	1.728
16	1.469	1.572	1.638	1.690	1.759	1.765
17	1.458	1.558	1.620	1.670	1.732	1.739
18	1.277	1.359	1.412	1.455	1.512	1.517
Average	1.000	1.000	1.000	1.000	1.000	1.000

Table A-4
Measured Sensor Activities And Reaction Rates

Surveillance Capsule T

Reaction	Location	Measured Activity (dps/g)	Saturated Activity (dps/g)	Radially Adjusted Saturated Activity (dps/g)	Radially Adjusted Reaction Rate (rps/atom)
^{63}Cu (n,α) ^{60}Co	Top	9.52E+04	7.67E+05	7.99E+05	1.22E-16
	Bottom	9.19E+04	7.40E+05	7.71E+05	1.18E-16
	Average				**1.20E-16**
^{54}Fe (n,p) ^{54}Mn	H-17 Charpy	3.34E+06	8.78E+06	9.16E+06	1.45E-14
	H-23 Charpy	3.23E+06	8.49E+06	8.86E+06	1.41E-14
	R-63 Charpy	2.90E+06	7.62E+06	7.96E+06	1.26E-14
	W-18 Charpy	3.51E+06	9.22E+06	7.93E+06	1.26E-14
	W-24 Charpy	3.71E+06	9.75E+06	8.38E+06	1.33E-14
	P-58 Charpy	3.51E+06	9.22E+06	7.93E+06	1.26E-14
	Average				**1.33E-14**
^{58}Ni (n,p) ^{58}Co	Middle	2.56E+07	1.18E+08	1.23E+08	1.76E-14
	Average				**1.76E-14**
^{238}U (n,f) ^{137}Cs (Cd)	Middle	2.92E+05	1.19E+07	1.19E+07	7.80E-14
^{238}U (n,f) ^{137}Cs (Cd)	Including ^{235}U, ^{239}Pu, and γ,fission corrections:				**6.44E-14**
^{237}Np (n,f) ^{137}Cs (Cd)	Middle	2.16E+06	8.78E+07	8.78E+07	5.60E-13
^{237}Np (n,f) ^{137}Cs (Cd)	Including γ,fission correction:				**5.52E-13**

Notes: 1) Measured specific activities are indexed to a counting date of February 3, 1975.
2) The average ^{238}U (n,f) reaction rate of 6.44E-14 includes a correction factor of 0.861 to account for plutonium build-in and an additional factor of 0.959 to account for photo-fission effects in the sensor.
3) The average ^{237}Np (n,f) reaction rate of 5.52E-13 includes a correction factor of 0.985 to account for photo-fission effects in the sensor.

Table A-4 cont'd

Measured Sensor Activities And Reaction Rates

Surveillance Capsule S

Reaction	Location	Measured Activity (dps/g)	Saturated Activity (dps/g)	Radially Adjusted Saturated Activity (dps/g)	Radially Adjusted Reaction Rate (rps/atom)
^{63}Cu (n,α) ^{60}Co	Top	2.25E+05	6.85E+05	7.13E+05	1.09E-16
	Bottom	2.24E+05	6.82E+05	7.10E+05	1.08E-16
	Average				**1.09E-16**
^{54}Fe (n,p) ^{54}Mn	P-9 Charpy	4.76E+06	6.36E+06	6.64E+06	1.05E-14
	P-7 Charpy	4.64E+06	6.20E+06	6.47E+06	1.03E-14
	R-6 Charpy	4.39E+06	5.87E+06	6.12E+06	9.71E-15
	P-5 Charpy	4.84E+06	6.47E+06	6.75E+06	1.07E-14
	P-1 Charpy	4.50E+06	6.01E+06	6.28E+06	9.95E-15
	S-9 Charpy	6.13E+06	8.19E+06	7.04E+06	1.12E-14
	S-7 Charpy	5.41E+06	7.23E+06	6.22E+06	9.86E-15
	R-8 Charpy	4.91E+06	6.56E+06	5.64E+06	8.94E-15
	S-5 Charpy	5.64E+06	7.54E+06	6.48E+06	1.03E-14
	S-1 Charpy	5.47E+06	7.31E+06	6.29E+06	9.96E-15
	Average				**1.01E-14**
^{59}Co (n,γ) ^{60}Co	Top	2.34E+07	7.12E+07	6.68E+07	6.54E-15
	Middle	2.07E+07	6.30E+07	5.91E+07	5.78E-15
	Bottom	2.01E+07	6.12E+07	5.74E+07	5.62E-15
	Average				**5.98E-15**
^{59}Co (n,γ) ^{60}Co (Cd)	Top	1.11E+07	3.38E+07	2.93E+07	2.86E-15
	Bottom	9.40E+06	2.86E+07	2.48E+07	2.43E-15
	Average				**2.64E-15**

Notes: 1) Measured specific activities are indexed to a counting date of November 23, 1977.
2) Measured reaction rates for iron as originally reported in Reference A-3 were subsequently identified in Reference A-5 as being biased high by 15% due to detector calibration issues. As a result, the Capsule S measured iron reaction rates listed above have been reduced to 85% of the original Reference A-3 values.

Table A-4 cont'd

Measured Sensor Activities And Reaction Rates

Surveillance Capsule V

Reaction	Location	Measured Activity (dps/g)	Saturated Activity (dps/g)	Radially Adjusted Saturated Activity (dps/g)	Radially Adjusted Reaction Rate (rps/atom)
^{63}Cu (n,α) ^{60}Co	Top	3.80E+04	7.80E+04	8.12E+04	1.24E-17
	Bottom	3.81E+04	7.82E+04	8.14E+04	1.24E-17
	Average				**1.24E-17**
^{54}Fe (n,p) ^{54}Mn	R-48 Charpy	1.58E+06	2.55E+06	2.66E+06	4.22E-15
	R-42 Charpy	1.62E+06	2.62E+06	2.73E+06	4.33E-15
	H-2 Charpy	1.47E+06	2.37E+06	2.48E+06	3.93E-15
	S-58 Charpy	1.90E+06	3.07E+06	2.65E+06	4.19E-15
	S-52 Charpy	1.87E+06	3.02E+06	2.60E+06	4.13E-15
	W-2 Charpy	1.75E+06	2.83E+06	2.44E+06	3.86E-15
	Average				**4.11E-15**
^{238}U (n,f) ^{137}Cs (Cd)	Middle	2.52E+05	1.64E+06	1.64E+06	1.08E-14
^{238}U (n,f) ^{137}Cs (Cd)	Including ^{235}U, ^{239}Pu, and γ,fission corrections:				**8.64E-15**
^{237}Np (n,f) ^{137}Cs (Cd)	Middle	1.23E+05	7.99E+05	7.99E+05	5.10E-15
^{237}Np (n,f) ^{137}Cs (Cd)	Including γ,fission correction:				**5.02E-15**
^{59}Co (n,γ) ^{60}Co	Top	3.11E+06	6.38E+06	6.11E+06	5.98E-16
	Middle	2.82E+06	5.79E+06	5.54E+06	5.42E-16
	Bottom	3.01E+06	6.18E+06	5.91E+06	5.79E-16
	Average				**5.73E-16**
^{59}Co (n,γ) ^{60}Co (Cd)	Top	1.53E+06	3.14E+06	2.77E+06	2.71E-16
	Middle	3.17E+04	6.51E+04	5.74E+04	5.62E-18
	Bottom	1.52E+06	3.12E+06	2.75E+06	2.69E-16
	Average				**1.82E-16**

Notes: 1) Measured specific activities are indexed to a counting date of March 30, 1985.
2) The average ^{238}U (n,f) reaction rate of 8.64E-15 includes a correction factor of 0.837 to account for plutonium build-in and an additional factor of 0.960 to account for photo-fission effects in the sensor.
3) The average ^{237}Np (n,f) reaction rate of 5.02E-15 includes a correction factor of 0.984 to account for photo-fission effects in the sensor.

Table A-4 cont'd

Measured Sensor Activities And Reaction Rates

Surveillance Capsule X

Reaction	Location	Measured Activity (dps/g)	Saturated Activity (dps/g)	Radially Adjusted Saturated Activity (dps/g)	Radially Adjusted Reaction Rate (rps/atom)
^{63}Cu (n,α) ^{60}Co	Top	2.28E+05	2.50E+05	2.60E+05	3.97E-17
	Unspecified	1.58E+05	1.73E+05	1.80E+05	2.75E-17
	Average				**3.36E-17**
^{54}Fe (n,p) ^{54}Mn	R-56 Charpy	1.72E+06	2.08E+06	2.17E+06	3.44E-15
	R-50 Charpy	1.46E+06	1.77E+06	1.84E+06	2.92E-15
	S-66 Charpy	2.03E+06	2.46E+06	2.11E+06	3.35E-15
	S-60 Charpy	1.77E+06	2.14E+06	1.84E+06	2.92E-15
	Average				**3.16E-15**
^{238}U (n,f) ^{137}Cs (Cd)	Middle	9.94E+05	2.77E+06	2.77E+06	1.82E-14
^{238}U (n,f) ^{137}Cs (Cd)	Including ^{235}U, ^{239}Pu, and γ,fission corrections:				**1.36E-14**
^{237}Np (n,f) ^{137}Cs (Cd)	Middle	7.07E+06	1.96E+07	1.96E+07	1.25E-13
^{237}Np (n,f) ^{137}Cs (Cd)	Including γ,fission correction:				**1.23E-13**
^{59}Co (n,γ) ^{60}Co	Top	4.01E+07	3.81E+07	3.58E+07	2.34E-12
	Middle	3.04E+07	2.89E+07	2.72E+07	1.77E-12
	Middle	2.39E+07	2.27E+07	2.14E+07	1.39E-12
	Bottom	2.22E+07	2.11E+07	1.98E+07	1.29E-12
	Average				**1.70E-12**
^{59}Co (n,γ) ^{60}Co (Cd)	Top	1.78E+07	1.69E+07	1.47E+07	9.56E-13
	Bottom	1.05E+07	9.95E+06	8.65E+06	5.64E-13
	Average				**7.60E-13**

Notes: 1) Measured specific activities are indexed to a counting date of May 1, 2002.

2) The average ^{238}U (n,f) reaction rate of 1.36E-14 includes a correction factor of 0.780 to account for plutonium build-in and an additional factor of 0.957 to account for photo-fission effects in the sensor.

3) The average ^{237}Np (n,f) reaction rate of 1.23E-13 includes a correction factor of 0.982 to account for photo-fission effects in the sensor.

Table A-5

Comparison of Measured, Calculated, and Best Estimate
Reaction Rates At The Surveillance Capsule Center

Capsule T

	Reaction Rate [rps/atom]				
Reaction	Measured	Calculated	Best Estimate	M/C	M/BE
$^{63}Cu(n,\alpha)^{60}Co$	1.20E-16	8.91E-17	1.15E-16	1.35	1.04
$^{54}Fe(n,p)^{54}Mn$	1.33E-14	1.10E-14	1.33E-14	1.21	1.00
$^{58}Ni(n,p)^{58}Co$	1.76E-14	1.52E-14	1.81E-14	1.16	0.97
$^{238}U(n,f)^{137}Cs$ (Cd)	6.44E-14	5.71E-14	6.67E-14	1.13	0.97
$^{237}Np(n,f)^{137}Cs$ (Cd)	5.52E-13	4.52E-13	5.33E-13	1.22	1.04

Capsule S*

	Reaction Rate [rps/atom]				
Reaction	Measured	Calculated	Best Estimate	M/C	M/BE
$^{63}Cu(n,\alpha)^{60}Co$	Rejected	6.51E-17	N/A	N/A	N/A
$^{54}Fe(n,p)^{54}Mn$	Rejected	7.84E-15	N/A	N/A	N/A
$^{59}Co(n,\gamma)^{60}Co$	Rejected	5.68E-12	N/A	N/A	N/A
$^{59}Co(n,\gamma)^{60}Co$ (Cd)	Rejected	2.94E-12	N/A	N/A	N/A

*Notes: 1) Measured reaction rates for Capsule S were rejected since they were incongruent with analogous results for similar Westinghouse plant designs. Furthermore, Reference A-5 reported that detector calibration problems existed at the laboratory that performed the Capsule S counting analysis.

2) The Capsule S calculated results reported above for the individual reaction rates were taken from the synthesized transport calculations at the core midplane after the fourth fuel cycle.

Table A-5 cont'd

Comparison of Measured, Calculated, and Best Estimate
Reaction Rates At The Surveillance Capsule Center

Capsule V*

	Reaction Rate [rps/atom]				
Reaction	Measured	Calculated	Best Estimate	M/C	M/BE
$^{63}Cu(n,\alpha)^{60}Co$	Rejected	3.15E-17	N/A	N/A	N/A
$^{54}Fe(n,p)^{54}Mn$	Rejected	3.16E-15	N/A	N/A	N/A
$^{238}U(n,f)^{137}Cs$ (Cd)	Rejected	1.42E-14	N/A	N/A	N/A
$^{237}Np(n,f)^{137}Cs$ (Cd)	Rejected	1.00E-13	N/A	N/A	N/A
$^{59}Co(n,\gamma)^{60}Co$	Rejected	1.49E-12	N/A	N/A	N/A
$^{59}Co(n,\gamma)^{60}Co$ (Cd)	Rejected	7.61E-13	N/A	N/A	N/A

*Notes: 1) Measured reaction rates for Capsule V were rejected since they were incongruent with analogous results for similar Westinghouse plant designs. Furthermore, Table X of Reference A-4 indicates that: "Data inconclusive for computing fluence rate" for all measured counting results except for iron from this capsule.

2) The Capsule V calculated results reported above for the individual reaction rates were taken from the synthesized transport calculations at the core midplane after the ninth fuel cycle.

Capsule X

	Reaction Rate [rps/atom]				
Reaction	Measured	Calculated	Best Estimate	M/C	M/BE
$^{63}Cu(n,\alpha)^{60}Co$	3.36E-17	3.19E-17	3.25E-17	1.05	1.03
$^{54}Fe(n,p)^{54}Mn$	3.16E-15	3.41E-15	3.22E-15	0.93	0.98
$^{238}U(n,f)^{137}Cs$ (Cd)	1.36E-14	1.64E-14	1.51E-14	0.83	0.90
$^{237}Np(n,f)^{137}Cs$ (Cd)	1.23E-13	1.23E-13	1.17E-13	1.00	1.05
$^{59}Co(n,\gamma)^{60}Co$	1.70E-12	1.96E-12	1.70E-12	0.87	1.00
$^{59}Co(n,\gamma)^{60}Co$ (Cd)	7.60E-13	9.85E-13	7.67E-13	0.77	0.99

Table A-6

Comparison of Calculated and Best Estimate Exposure Rates
At The Surveillance Capsule Center

Capsule ID	$\phi(E > 1.0\ MeV)$ [n/cm^2-s]			
	Calculated	Best Estimate	Uncertainty (1σ)	BE/C
T	1.66E+11	1.92E+11	6%	1.16
S	1.16E+11	N/A	N/A	N/A
V	4.81E+10	N/A	N/A	N/A
X	4.63E+10	4.24E+10	6%	0.92

Notes: 1) Best estimate results are not reported for Capsules S and V since all measured reaction rates were rejected.
2) Calculated results are based on the synthesized transport calculations taken at the core midplane following the completion of each respective capsules irradiation period.

Capsule ID	Iron Atom Displacement Rate [dpa/s]			
	Calculated	Best Estimate	Uncertainty (1σ)	BE/C
T	2.81E-10	3.17E-10	7%	1.13
S	1.99E-10	N/A	N/A	N/A
V	7.87E-11	N/A	N/A	N/A
X	7.70E-11	6.99E-11	7%	0.91

Notes: 1) Best estimate results are not reported for Capsules S and V since all measured reaction rates were rejected.
2) Calculated results are based on the synthesized transport calculations taken at the core midplane following the completion of each respective capsules irradiation period.

Table A-7

Comparison of Measured/Calculated (M/C) Sensor Reaction Rate Ratios Including all Fast Neutron Threshold Reactions

Reaction	M/C Ratio			
	Capsule T	Capsule S	Capsule V	Capsule X
$^{63}Cu(n,\alpha)^{60}Co$	1.35	N/A	N/A	1.05
$^{54}Fe(n,p)^{54}Mn$	1.21	N/A	N/A	0.93
$^{58}Ni(n,p)^{58}Co$	1.16	N/A	N/A	
$^{238}U(n,p)^{137}Cs$ (Cd)	1.13	N/A	N/A	0.83
$^{237}Np(n,f)^{137}Cs$ (Cd)	1.22	N/A	N/A	1.00
Average	1.21	N/A	N/A	0.95
% Standard Deviation	6.9	N/A	N/A	10.2

Notes: 1) All measured reaction rates for Capsules S and V were rejected.
2) The overall average M/C ratio for the set of 9 sensor measurements is 1.10 with an associated standard deviation of 14.7%.

Table A-8

Comparison of Best Estimate/Calculated (BE/C) Exposure Rate Ratios

Capsule ID	BE/C Ratio	
	$\phi(E > 1.0\ MeV)$	dpa/s
T	1.16	1.13
S	N/A	N/A
V	N/A	N/A
X	0.92	0.91
Average	1.04	1.02
% Standard Deviation	16.5	15.5

Note: Best estimate results were not determined for Capsules S and V since all measured reaction rates were rejected.

Appendix A References

A-1. Regulatory Guide RG-1.190, "Calculational and Dosimetry Methods for Determining Pressure Vessel Neutron Fluence," U. S. Nuclear Regulatory Commission, Office of Nuclear Regulatory Research, March 2001.

A-2. WCAP-8631, Revision 0, "Analysis of Capsule T from the Florida Power and Light Company Turkey Point Unit No. 3 Reactor Vessel Radiation Surveillance Program," December 1975.

A-3. E. B. Norris, "Reactor Vessel Material Surveillance Program, Capsule S – Turkey Point Unit No. 3, Capsule S – Turkey Point Unit No. 4," Final Report SwRI Project No. 02-5131 and SwRI Project No. 02-5380, Southwest Research Institute, May 1979.

A-4. P. K. Nair and E. B. Norris, "Reactor Vessel Material Surveillance Program for Turkey Point Unit No. 3: Analysis of Capsule V," Final Report SwRI Project No. 06-8575, Southwest Research Institute, August 1986.

A-5. WCAP-14044, Revision 0, "Westinghouse Surveillance Capsule Neutron Fluence Reevaluation," April 1994.

A-6. A. Schmittroth, *FERRET Data Analysis Core*, HEDL-TME 79-40, Hanford Engineering Development Laboratory, Richland, WA, September 1979.

A-7. RSIC Data Library Collection DLC-178, "SNLRML Recommended Dosimetry Cross-Section Compendium", July 1994.

APPENDIX B

LOAD-TIME RECORDS FOR CHARPY SPECIMEN TESTS

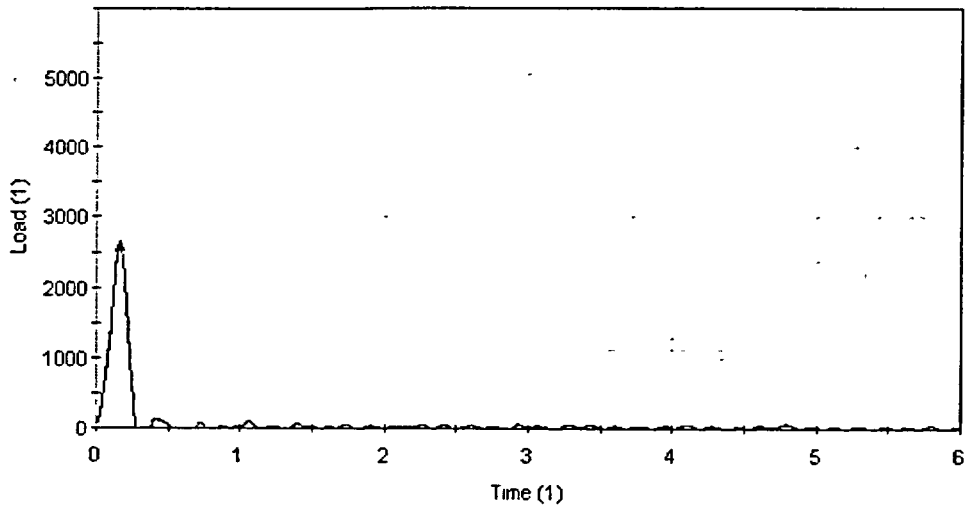

S62, 0°F

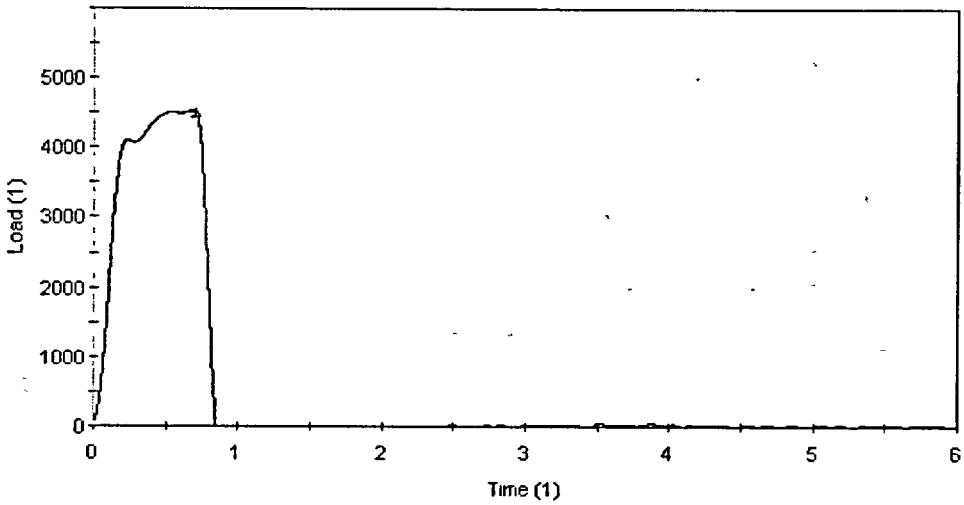

S60, 25°F

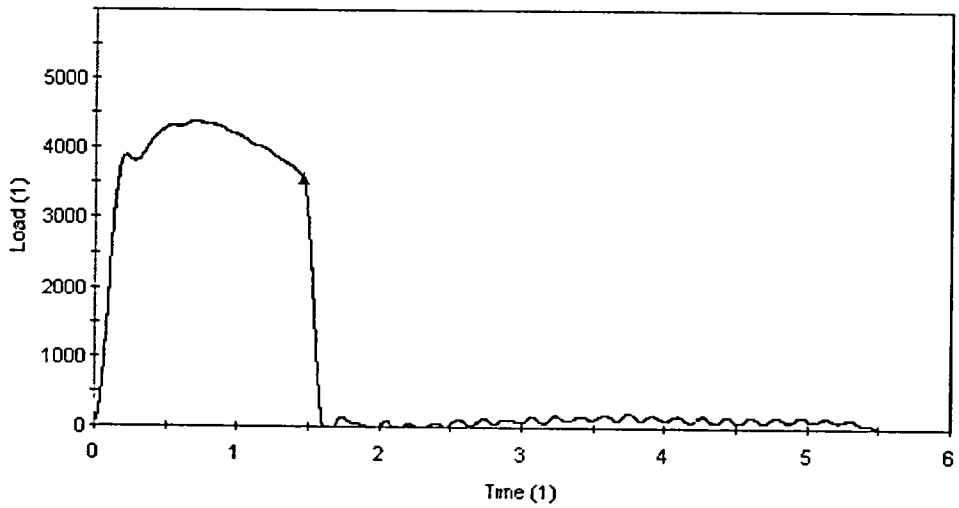

S63, 50°F

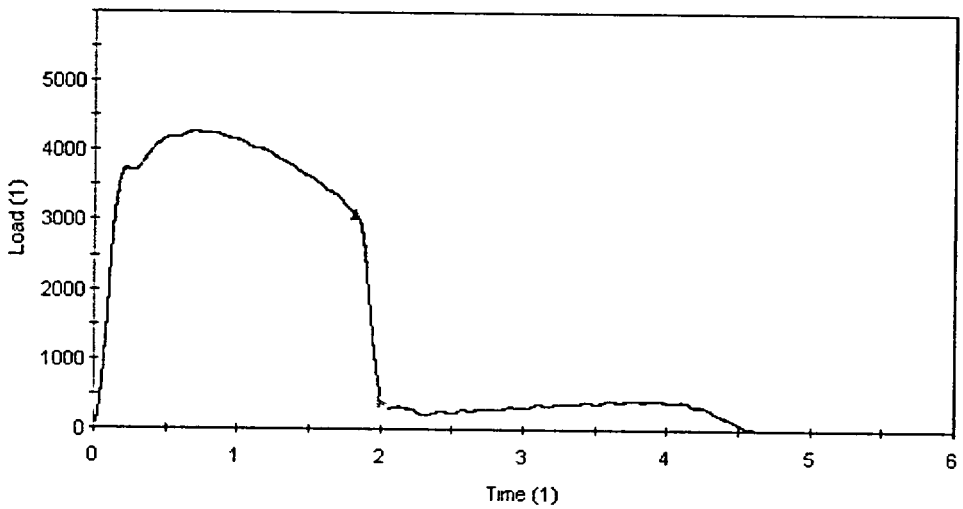

S65, 90°F

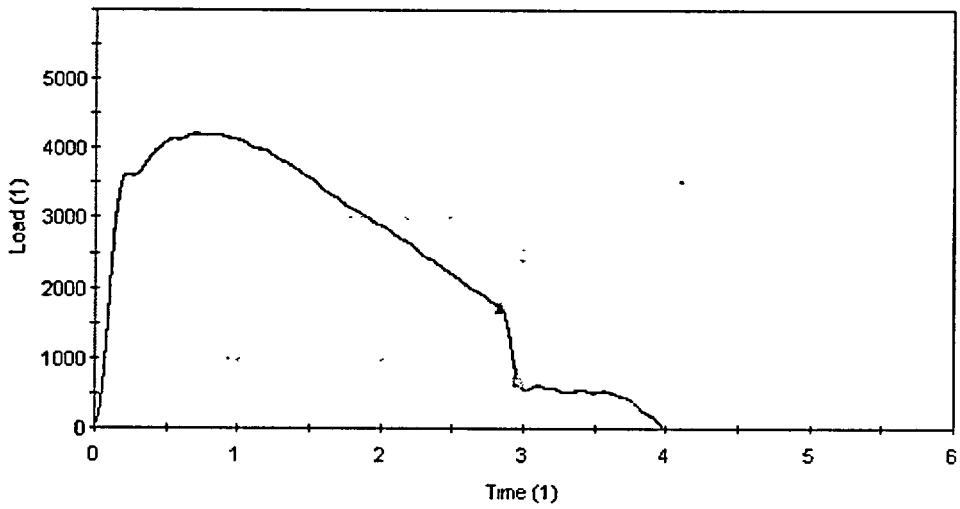

S66, 130°F

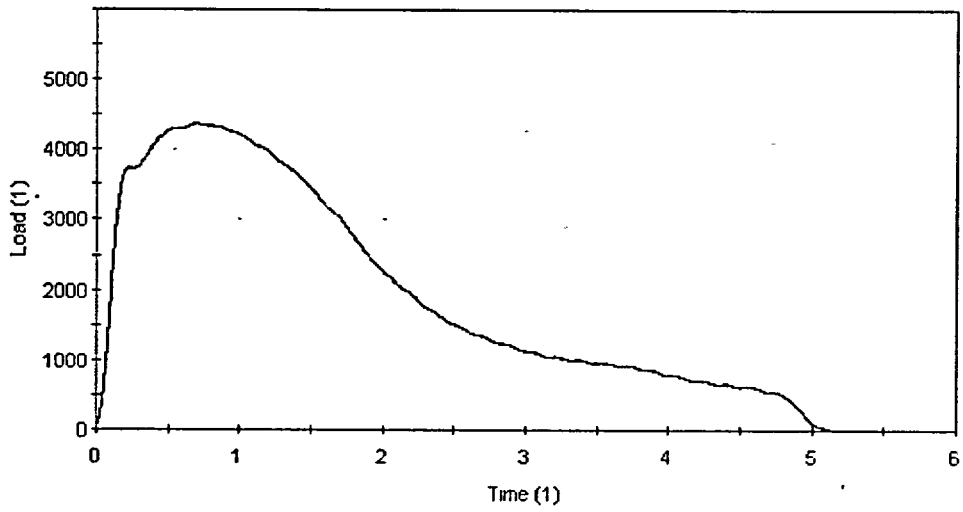

S64, 150°F

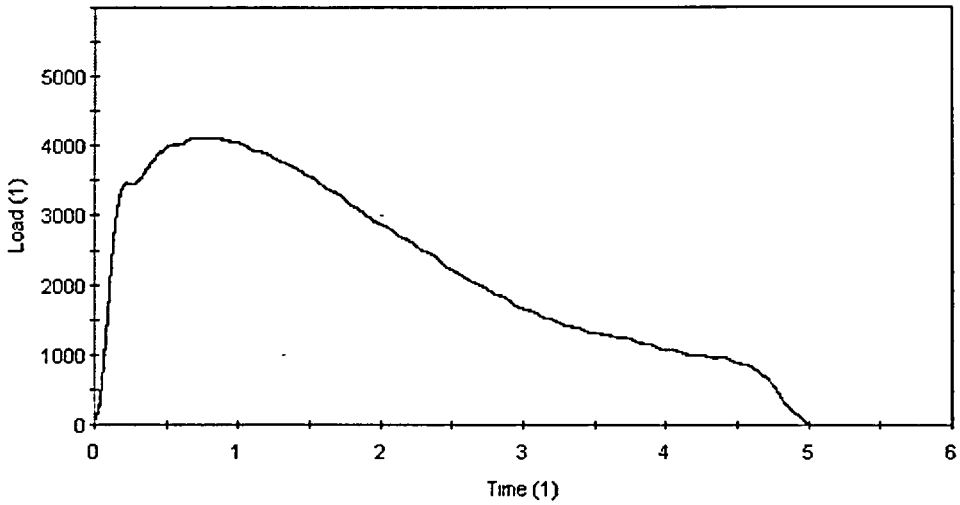

S61, 160°F

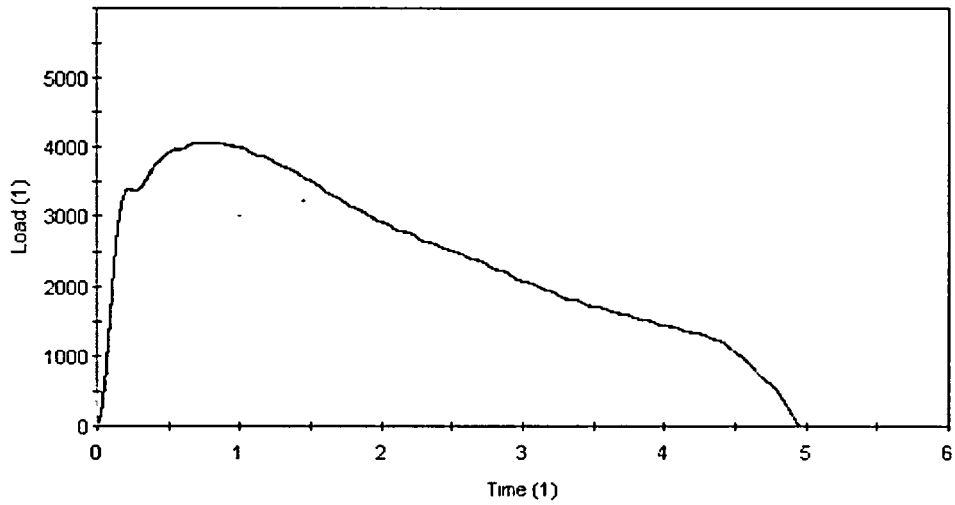

S59, 180°F

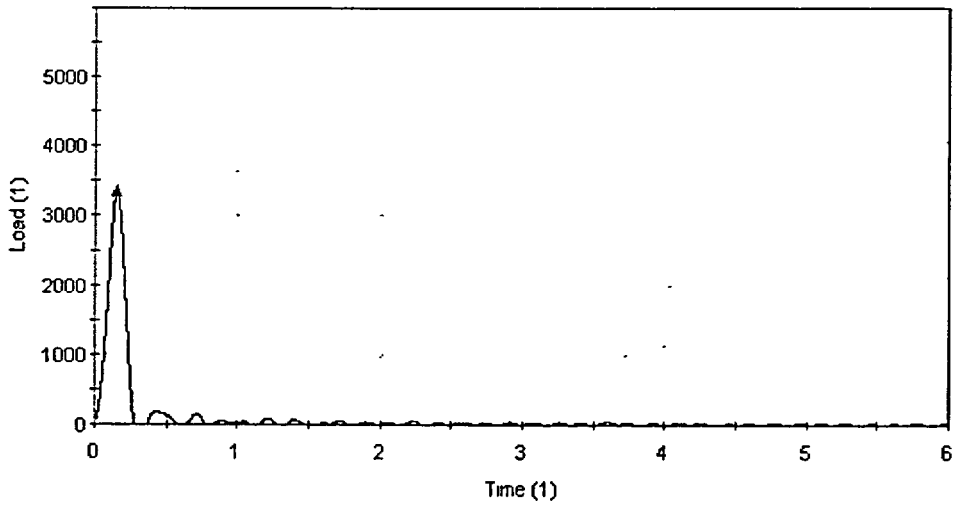

R51, 60°F

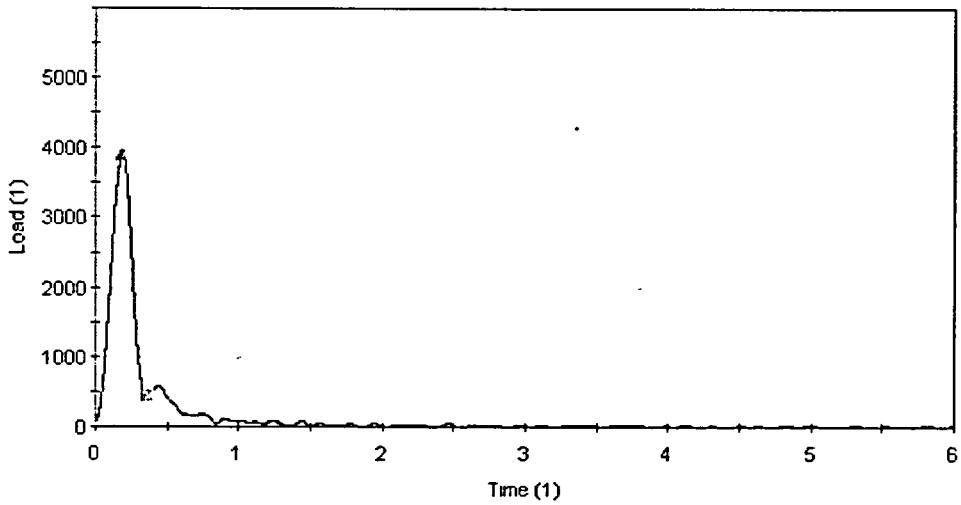

R50, 100°F

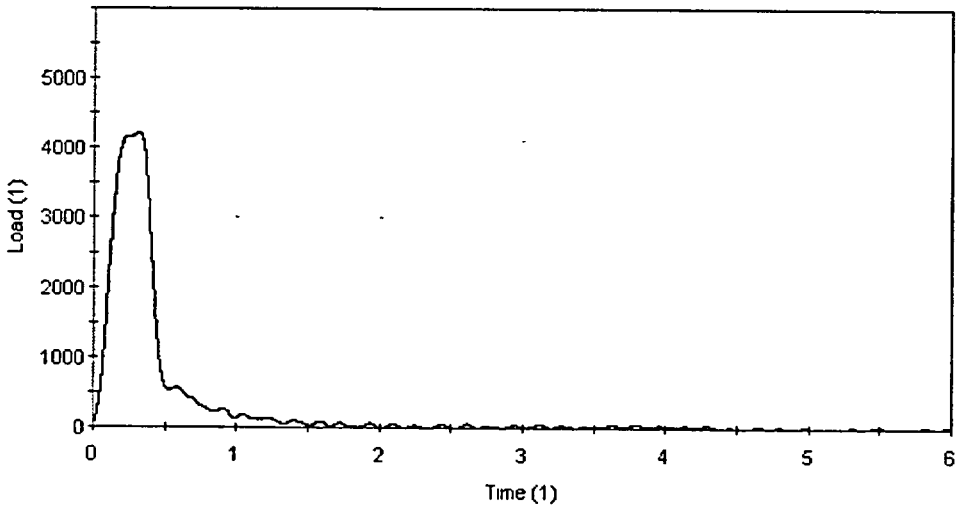

R49, 150°F

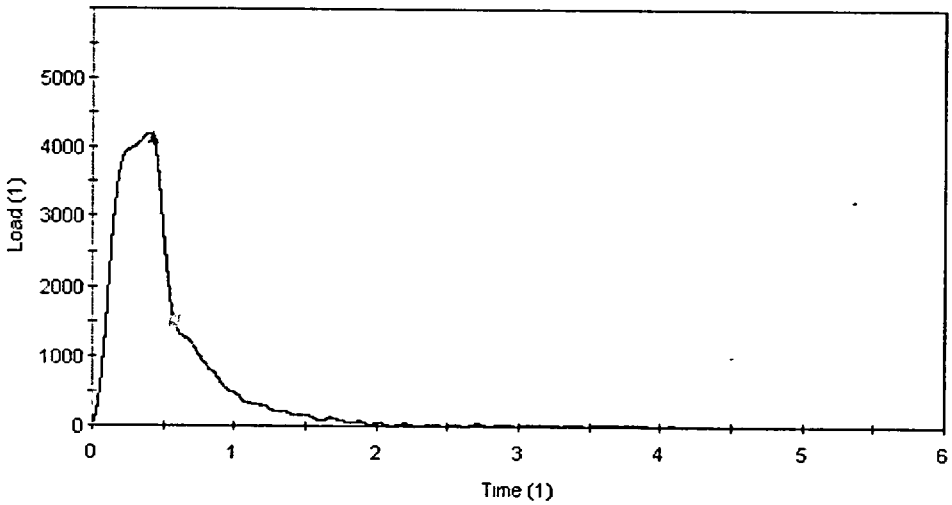

R55, 200°F

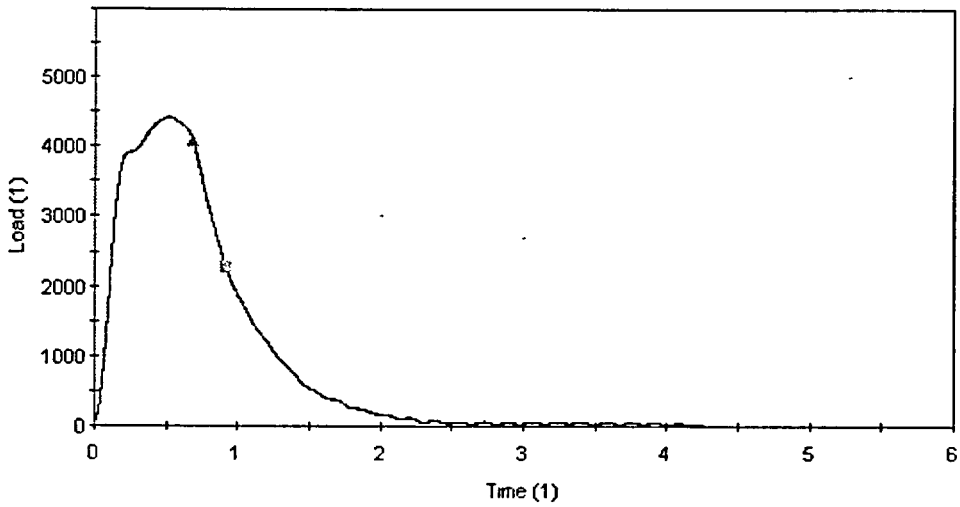

R54, 225°F

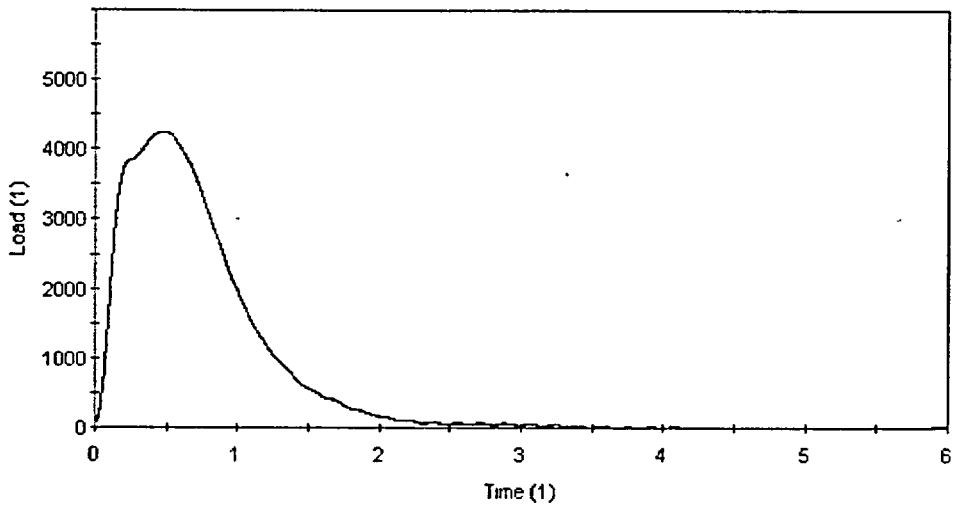

R56, 250°F

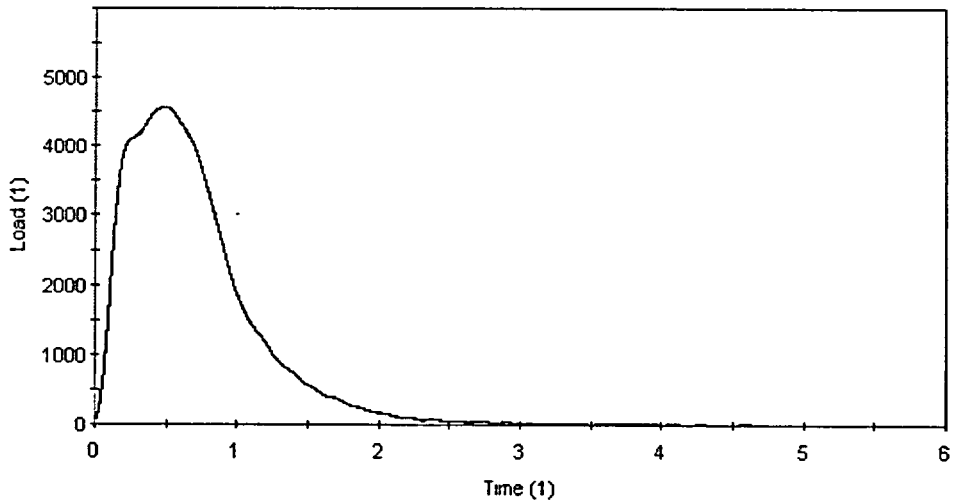

R52, 275°F

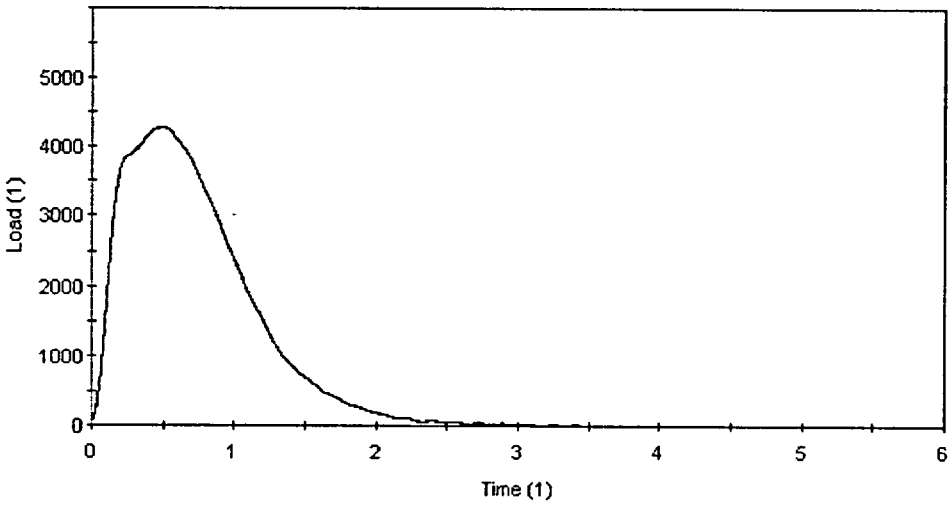

R53, 325°F

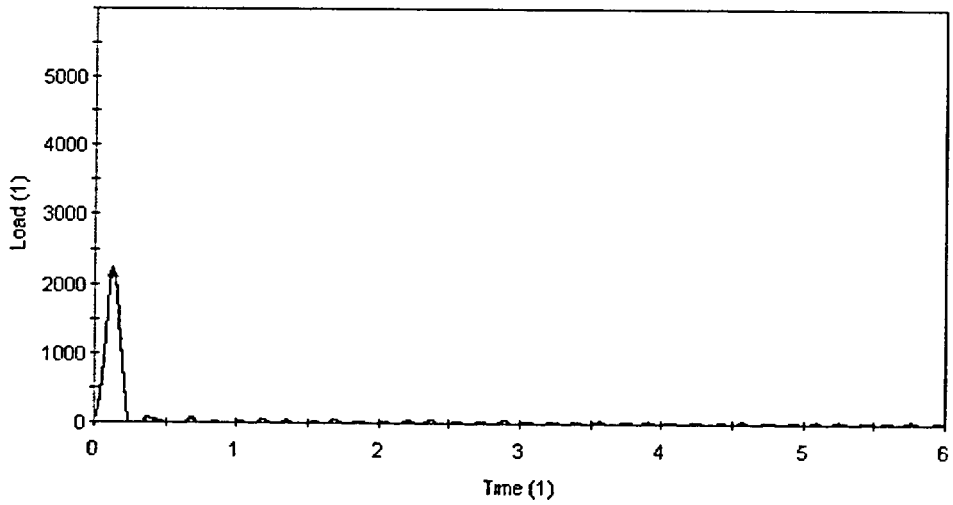

W12, 80°F

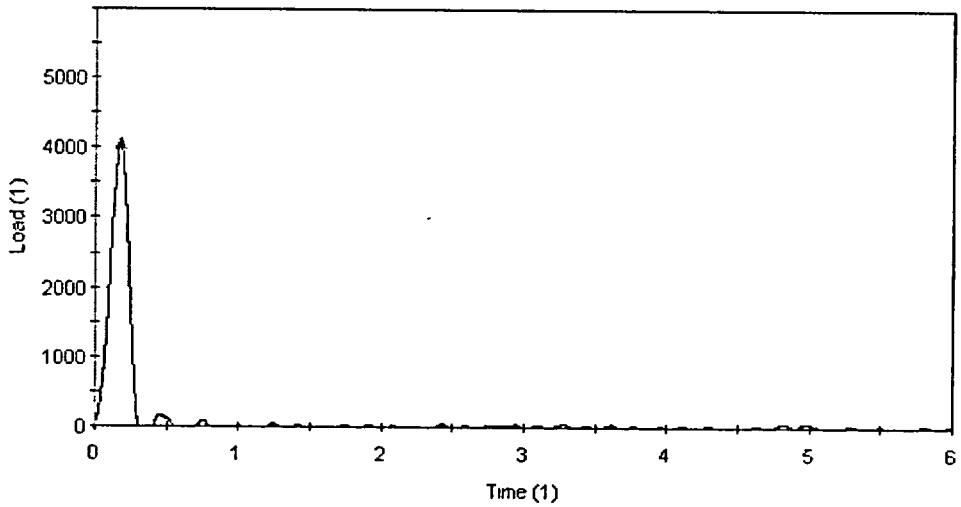

W13, 20°F

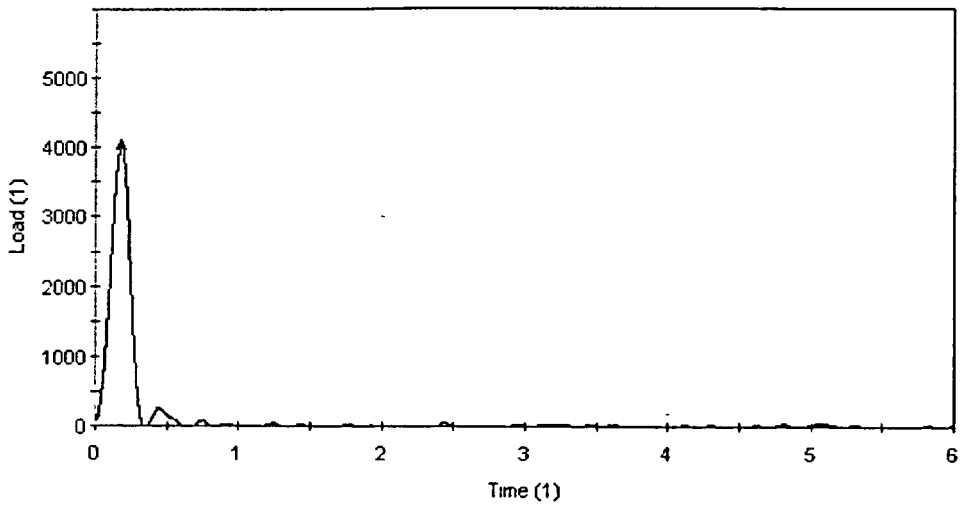

W10, 125°F

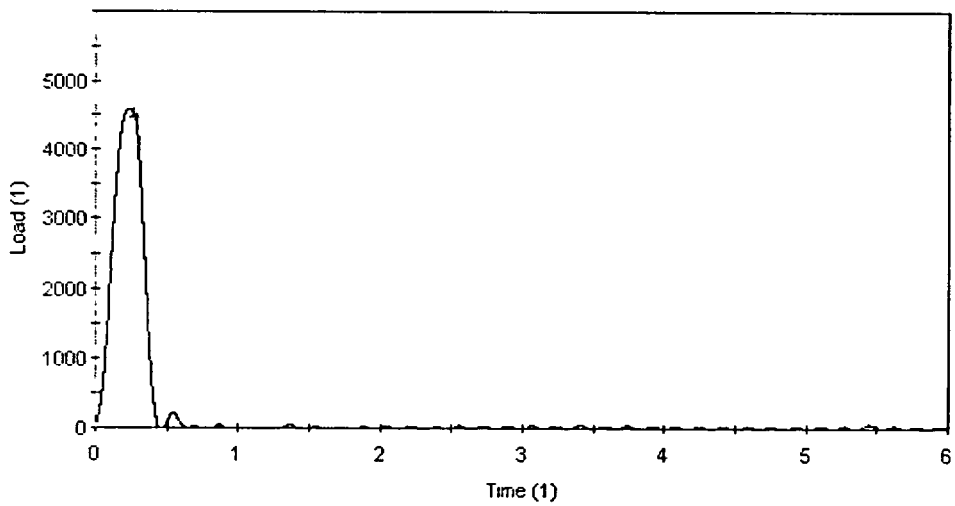

W14, 150°F

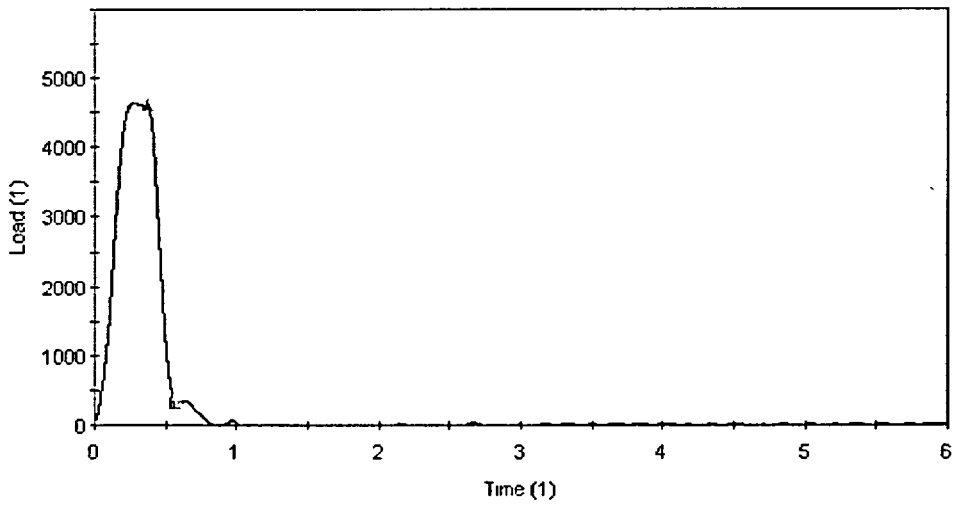

W11, 175°F

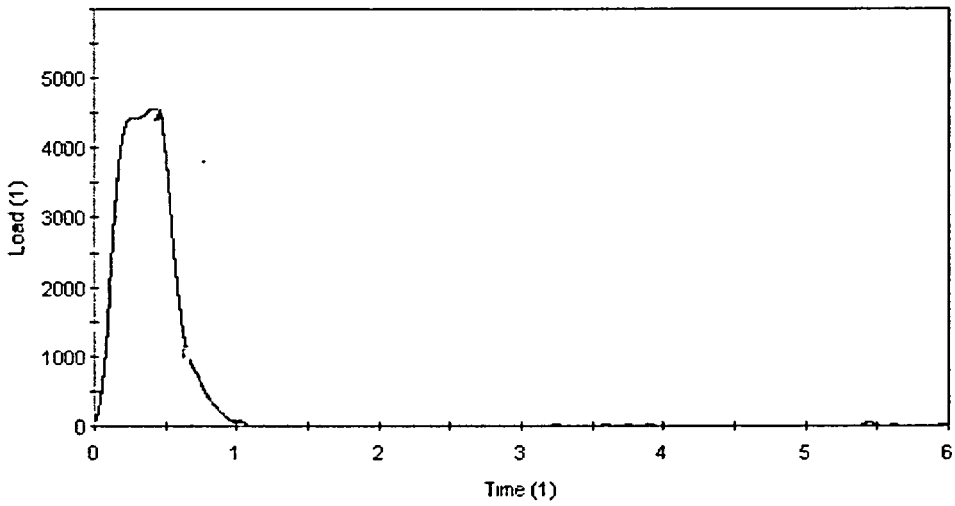

W16, 225°F

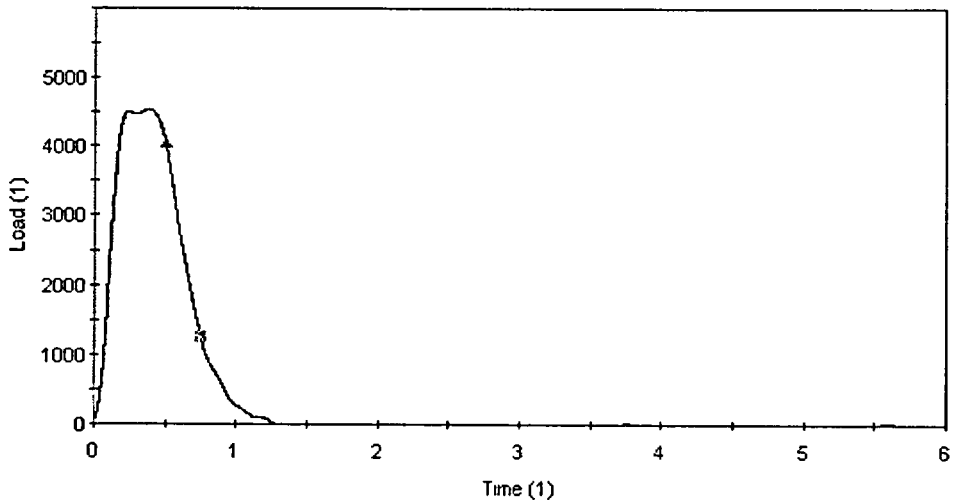

W15, 250°F

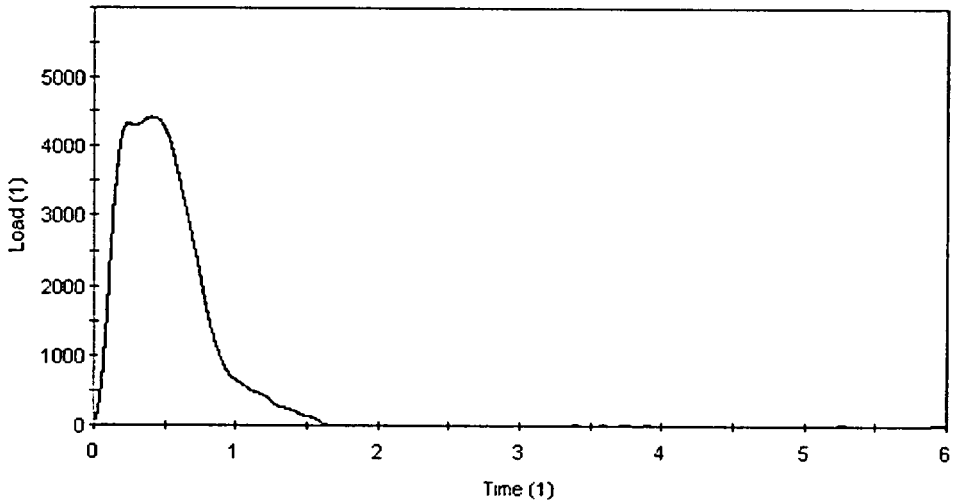

W9, 325°F

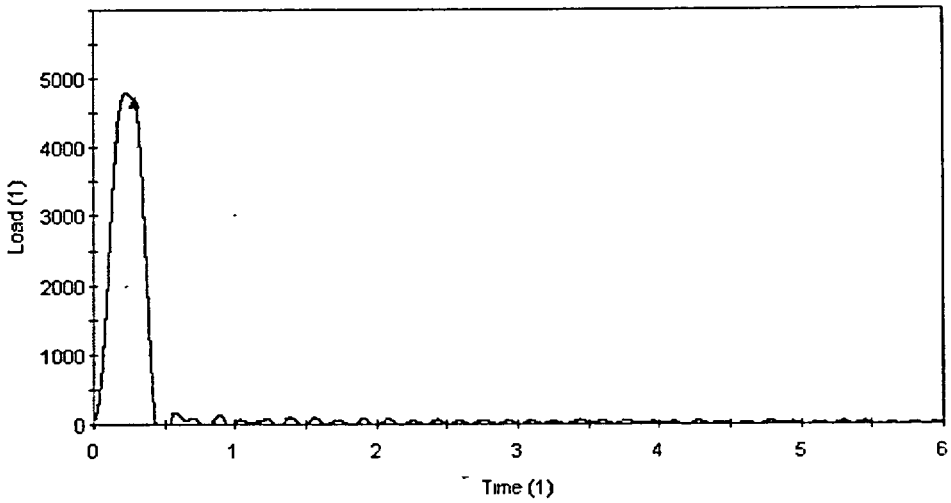

H9, -30°F

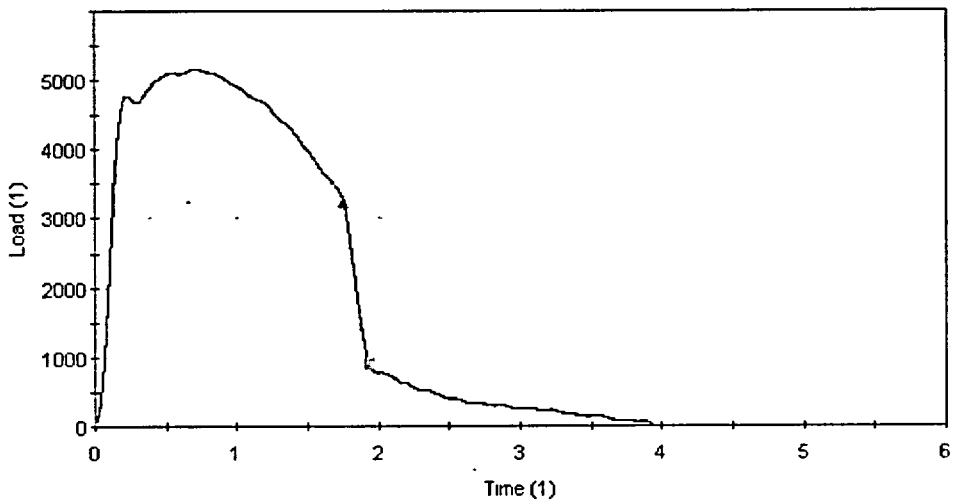

H12, -30°F

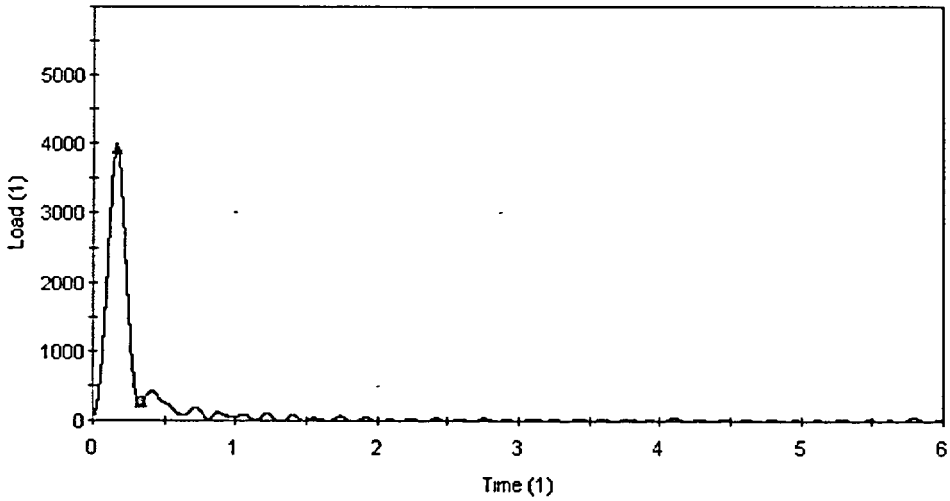

H11, -10°F

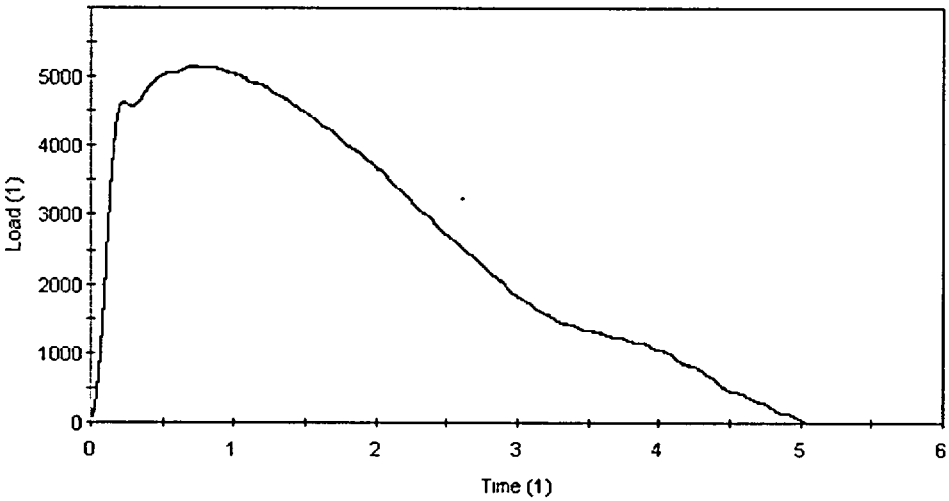

H10, 20°F

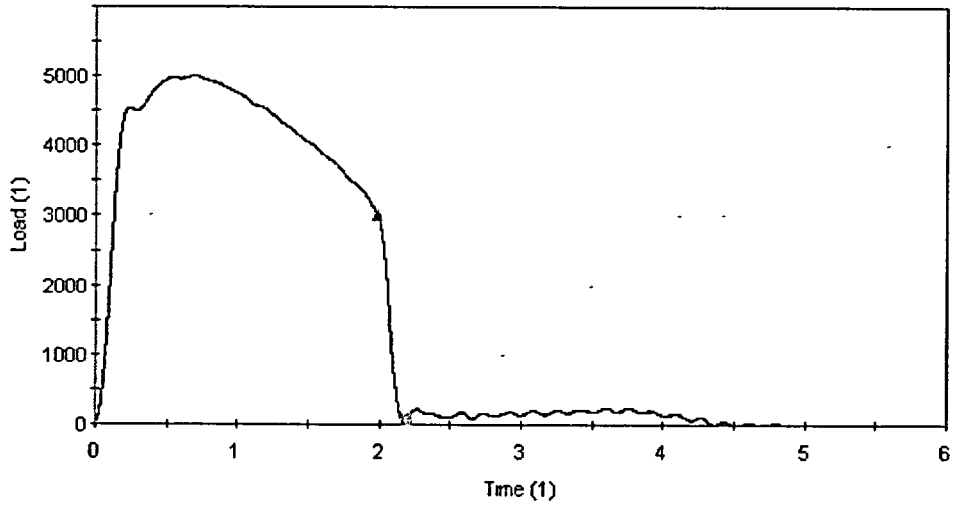

H14, 25°F

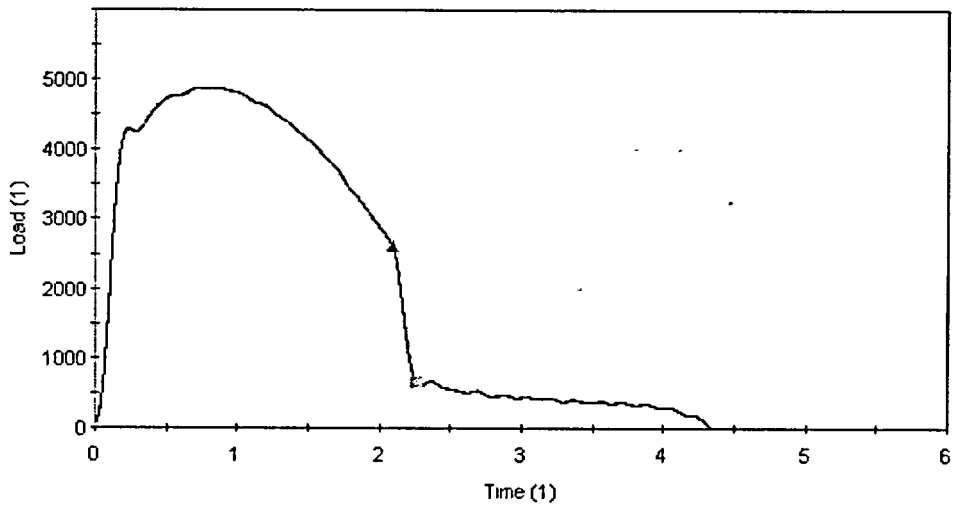

H16, 75°F

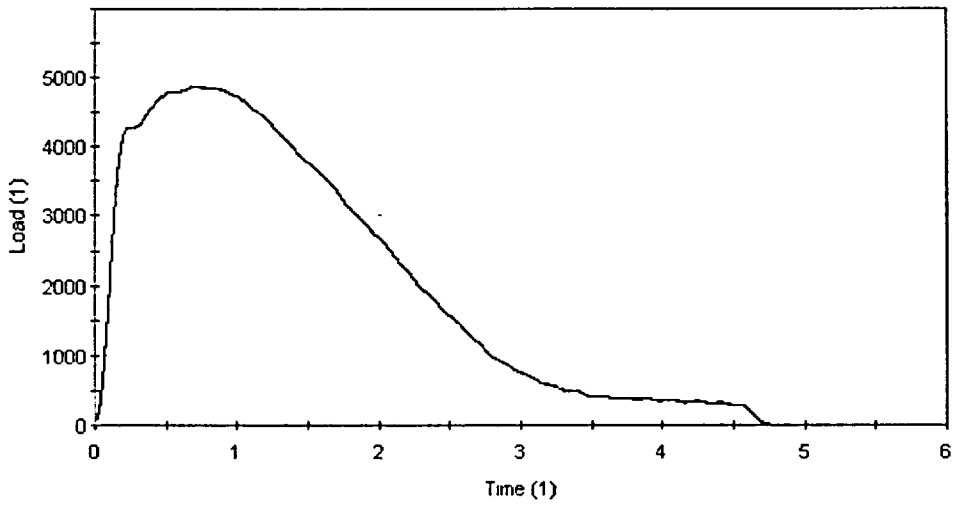

H15, 100°F

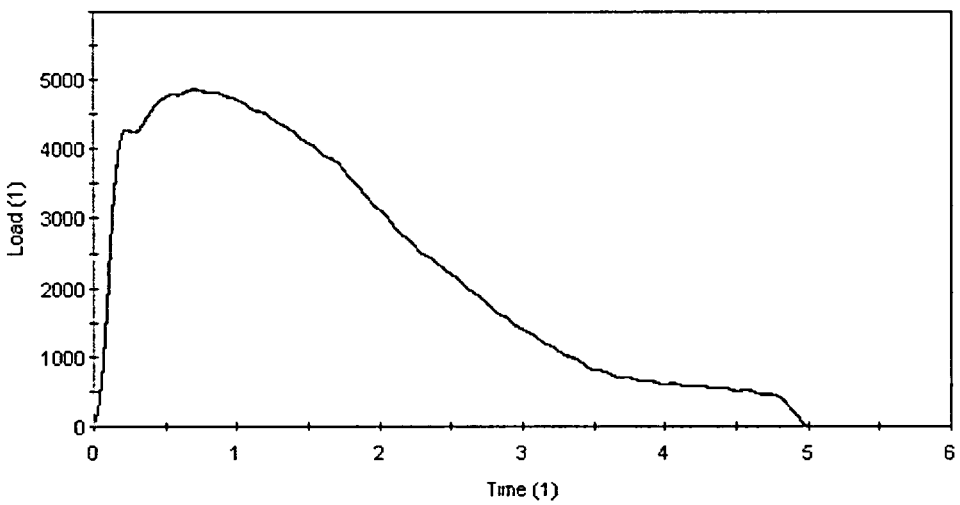

H13, 130°F